Air pollution management through urban plantation

Savita Datta

A thesis submitted for the partial fulfilment of the degree of
Doctor of Philosophy

Department of Earth and Environmental Sciences
Indian Institute of Science Education and Research Mohali
Knowledge City, Sector 81, SAS Nagar, Manauli PO, Mohali 140306
Punjab, India

March 2023

This thesis is dedicated to my family, who supported me through all my highs and lows.

Declaration

The work presented in this thesis has been carried out by me under the guidance of Dr. Baerbel Sinha at the Indian Institute of Science Education and Research Mohali. This work has not been submitted in part or in full for a degree, a diploma, or a fellowship to any other university or institute. Whenever contributions of others are involved, every effort is made to indicate this clearly, with due acknowledgement of collaborative research and discussions. This thesis is a bona fide record of original work done by me and all sources listed within have been detailed in the bibliography.

Savita Datta

(PH16044)

In my capacity as the supervisor of the candidate's thesis work, I certify that the above statements by the candidate are true to the best of my knowledge.

Dr. Baerbel Sinha

Acknowledgement

Successful completion of any project requires efforts and support of many people. I take this opportunity to express my gratitude to everyone I've had the pleasure of working with on this and other similar projects.

First, I would like to express my deepest gratitude to my supervisor Dr. Baerbel Sinha. I am forever thankful to her for sharing her knowledge, expertise, guidance and consistent encouragement from the beginning until my final research thesis is completed. Thanks for your time and extreme patience and intellectual contributions to my development. She has always believed in me and motivated me to give one's best effort in any work. Without her guidance, this dissertation would not have been possible. I also thank her for allowing me to work with the best resources and access the best atmospheric science training.

I sincerely thank Dr. Vinayak Sinha who first gave me chance to work in this field and for his constant motivation, invaluable suggestions, mentoring and support during the different stages of this thesis work. He provided me extensive personal and professional guidance and taught me a great deal about both scientific research and life in general. I am also thankful to my monitoring committee members - Dr. Vinayak Sinha and Dr. Sunil Patil for their insightful suggestions and motivation. I also sincerely appreciate the valuable comments and suggestions of all the anonymous editors and esteemed reviewers, which helped me improve the quality of my peer-reviewed articles.

I can't miss thanking all my present and past group members from Aerosol Research Group and Atmospheric Chemistry and Emissions Group at IISER Mohali. Special thanks to all my colleagues - Chinmoy, Vinod, Praphulla, Gaurav, Abhishek, Saryu, Harshita, Haseeb, Ashish, Shabin, Pallavi, Pooja, Tess, Astha, Raj and Anita for the fun and support. I would also like to thank all final year thesis students and project assistants who worked in the lab - Vidit, Lejish, Ishnoor, Shubham, Sneha, Saurabh, Bharti, Priya, Ritika, Abhilasha and Adarsh for all support and time to time help. Their presence greatly enhanced my experience. Thanks all who helped me in intensive fieldwork. I would like to express my gratitude to Vinod, Praphulla, Abhishek, Saryu, Harshita, Haseeb and Ashish to help me learn the different instrumental techniques in the lab. I must say that I have thoroughly enjoyed my academic and research activities and it was a journey filled with learnings.

I would like to express my gratitude to the IISER Mohali Atmospheric Chemistry Facility for the data and the Ministry of Human Resource Development (MHRD), India, and IISER Mohali for funding the facility. I also thank University Grants Commission (UGC) for JRF/SRF fellowship. I want to acknowledge the DST Climate Change Program (SPLICE) DST/ CCP/MRDP/100/2017(G) for funding support towards sampling and fieldwork for plant chamber experiments. I also thank all academic and non-academic staff at IISER Mohali who made my journey comfortable and safe.

Finally, I am thankful to my family who always supported me patiently. Being married and mother of two kids, means path full of constraints. In such journey, while doing PhD means you really need a big support system. I would like to thank my parents, parents-in-law, and all relatives whose love and blessings are always with me. I want to thank my husband and my kids for their love, support and care.

Savita Datta

Synopsis

Thesis title: Air pollution management through urban plantation

Candidate: Ms Savita Datta (PH16044)

Chapter 1: Introduction

In the Introductory chapter of my thesis, I describe the role of vegetation in combating air pollution. Population growth, urbanization, and industrialization have caused significant air pollution problems in India. The combination of anthropogenic and natural environmental factors in urban areas leads to poor air quality, especially in developing nations like India, which is reported to have among the worst levels of air pollution worldwide. The environmental impacts of urbanization are generally believed to follow a Kuznets curve with an inverted U shape. In the initial stage of urbanization and rapid economic development, air quality decreases with increasing urbanization. However, when the population becomes aware of the ill-effects of pollution on everyone's health, voters demand a cleaner environment. This results in policy interventions that reduce air pollution levels. Globally several countries in the developed world have passed the inflection point of the Kuznets curve, while India is affected by heavy indoor and outdoor pollution. In India, urban growth is limited to a few megacities. So, the overall urbanization rate in India is low, but these megacities have extremely high population densities and are becoming regional air pollution hotspots.

Due to adverse impacts on the respiratory and pulmonary systems, air pollution is a severe cause of morbidity and early mortality. Various government policies imposed to regulate air pollution seem to have limited effect and have not shown a significant reduction in average mortality due to pollution exposure. Even the recent report of the *Lancet* commission on air pollution and health states that ambient air pollution is still the primary cause of early deaths in lower and middle-income countries. It is believed that the reduction in poverty-related mortality in these countries was partially offset by increased deaths due to air pollution. Harmful gases and suspended particle matter in the air caused by natural or anthropogenic activities contributed 17.8% of the total all-cause mortality in India in 2019. Therefore, considerably more work needs to be done to improve the situation and reach compliance with air quality standards. Developed countries already have a well-organized urban air quality management system. In contrast, developing countries are still working to improve monitoring systems, upgrade source and emission inventories, and effectively implement pollution control and management strategies.

Trees have always served as a support system for physical and mental welfare of humans. Urban green spaces, which may include trees, shrubs, herbs, and grasses, are a crucial component and contributor to sustainable development. Trees, when chosen wisely, have the potential to significantly reduce air pollution, which helps enhance both the environment and human health. They absorb gaseous air pollutants through leaf stomata and sequester particulate matter and gases via dry deposition on their surface. In India, the urban plantation has been promoted as a short-term intervention measure to improve urban air quality.

However, urban sites are high-stress environments, and different biotic and abiotic factors impede a tree's growth and cause tree mortality. Though trees are planted to reduce pollution and benefit from ecosystem services, it is difficult for vegetation to flourish in polluted environments. Trees that fail to thrive contribute little towards improving the environment, so their plantation needs to be avoided in certain locations. In addition, trees are known to emit volatile organic compounds (VOCs) termed as biogenic volatile organic compounds (BVOCs) through plant biochemical pathways. VOCs are precursors of tropospheric ozone (TO) and secondary organic aerosol (SOA) in cities with high NOx levels. Emission of BVOCs can also be triggered due to various urban stresses and lead to an increase in BVOC burden by significant emission of stressed BVOCs. Due to this, plantation of the wrong species and plantation in the wrong places may deteriorate air quality instead of improving it. Trees that emit allergenic pollen, too, negatively impact human well-being and need to be avoided.

Thus, my research focuses on accurately quantifying how urban vegetation affects air quality and how to choose the appropriate tree species for planting to reduce air pollution.

The research questions addressed in my thesis are as follows:

1. What role do trees and vegetation play in an urban environment in the fight against air pollution? Do they improve or deteriorate air quality in Indian cities?
2. What are the isoprene and monoterpene emission rates and trends of various tree species used for urban plantations in India?
3. What are the main shortcomings of the current process for selecting trees for urban plantations, and why is there a need for a better index?

4. What is the best approach towards quantifying the impact of urban trees and plants on air quality and ranking species according to their ability to both tolerate the stress of pollution and reduce pollution levels at a plantation site and downwind?
5. Which different modelling approaches exist for estimating the air pollution uptake potential of trees, and how do their performances compare in the urban environment?
6. Do these models contain all the feedback processes which affect plant stomatal aperture, or are there missing processes?
7. Which changes in existing models would improve their performance in reproducing the measured plant stomatal conductance?
8. Are trees helpful in mitigating the exposure to air pollutants and trace gases for which emissions peak in the evening post sunset or the early morning before sunrise, for example for compounds emitted by traffic (NOx and PAHs)?
9. Which uptake models are best capable of assessing the nighttime stomatal flux?

Chapter 2: Material and methods: field measurements and modelling

In Chapter 2 of the thesis, I discussed the methods adopted to conduct the research. My thesis work involved field observations and measurements, and to better comprehend the connection between plants and air pollution, my fieldwork results have also been integrated with modelling tools. I conducted field experiments to measure BVOC emission and acquired measurements using a leaf porometer on selected full-grown trees in their natural environment. I designed and optimized a dynamic plant cuvette using polyvinyl fluoride bags (54 L Tedlar® bags with 95% transmittance, 0.0508 mm thickness, dimensions: 24" x 36", Jensen Inert Products, part no. GST002S-2436TJC, USA) with three sealed, one open side and ¼" OD Jaco fittings on two sides for inlet and outlet of air. The BVOC emission factor measurement experiments were carried out on 14 species (*Mangifera indica, Putranjiva roxburghii, Diospyros blancoi, Swietenia macrophylla, Populus deltoides, Polyalthia longifolia, Mimusops elengi*, *Magnolia grandiflora*, and *Nyctanthes arbor-tristis, Ficus benjamina, Kigelia pinnata, Plumeria alba, Tecoma stans, and Ricinus communis*), growing in the open environment at the experimental site, near the central analytical facility (CAF) at the Indian Institute of Science Education and Research Mohali (30.667°N–76.729°E, 310 masl) in S.A.S Nagar district, Punjab. Chapter 2 also provides a detailed description of the chamber setup and the method used to measure the leaf dry weight and leaf area for calculating the emission factors. Alongside, I measured the stomatal conductance of 15 species on the campus using a handy porometer, the SC-1 model (by Decagon devices Inc., presently the METER Group Inc.). The device is based on steady state technique that measures the flux rate to water vapor with a 10% uncertainty and a resolution of 0.1 $mmolm^{-2}s^{-1}$. In this chapter, I further described the working process of the device. The instrument has two Relative Humidity (RH) sensors in series in the path of diffusion. This can be used to calculate vapor flux by comparing the RH difference between values observed by two sensors and assuming that the temperature at both sensors is the same. I also discussed the calibration process of the porometer, which is required to ensure the measurements are within the certified uncertainty limits. Next, I explained the DO_3SE model used to study stomatal conductance behavior influenced by various environmental factors to assess the gaseous flux potential of a tree. As the model requires continuous data, the chapter also includes a description of the methodology used to fill in any data gaps in the input file of four years (2018-2021) of air monitoring data. The input data file comprises ambient temperature, PAR, relative humidity, barometric pressure, water vapor pressure deficit, wind speed, rain, ozone (O_3), sulphur dioxide (SO_2) nitrogen dioxide (NO_2) and carbon dioxide (CO_2). A section in the chapter also discusses the instrument models measuring and logging meteorological data.

Chapter 3: A new index to assess the air quality impact of urban tree plantations

At the start of my research, I reviewed around 250 plant species that are planted as part of urban plantation schemes in the North-West Indo Gangetic Plain. The main focus was on their BVOC emissions and, thus, their impact on urban air quality. I compiled the BVOC emission factors of these species reported in the literature and created a list of all species with known BVOC emissions. Also, conducted field experiments to measure BVOC emissions of 10 trees and 4 shrubs. The list included some missing species (7) for which I published the first BVOC emission measurements and some species for which contradictory results had been published (2) to study their impact on urban air quality. I also included a few species for which the BVOC emission potential was known, but the environmental response functions have not been studied. In this chapter, I presented the results of the literature review and my measurement results for the additional species shortlisted, namely (*Mangifera indica, Putranjiva roxburghii, Diospyros blancoi, Swietenia macrophylla, Populus deltoides, Polyalthia longifolia, Mimusops elengi*, *Magnolia grandiflora*, and *Nyctanthes arbor-tristis, Ficus benjamina, Kigelia pinnata, Plumeria alba, Tecoma stans, and Ricinus communis*). There are 7 tree species for which isoprene and 6 tree species for which monoterpenes have been reported for the first time in my thesis from my field measurements. I also discussed the need for better methodologies to evaluate a tree's eligibility for urban and roadside plantations. Urban greening is offered as a strategy to reduce the urban heat island and improve the urban air quality in India and worldwide. Through my investigation, I debated the drawbacks of the existing tree selection methods for urban plantation schemes that are accepted in India.

At present, there are two indices used for choosing a species - The air pollution tolerance index (APTI) and the other one is the anticipated performance index (API). API assesses a tree's overall performance based on its ability to tolerate pollution and its potential to reduce pollution through its morphological characteristics. It also includes the economic worth of a tree. The argument was justified by contrasting the urban air impact of two equally recommended species as per API score: *Mangifera indica* (API = 5.9 ± 0.9) and *Polyalthia longifolia* (API = 4.8 ± 1.0*)*. *Mangifera indica* is a high isoprene and moderate monoterpene emitter, whereas *Polyalthia longifolia* is a non-isoprene emitter and a low monoterpene emitter. Both are equally recommended for urban plantation at present. The impact of both species on ozone formation differs by two orders of magnitude when these species are planted in a NO_x rich roadside environment. *Polyalthia longifolia* sequesters more ozone through its stomata than can be formed from its precursor emissions even in summer, reducing ozone levels both at the site and downwind. For *Mangifera indica* the ozone formation potential of its precursor emission flux is four times larger than the stomatal uptake during peak daytime. Hence, the plantation of *Mangifera indica* fuels tropospheric ozone production. I found that the high API of *Mangifera indica* resulted from its high APTI and economic value. Whereas pollution tolerance is necessary for selecting trees to be planted in polluted environments, it is not sufficient to evaluate the impact of trees on urban air quality.

Due to this, I proposed a new and better index, the Air Quality Impact Index (AQII), to evaluate the impact of vegetation on urban air quality. This new index does not consider profit as a priority for urban greenery and instead incorporates the effect of ozone and aerosol precursor emission, stomatal conductance or pollution uptake potential, pollen allergy potential and drought tolerance, tree habit and aerodynamic properties of the proposed species into the decision making process, as air pollution mitigation should be the prime objective of urban plantations. I calculated this new AQII for 98 species. For 52 species, API score is available in the literature, and the AQII was compared with their old API score. I suggested species with an AQII score ≥17 as good choices for urban plantations. *Polyalthia longifolia* has a score of 22 and is recommended. Such a high score results from a species having low isoprene and monoterpene emission potential and no allergenic windblown pollen. On the other hand, species with an AQII score < 11 are usually not very well suited for urban plantation or, at the very least require a careful site-specific impact assessment. Usually, species with a low score are prolific emitters of isoprene and monoterpenes and have allergenic windblown pollen. Hence their plantation is best avoided in urban areas. A moderate score between 11 and 17 is usually either due to the high ozone or aerosol precursor emission potential or due to allergenic windblown pollen release potential. Hence, such species can be considered for urban plantation but with a site-specific assessment that evaluates how important the parameter that causes the low score is in a particular plantation context. *Mangifera indica,* has a score of 11 and would necessitate a detailed impact assessment before being selected for urban plantations.

Chapter 4: Nocturnal pollutant uptake contributes significantly to the total stomatal uptake of *Mangifera indica*

This chapter compares two widely employed approaches, multiplicative and photosynthetic, to analyze the behavior of stomatal flux in trees. Through stomatal uptake, the leaves of vegetation act as a surface for dry deposition and sequester trace gases, including ozone and its precursors. So far, it has been asserted that the multiplicative approach performs better for leaf-level and regional-level applications. However, my work has shown that the photosynthetic approach is superior to the multiplicative, even for leaf-level applications. To validate the hypothesis of my investigation, I optimized the well-known DO_3SE (Deposition of Ozone for Stomatal Exchange) model for *Mangifera indica*. DO_3SE is a dry deposition model specifically designed to assess tropospheric ozone risk to forests and crop yield. The model can be tuned for various environmental variables and photosynthetic parameters like temperature, photosynthetic active radiation (PAR), relative humidity, water vapor pressure deficit, soil moisture, phenology, rate of carboxylation (V_{cmax}) and electron transport rate (J_{max}) in the multiplicative and photosynthetic mode for the stomatal flux estimation. I ran the model over four consecutive years (2018-2021) with measured meteorological data, ambient ozone (O_3) mixing ratios measured carbon dioxide (CO_2) mixing ratios as the input file. Next, the output stomatal conductance obtained from both model runs was compared with that obtained from the field measurements in four years and different periods. The analysis showed that the daytime stomatal conductance was overestimated by the multiplicative model. The same model also prescribed zero conductance at night, whereas field measurement readings between 9 p.m. and 4 a.m. reveal an average conductance of 100 mmol $(H_2O)m^{-2}s^{-1}$. This acts as a drawback for nighttime stomatal conductance assessment as many species do not close their stomata fully at night.

Next, I showed the use of the model to estimate the pollutant uptake potential of tree species and compared the results of both models. For *Mangifera indica,* the annual ozone uptake potential is 2.09 kg per tree with the photosynthetic model. Significant results were also obtained for the yearly uptake of SO_2 and NO_2, whose concentrations peak in the evening or at night. The values are 0.22 kg per tree and 0.93 kg per tree, respectively, for SO_2 and NO_2. Here, the nocturnal flux by the photosynthetic model is estimated to be 64%, 39%, 46%, and 88% of the total for NO_2 uptake in winter, summer, monsoon, and post-monsoon, respectively. For SO_2, nocturnal flux contributes 38%, 30%, 31%, and 48% of the total uptake in winter, summer, monsoon, and post-monsoon, respectively. Additionally, in this chapter, I have suggested how the DO_3SE photosynthetic and multiplicative models might be improved in future versions of the models.

Chapter 5: Conclusion: results and findings in brief

In the fifth chapter, I have discussed the major findings of my work. My work examined the importance of green spaces in the polluted urban environment for better public health. I briefly explained the results and the answers to the research questions posed at the outset of my thesis. The chapter also provides a brief overview of the prospects for the future. Key messages of the work are:

- The urban plantation is restricted to limited space. Thus, selecting tree species for greening policies becomes essential. However, the existing selection criteria in India needs to be revised with a holistic evaluation that also considers the air quality impact of urban greenery.
- Flux-based modelling is the state of the art method for determining the stomatal uptake of air contaminants. Two fundamental approaches to studying the stomatal flux response are multiplicative and photosynthetic. My analyses and results show that the latter which is based on the photosynthesis process response is superior to the multiplicative model, even for leaf-level applications.

Table of Contents

List of Publications

- **<u>Datta, S.,</u>** Sharma, A., and Sinha, B., Nocturnal pollutant uptake contributes significantly to the total stomatal uptake of *Mangifera indica,* Environmental Pollution, 310,119902, 2022.

- **<u>Datta, S.,</u>** Sharma, A., Parker, V., Hakkim, H., Kumar, A., Chauhan, A., Tomar, S.S., and Sinha, B., A new index to assess the air quality impact of urban tree plantation, Urban Climate, 40, 100995, 2021.

- Mishra, A.K., Sinha, B., Kumar, R., Barth, M., Hakkim, H., Kumara, V., Kumar, A., **<u>Datta, S.,</u>** Guenther, A. and Sinha, V., Cropland trees need to be included for accurate model simulations of land-atmosphere heat fluxes, temperature, boundary layer height, and ozone, Science of The Total Environment, Vol.,751, 141728, 2021.

- Vettikkat, L., Sinha, V., **<u>Datta, S.,</u>** Kumar, A., Hakkim, H., Yadav, P., and Sinha, B., High DMS and monoterpene emitting big leaf Mahogany trees: discovery of a missing DMS source to the atmospheric environment, Atmos. Chem. Phys. 20, 375–389, 2020.

Chapter 1

Introduction

1.1 Urbanization and its impact on air pollution and health

The late 20^{th} century is characterized by the growth of urban areas and cities. The percentage of the global population living in urban areas increased from ~30% to >50% between 1950 and 2010 (Jiang and O'Neill, 2017). In India, urbanization rates are still relatively low and stood at 31% in 2010. However, urban growth in India has been unbalanced and focused on a limited set of megacities to which people are migrating in search of better income options or for living superior lifestyles (Sarkar, 2019). The rise in urbanization, industrialization and development degraded the environment of these megacities and increased pollution levels, consequently deteriorating the health of humans living in them. This air pollution health penalty offsets some of the gains in life expectancy and health outcomes brought by better access to healthcare and schooling and higher incomes (Kim and Kim, 2016). The global burden of disease study indicates that more than 6 million deaths worldwide were caused by ambient air pollution (Landrigan, 2017).

The environmental impacts of urbanization are generally believed to follow a Kuznets curve with an inverted U shape (Wang et al., 2022). In the initial stage of urbanization and rapid economic development, air quality decreases with increasing urbanization. However, when the population becomes aware of the ill-effects of pollution on everyone's health, voters demand a cleaner environment. This results in policy interventions that reduce air pollution levels. Globally, not only countries in the global North but also China is believed to be past the inflection point of the Kuznets curve for urban air pollution (Liu et al., 2022). In lower middle-income countries like India, air pollution is still one of the major concerns impacting well-being in cities and towns. Harmful gases and suspended particle matter in the air caused by natural or anthropogenic activities contributed 17.8% of the total all-cause mortality in India in 2019 (Pandey et al., 2021).

Political demands for cleaner air in Indian megacities are already-motivating many government and private agencies to focus and work on policy-making, concentrating on sustainable development. While combating air pollution at the source by promoting cleaner residential fuel choices (Dabadge et al., 2018; Swain and Mishra, 2020; Sharma et al., 2022), shifting towards cleaner transport fuels (Hakkim et al., 2022), and reducing open waste burning (Chaudhary et al., 2022; Sharma and Sinha, 2023) is preferable, such interventions take time. Hence, the political focus has shifted towards short-term intervention measures that range from greening cities to the deployment of smog towers and smog guns. This thesis focuses on evaluating the impact of urban plantations on urban air quality.

1.2 Pollution mitigation by vegetation

Trees have been an essential part of life since ancient times, whether for wood, food, or shelter, their role in the climate system, or the monsoon system. But they are now more acknowledged for air pollution removal in cities, for combating heatwaves and mitigating the urban heat island (Chun and Guldmann, 2018). Researchers realized the increasing air pollution problem associated with socio-economic growth decades back (Seinfeld, 1989; Mage et al., 1996), and studies began to evaluate sources of air pollution, the atmospheric chemistry that leads to secondary pollution, and devise mitigation strategies. Being a developing country, the problem of air pollution in India is still a challenge and studies on pollution trends document that air pollution continues to rise (Guttikunda et al., 2014; Chandrappa and Chandra Kulshrestha, 2016; Gurjar et al., 2016). Hence, tree plantation was promoted as a short-term mitigation strategy to reduce air pollution in India (Shannigrahi et al., 2003; Kapoor et al., 2013). Trees provide many positive ecosystem services in an urban environment, like carbon sequestration, boosting and ameliorating microclimate (Georgi and Zafiriadis, 2006), enhancing beauty, supporting biodiversity and strengthening mental wellness (Marselle et al., 2020). In addition, trees are also known for removing of air pollution (Grote et al., 2016), primarily, because trees can be relatively efficient in removing coarse mode dust via a process known as dry deposition (Abhijith et al., 2017; Viippola et al., 2018). They also absorb gaseous contaminants through the leaf stomata (Nowak et al., 2006; Selmi et al., 2016). Since tree plantations came to be viewed as one of the most convenient and popular options to reduce air pollution, urban planners and policy makers started adopting plantation schemes in their air pollution mitigation plans.

Where urban afforestation projects are actively advocated as a planning tool to mitigate climatic change, adopt sustainable socio-economic growth, and improve the health and well-being of human beings, the availability of land for plantation is a constraint. The reduction in the number of green spaces results from deforestation required for development and urbanization. In such cases, compensatory afforestation often promotes a limited set of tree species. Due to the restricted space, urban plantations include only tiny swaths of woodland

and semi-natural ecosystems. So, selecting species also becomes essential to get more benefits from less green coverage. Urban plantations occur mostly in parks, and gardens, where aesthetical principles often guide species selection, and along roads where the choice of species for curbside plantations is usually driven by the ease with which trees can be cut when the need to widen the road arises.

1.3 Impact of pollution and urban environment on trees

Even though trees are planted to reduce pollution and provide ecosystem services, it is difficult for vegetation to flourish in polluted environments. The gaseous pollutants like SO_2, NO_2, and O_3 penetrate the leaves, and plant physiological systems are harmed by cytotoxicity caused by oxidative stress mechanisms (Emberson et al. 2000; Singh et al., 2022). Particulate matter accumulates on leaf surfaces, clogs stomata, hinders photosynthesis, and can cause cellular-damaging actions (Grantz et al., 2003; Singh et al., 2022). Particles also impede the uptake potential of plants for gas-phase constituents by providing smaller entries and reducing flux. This is why studies have shown a reduction of carbon sequestration potential with increased air pollutant exposure (Karmakar et al., 2019). In addition, the urban environment may also indirectly stress trees by fostering conditions that allow some pests and insects to flourish on them (Tubby and Webber, 2010). Different biotic and abiotic factors that impede a tree's growth and cause tree mortality affect them. Thus, the vulnerability and susceptibility of vegetation towards contaminated environments drew attention.

Urban sites are high-stress environments, so when choosing trees for these locations, stress tolerance capacity is an essential criterion for selecting species that can withstand harsh urban conditions. Ascorbic acid, chlorophyll, relative water content, and leaf-extract pH levels of green biomass of plant species are the parameters that are usually examined to define the air pollution tolerance of tree species. High concentrations of ascorbic acid, a potent reductant, help plants tolerate pollution. As a result of pollution exposure, the level of this acid decreases. Therefore, plants that maintain a high ascorbic acid level despite growing in a polluted environment are considered air pollution tolerant (Keller and Schwager, 1977; Lee, 1991). Under the stress of pollution, the chlorophyll levels of leaves fall (Giri et al., 2013). Thus, species that maintain high chlorophyll levels even in polluted conditions are supposed to be more tolerant. Air pollutants like O_3 and SO_2 can increase the cell permeability of leaves, and induce stomatal sluggishness, which may result in water loss (Keller, 1986). Thus, plants able to retain high relative water content are believed to have the ability to handle pollution well.

Acidic pollutants like SO_2 reduce the intercellular pH level in the leaves (Pfanz et al., 1987). Therefore, plants may be more tolerant to air contaminants in polluted environments if their leaf-extract pH is greater. These parameters are combined to form a formula known as the air pollution tolerance index (APTI). This index quantifies a plant species as tolerant or sensitive in polluted environments (Singh et al., 1991). Since then, the method has remained popular to investigate plants and trees based on their tolerance level and to select the more pollution tolerant species for plantation on the urban roadside (Sulistijorini et al., 2008; Mohammed et al., 2011; Krishnaveni et al., 2014; Kamble et al., 2021) and industrial regions (Das and Prasad, 2010; Bakiyaraj and Ayyappan, 2014; Bharti et al., 2017).

1.4 Feedback effect of urban trees on urban air quality

Is green infrastructure a reliable option to improve urban air quality? This question occupies a center point in my PhD thesis.

While the contribution of trees to ecosystem services such as storing atmospheric carbon, combatting the urban heat island effect, promoting biodiversity and improving mental health and the quality of life has been widely acknowledged (Khera et al., 2009; Karlik, 2012; Grote et al., 2016; Chun and Guldmann, 2018; Jaganmohan et al., 2018; Marselle et al., 2020), their impact on urban air quality deserves a closer look. Trees are known to emit volatile organic compounds (VOCs) known as biogenic organic compounds (BVOCs). VOCs are precursors of tropospheric ozone (TO) and secondary organic aerosol (SOA) and can accelerate secondary pollutant formation in cities with high NOx levels. As a consequence, their emissions can aggravate photochemical smog. The impact of urban trees on urban ozone levels has been controversially discussed in the air quality modelling community. Some studies reported a net reduction in urban ozone levels due to tree plantations and no impact of species selection on urban air quality (Nowak et al., 2000; Sicard et al., 2018), while other studies found that careful species selection was crucial for reaching air quality targets (Taha, 1996; Calfapietra et al., 2013; Bonn et al., 2018; da Silva et al., 2018; Simon et al., 2019). However, most studies have so far been conducted in Europe and America (Benjamin and Winer, 1998; Karlik, 2012; Sicard et al., 2018; Gómez et al., 2020), while only very few pioneering studies investigated the air quality impact of Indian tree species (Singh et al., 2014). My thesis aims to expand the knowledge about the air quality impact of Indian trees.

1.5 Motivation, objectives, and outline of the thesis

Until date, most literature evaluating the impact of urban plantations on urban air quality and ozone levels is mainly from the developed world. Very little work has been reported for tropical and subtropical sites. I conducted my research on a suburban academic campus established around 2008. During the construction of the campus, conscious efforts were made to to preserve, transplant, and replant trees. After the completion of the first construction phase, additional vegetation was planted to maintain an eco-friendly green environment on the campus and shade roads and buildings. While there has been a prominent increase in the greenery over the past years, high ozone episodes occur regularly. The site is frequently out of compliance with the national ambient air quality standard for ozone (Kumar et al., 2016). Therefore, I was curious to know whether the planation of tropospheric ozone precursor emitting species present on campus land could be contributing to those exceedances. This motivated me to look into the efficiency of trees in mitigating air pollution.

Research questions addressed through the present investigation are as follows:

10. What role do trees and vegetation play in an urban environment in the fight against air pollution? Do they improve or deteriorate air quality in Indian cities?
11. What are the isoprene and monoterpene emission rates and trends of various tree species used for urban plantations in India?
12. What are the main shortcomings of the current process for selecting trees for urban plantations, and why is there a need for a better index?
13. What is the best approach towards quantifying the impact of urban trees and plants on air quality and ranking species according to their ability to both tolerate the stress of pollution and reduce pollution levels at a plantation site and downwind?
14. Which different modelling approaches exist for estimating the air pollution uptake potential of trees, and how do their performances compare in the urban environment?
15. Do these models contain all the feedback processes which affect plant stomatal aperture, or are there missing processes?
16. Which changes in existing models would improve their performance in reproducing the measured plant stomatal conductance?
17. Are trees helpful in mitigating the exposure to air pollutants and trace gases for which emissions peak in the evening post sunset or the early morning before sunrise, for example for compounds emitted by traffic (NOx and PAHs)?

18. Which uptake models are best capable of assessing the nighttime stomatal flux?

Questions 1 to 4 has primarily been addressed in chapters 3, where I present BVOC measurements on 14 tree and shrub species and the current knowledge about the impact of 98 species on urban air quality. I discuss the shortcomings of the indices currently used to shortlist trees for urban plantation and present a more suitable and holistic index for the purpose.

Questions 5 to 9 are the focus of chapter 4 of my thesis. In this thesis chapter, I explore which of the currently used model is more suitable to model stomatal conductance in the subtropical climate zone and able to correctly model nighttime fluxes. I also find several shortcomings in both existing models and propose strategies for improving these models further. Chapter 2 describes the research methodology, instruments used and experiments conducted to address my research questions.

Chapter 2

Material and methods: field measurements and modelling

The content of sections 2.3.1 and 2.4 of this chapter has been published as electronic supplement to chapter 4 in the international peer reviewed journal Environmental Pollution as Datta et al., 2022 with co-authors Sharma, A., and Sinha, B.

My thesis work comprised of intensive field observations and measurements that were combined with modelling tools to better understand the relationship between plants and air pollution. Before starting my experimental work, I carried out a comprehensive literature review of prior research on the relation between natural vegetation and air pollution. In this chapter, I provide a detailed description of my field site and a detailed description of the measurement and modelling tools used in my work.

2.1 Field surveys and literature assessment

My work started with a literature review of BVOC emissions from Indian plants with a special focus on plants that potentially affect urban air quality. I started with a list of ~250. species that are known to be used in urban plantation in the north west IGP from a book entitled “Trees of Delhi” (Krishen, 2006). I surveyed the literature and complied all that is known about the BVOC emissions, pollution tolerance, allergy potential and stomatal conductance of these species. Till the early 2000s measurements of the BVOCs emission potential were restricted to mainly temperate species and temperate regions. Later researchers from India took on the very important task to study tropical and subtropical species for the first time in 2003 (Varshney and Singh, 2003). They reported isoprene emission factors, normalized to 30℃ and 1000 PAR, of 40 Indian species using dynamic branch chamber method. Further work, provided isoprene emission factors for 121 and monoterpene emission factor for 107 Indian tropical and subtropical species (Padhy and Varshney, 2005; Singh et al., 2008; Singh et al., 2011; Malik et al., 2018). Subsequently, I conducted a field survey and located a few tree species that have not been studied before and grow near my field site. The region is home to tropical and subtropical evergreen and deciduous plants, as well as a few temperate species. VOC emission screening was conducted on these trees and shrubs as described in greater detail in section 2.2.1. and the results are presented in chapter 3 of this thesis. Overall, 68 species of trees and 33 species of shrubs are found on campus. The BVOC emission potential of 3 trees (*Putranjiva roxburghii*, *Diospyros blancoi*, and *Swietenia macrophylla*) and 3 shrubs (*Nyctanthes arbor-tristis, Plumeria alba,* and *Ricinus communis*) had not been reported in the literature and was first reported in my thesis. In addition, I studied *Mimusops elengi* for which contradictory results had been report, *Magnolia grandiflora* for which only monoterpene emission had been reported, *Ficus benjamina* for which emission reported through static sampling method and 5 species (*Mangifera indica, Polyalthia longifolia, Kigelia pinnata, Populus deltois* and *Tecoma stans*) for which emissions were known but environmental response functions and seasonality of emissions had not been studied. My field measurements were conducted near the central analytical facility at the Indian Institute of Science Education and Research Mohali (30.667°N–76.729°E, 310 m.a.s.l.) in S.A.S Nagar district, Punjab. The site is close to Chandigarh, Himachal Pradesh, and Haryana. The study location is currently transitioning from a VOC rich suburban to a NOx rich urban atmospheric environment and therefore provides an interesting location to study the impact of trees on air quality as well as the impact of deteriorating air quality on trees. However, the BVOC emission potential under fixed temperature and light conditions alone in insufficient to understand the impact of trees on air quality in a changing climate. BVOC emissions can change in response to environmental conditions and the same environmental conditions also affect the abilities of a plant to sequester air pollutants such as ozone, NO_2 and SO_2 through stomatal uptake. The environmental response functions, which can be used to determine how a plant will behave in a changing climate require repeated observations in different seasons. Even for simple parameters such as stomatal conductance environmental response functions for tropical and subtropical species are hardly available in the literature.

2.2 Field experiments

I carried out field experiments to measure BVOCs emission and stomatal conductance on full grown trees in their natural environment by mounting a dynamical plant chamber on branches of the tree. This approach is different from previous studies which often uses saplings in pots and studied plants in a protected environment such as a growth chamber. The fieldwork continued for four years at different periods and seasons, from April 2018 to February 2022 (shown in table 2.1). Field trips to the Himalaya's that had been planned for the year 2020 had to be canceled because of the Covid-19 pandemic. The instrument details used in the field and lab experiments are described in greater detail in the section 2.2.1 and 2.2.2 below.

2.2.1 BVOC flux measurement using branch cuvette method

The objective was to measure and analyze the trend of BVOC emission from selected trees and shrubs growing in the open environment. There is no standardized commercially available branch enclosure system, unlike leaf cuvettes. Researchers modify the basic design into their setup depending on the apparatus availability and environmental requirements. Few groups used Teflon bags as static chambers without any control on water vapor or mitigation of ozone to measure isoprene and monoterpene emission (Zimmerman et al., 1978). Many used a dynamic setup with proper maintenance of input and output flow (Evans et al., 1982; Helmig et al., 2007). A polycarbonate sheet was also used as a chamber to study isoprene emission rates from Indian tree species (Varshney and Singh, 2003). So, the first step was to build a setup and optimize it for field measurements. I adopted a dynamic branch cuvette method, suitable for highly reactive and volatile compounds. Along with my group, I designed a dynamic branch cuvette setup with continuous inflow and outflow. Section 2.2.1.1 describes the details of setup used in the field.

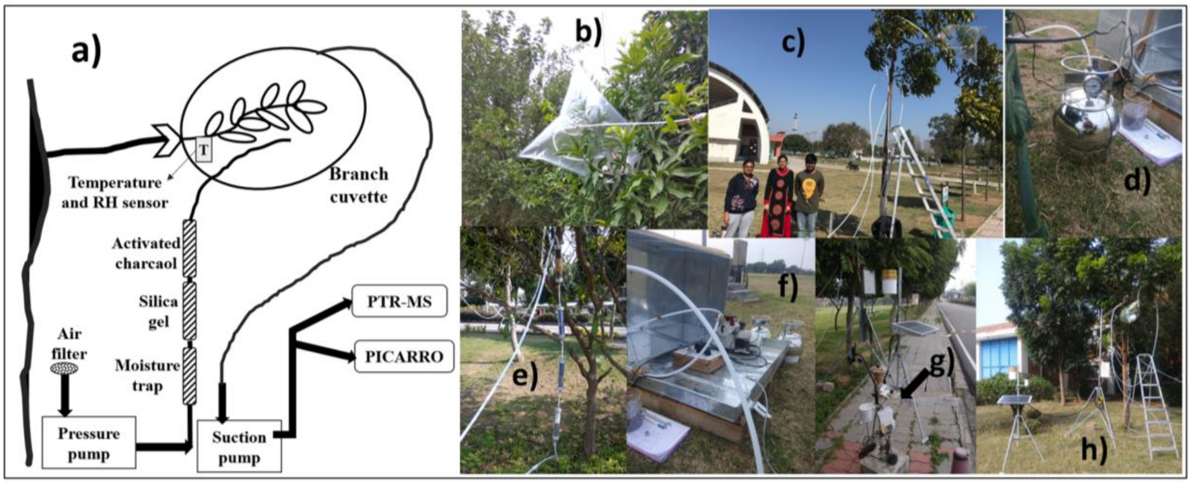

Figure 2.1: Images taken during different field experiments, measuring emission flux from trees. Image a) shows primary setup. b), c) show chambers on trees. d) shows canister filling during sampling on trees that grew too far from the lab to allow for online measurements. e) shows the setup for the generation of background air using a steel wool moisture trap, silica beads, and activated charcoal. f) shows power supply connection to pump. g), and h) shows portable MET stations from Decagon devices Inc. and Campbell Scientific Inc. respectively.

2.2.1.1 Optimization of dynamic branch cuvette setup

The basic experiment setup is shown in the figure 2.1a along with images taken in the field while conducting chamber experiments on various species Continuous measurements of isoprene and monoterpene were measured using proton transfer reaction mass spectrometer (PTR-MS, HS Model 11-07HS-088; Ionicon Analytik Gesellschaft, Austria)) on naturally growing trees. For measurements of carbon dioxide assimilation, the output air was also connected to the cavity ring-down spectrometer (CRDS Model G2508, Picarro, Santa Clara, USA).

For leaf level measurements of emission rate, it is required that the chamber material is inert, does not contaminate the air and is transparent to photosynthetic active radiation (PAR). I chose polyvinyl fluoride bags (54 L Tedlar® bags with 95% transmittance, 0.0508 mm thickness, dimensions: 24” x 36”, Jensen Inert Products, part no. GST002S-2436TJC, USA), with three sealed, one open side and ¼” OD Jaco fittings on two sides for inlet and outlet of air. Previous studies have already used and mentioned the practical potential and advantages of this setup (Ortega and Helmig, 2008; Ortega et al., 2008). The selected tree branch was put inside the cuvette carefully so that leaves do not touch the boundary walls. Then I sealed the open end using parafilm and nylon rope. First a high-capacity Teflon VOC pump (ModelN145.1.2AT.18, KNF, Germany) is used for ambient air suction and air is pushed into the cuvette via a mass flow controller (EL-FLOW, Bronkhorst High-Tech, the Netherlands; uncertainty 2 % as stated) while maintaining a flow of 30 L min^{-1}. For the protection of pump from big size impurities, a filter holder with aquarium wool is deployed at the suction end. The system is designed to provide dry zero air into the cuvette. Hence, next ambient air is made to pass through a series of self-designed traps containing steel wool (moisture trap), silica gel (desiccant) and activated charcoal (VOC and ozone scrubber) respectively. Intermediate measurement of background air at input for isoprene and monoterpene with PTR-MS and O_3 using portable ozone monitor (PO3M; 2BTechnologies, Colorado, US) ensures the performance of the zero-air setup. Another Teflon VOC pump is used at the output side of the cuvette and at a ~30 L min^{-1} suction rate to keep the setup dynamic. All flows are flowing through 9.5 mm ID Teflon tubings except for a few centimeter connections near traps, chamber and near measuring instruments that are running through 0.63, 3.2, and 6.3mm ID Teflon tubings.

To study emission flux at the ambient condition, it is required to keep cuvette internal environment as similar as possible to that of the open surrounding. For continuous temperature and relative humidity recording, I used a portable temperature humidity sensor (HTC Easylog, India) inside the cuvette suspended with a branch also supported with a Teflon rod to minimize weight stress on the branch. Sidewise, ambient temperature, humidity, PAR, and soil moisture (SM) were measured next to the tree with portable meteorological stations from Decagon Devices, USA and Campbell Scientific Inc.. All sensor description has been briefed in section 2.4.

For online sampling, output air from the cuvette was introduced into the PTR-MS for the measurements of isoprene and monoterpene and into the PICARRO CRDS for the measurements of cuvette carbon dioxide mixing ratio. Both the instruments are deployed at Central Analytical Facility (CAF), IISER, Mohali. For offline measurements, samples were collected into a passivated 6 L steel canisters (SilcoCan Restek, USA) slowly within a period of half an hour at a flow rate of 500 mL using another Bronkhorst mass flow controller of maximum capacity 500 sccm and a Teflon VOC pump (model N86 KT.45.18; KNF, Germany). The collected air then analyzed with PTR-MS and CRDS.

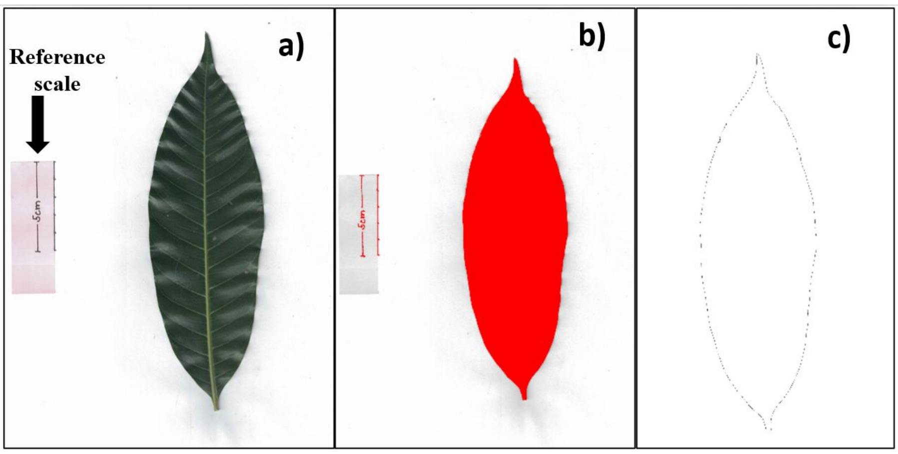

Figure 2.2: shows scanned and processed photographs of Mango leave. a) scanned image of mango leave with reference scale of 5 cm. b) red color threshold set image c) boundary line of the image in output file for which software calculated area.

2.2.1.2 Estimating leaf area and dry weight

All the species under the experiment were growing in the open environment and aged between 5-7 years at the time of the study. After every field experiment, leaves in the chamber were picked off to estimate leaf area and dry weight. For leaf area, first I scanned all leaves with Brother DCP-L2540DW printer cum scanner. For scanning leaves were kept, one by one, on A4 sheet with reference scale of 5 cm as shown in the Figure 2.2a. Individual scanned images, then processed with ImageJ software (Schneider et al., 2012) that measures area basis of set pixel threshold (Figure 2.2b, and c). Once area is found, the harvested leaves were kept in hot air oven at 60˚C for 24 to 48 hours and then weighed.

As listed in table 2.1, branch cuvette was deployed on 14 species. Continuous online measurements were taken on 9 species (*Mangifera Indica, Putranjiva roxburghii, Diospyros blancoi, Swietenia macrophylla, Populus deltoides, Polyalthia longifolia, Mimusops elengi*, *Magnolia grandiflora*, and *Nyctanthes arbor-tristis*) grown in less than 100 m distance from the laboratory housing the measuring instruments and offline samples, with the same cuvette design, were collected in canisters and analyzed within 6 hours after experiment on 5 species (*Ficus benjamina, Kigelia pinnata, Plumeria alba, Tecoma stans, and Ricinus communis*) that grew too far from the lab to allow for online measurements. In offline measurements, 5 canisters per tree along with intermediate backgrounds were collected during different hours of the day to record diurnal profiles.

Table 2.1. List of all trees included in the BVOCs flux measurements experiment and their period and days of installation. Species names in the shaded cells are those on which experiment was carried out offline.

Name of the species	Winter		Summer		Monsoon		Post-monsoon	
	Start date	**End date**	**Start date**	**End date**	**Start date**	**End date**	**Start date**	**End date**
Mangifera Indica	16/01/2019	21/01/2019	19/04/2018 25/06/2021	26/04/2018 01/07/2021	27/08/2018	05/09/2018		
Putranjiva roxburghii	25/02/2019	26/02/2019			10/09/2019	12/09/2019		
Diospyros blancoi	27/02/2019	28/02/2019						
Swietenia macrophylla	24/01/2019	29/01/2019	22/05/2018	24/05/2018	25/09/2018	04/10/2018	15/11/2018	22/11/2018
Populus deltoides			15/06/2019	16/06/2019	08/08/2018	15/08/2018	28/11/2018	08/12/2018
Polyalthia longifolia			03/04/2021	10/04/2021			25/11/2019	29/11/2019
Mimusops elengi	12/02/2019	16/02/2019	20/05/2019	27/05/2019	27/07/2018	02/08/2018		
Magnolia grandiflora	01/03/2019	02/03/2019						
Nyctanthes arbor-tristis			05/03/2019	06/03/2019				
Ficus benjamina			12/03/2019	13/03/2019				
Kigelia pinnata			15/03/2019	16/03/2019				
Plumeria alba			18/03/2019	19/03/2019				
Tecoma stans			19/03/2019	20/03/2019				
Ricinus communis			22/03/2019	23/03/2019				

2.2.2 Measurements of stomatal conductance

Stomatal conductance measures the water vapor or carbon dioxide diffusion rate into and out of the leaf stomata. In my work, I wanted to measure leaf stomatal conductance in the field and cover as many species as possible around the experiment site, as stomatal conductance had not been reported for most species. A portable leaf porometer measuring device was chosen for such a requirement. The model, SC-1 steady state technique porometer made by Decagon devices Inc., and presently the METER group Inc., measures flux rate to water vapor with a 10% uncertainty and a resolution of 0.1 $mmolm^{-2}s^{-1}$.

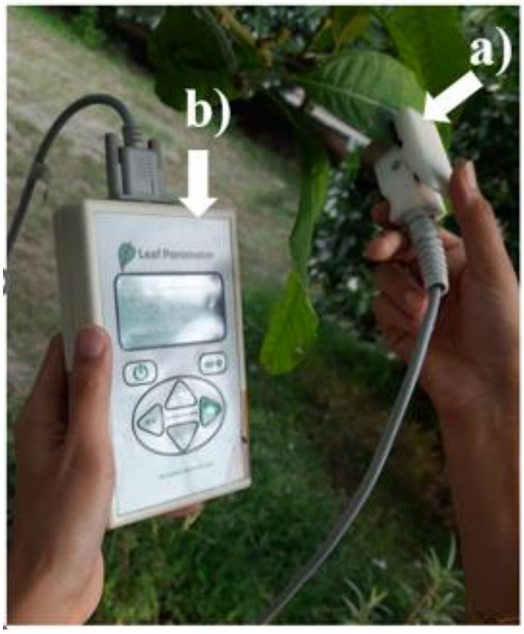

Figure 2.3: Porometer in use during measurement taken on Mangifera Indica. Device shows two parts: a) the sensor head and b) data logger head.

The present model, as shown in figure 2.3, while taking measurements in the field, consists two parts. First marked as a) is the sensor head that is deployed with two RH sensors in aluminum body to maintain temperature equilibrium, and desiccant dryer at bottom. The different parts in sensor head are revealed in the figure 2.4a). The second is logger unit that operates the stomatal conductance calculation and save the measurements. The basic principle of this instrument is measuring unknown conductance of the leaf by keeping it in series with two known conductance. The instrument has two RH sensors in series in the path of diffusion. This can be used to calculate vapor flux by comparing RH difference between values observed by two sensors and assuming that temperature at both the sensors is same. The instrument consider steady state approach of measurements and eq. (1) to eq. (8) describes the numerical methodologies to calculate final stomatal conductance.

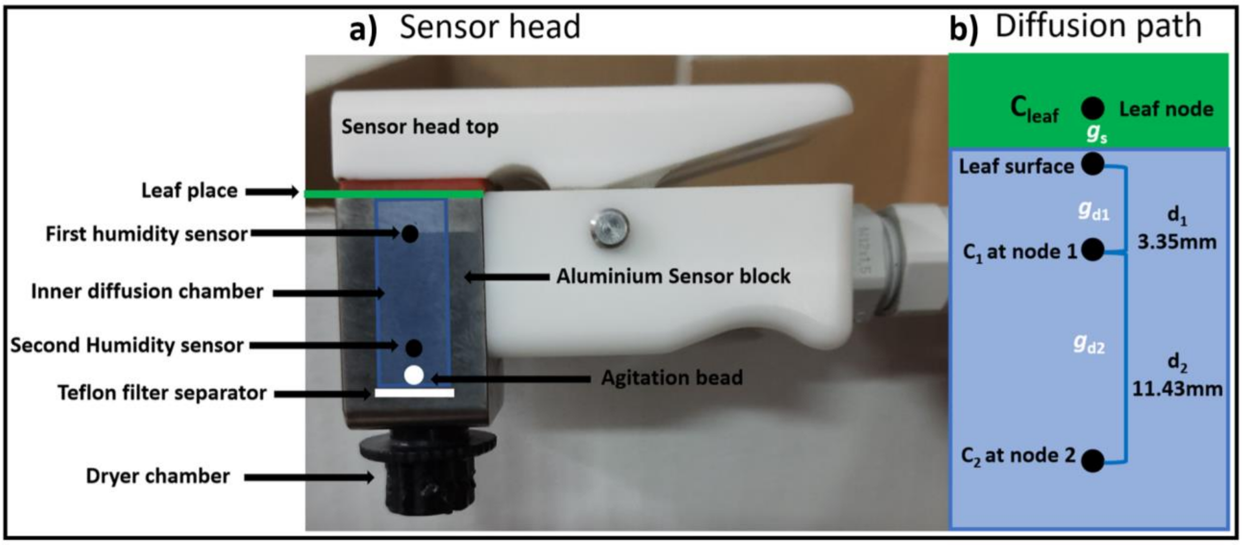

Figure 2.4: Description of senor head and functioning of diffusion path.

2.2.2.1 Calculation of stomatal conductance

Figure 2.4b) describes functions and parameters of sensor head and diffusion path. Below are assumptions for calculation:

1) All conductance in series, hence flux is same between any connecting node.
2) Leaf temperature is taken as temperature measured at first sensor.
3) Internal RH fraction of a leaf is 1.

Now, diffusion flux between two conductance nodes, from Fick's law

$$F_{vapor} = g_{d_2}(C_1 - C_2) \tag{1}$$

and between leaf and node 1

$$F_{vapor} = g_{s+d_1}(C_{leaf} - C_1) \tag{2}$$

Next, relation between mole fraction of water vapor, C, at two nodes and at leaf surface and humidity are related as:

$$C_i = \frac{rh_i e_s(T_{ai})}{P_{atm}} \quad , \quad C_{leaf} = \frac{e_s(T_{a1})}{P_{atm}} \quad \text{using second and third assumption} \tag{3}$$

rh is measured humidity, and i is variable for node 1, and 2

Here, $e_s(T_a) = 0.611 \exp\left(\frac{17.502*T_a}{T_a+240.91}\right)$

is Tetens formula (Buck, 1981) for saturation vapor pressure (kPa) with respect to temperature (^{0} C) measured at two sensors.

Also, $g_{d_1} = \frac{\rho D_{vapor}}{d_1}$, $g_{d_2} = \frac{\rho D_{vapor}}{d_2}$, and g_{s+d_1} = to be evaluated (4)

are conductance to water vapor along diffusion path linking node1and leaf surface, linking both nodes, and total conductance between stomata and node 1. Here,

d_1 = 3.35mm, the distance between leaf surface and first humidity sensor
d_2 = 11.43mm, the distance between two humidity sensors
ρ = air molar density mol m^{-3}

D_{vapor} = water vapor diffusivity, m^2 s^{-1}

Therefore, $\rho D_{vapor} = (44.6)(2.12 * 10^{-5})\left(\frac{T}{273.15}\right)^{0.75}$

$2.12 * 10^{-5}$ is water vapor diffusivity, (m^2 s^{-1}) in air at 0^{0} C temperature and 101.3 kPa pressure (STP).

Now, as per assumption 1,

eq. (1) = eq. (2)

$$F_{vapor} = g_{s+d_1}\left(C_{leaf} - C_1\right) = g_{d_2}(C_1 - C_2)$$

$$g_{s+d_1} = \frac{g_{d_2}(C_1 - C_2)}{(C_{leaf} - C_1)} \qquad (5)$$

Solving eq. (5) using equations (3), and (4)

$$g_{s+d_1} = \frac{\frac{\rho D_{vapor}}{d_2}(rh_1 e_s(T_{a1}) - rh_2 e_s(T_{a2}))}{e_s(T_{a1})(1 - rh_1)} \qquad (6)$$

To find stomatal conductance, followed combination formula for conductance in series

$$\frac{1}{g_{s+d_1}} = \frac{1}{g_s} + \frac{1}{g_{d_1}}$$

Or, $$\frac{1}{g_s} = \frac{1}{g_{s+d_1}} - \frac{1}{g_{d_1}} \qquad (7)$$

Using equations (4) and (6), then rearranging eq. (7)

$$g_s = \frac{\rho D_{vapour}}{\frac{(e_s(T_{a1})(1 - rh_1))d_2}{rh_1 e_s(T_{a1}) - rh_2 e_s(T_{a2})} - d_2}$$

Rearranging, and taking $g_{sto\_H_2O}$ for g_s

$$g_{sto\_H_2O} = \frac{\rho D_{vapor}\left(rh_1 e_s(T_{a1}) - rh_2 e_s(T_{a2})\right)}{\left(e_s(T_{a1})(1-rh_1)\right)d_2 - \left(rh_1 e_s(T_{a1}) - rh_2 e_s(T_{a2})\right)d_1} \tag{8}$$

This provides final equation of stomatal conductance calculation for water vapor in mol m^{-2} s^{-1}. However, the calibration factor stored in the instrument program is used to calibrate the final display value of stomatal conductance.

$$g_{sto\_H_2O} = \frac{\rho D_{vapor}\left(rh_1 e_s(T_{a1}) - rh_2 e_s(T_{a2})\right)}{\left(e_s(T_{a1})(1-rh_1)\right)d_2 - \left(rh_1 e_s(T_{a1}) - rh_2 e_s(T_{a2})\right)d_1} * calibration\ factor \tag{9}$$

2.2.2.2 Calibration of porometer device

RH sensors are known to change in efficiency with time as they age. In addition, ambient RH and temperature are known to affect the accuracy of the measurements as some limited air exchange happens when the leaf porometer is clipped onto the leaf. A regular calibration of the device can help limit inaccuracy. The instrument has to be calibrated using filter papers, wetted with milli-Q water, placed on calibration plate and keeping it between sensor head at place of leaf to measure conductance. The set-up is designed to give 240 mmol$m^{-2}s^{-1}$ stomatal conductance. Regular calibration was carried out to ensure measurement data stay within uncertainty limits.

While in auto calibration mode, the instrument saves the calibration value, when three measurements in continuous manner are within 7.5% uncertainty to each other. This saved calibration can be identified by a particular calibration number (CALNUM), but the correction factor is not saved together with the calibration ID. After saving the calibration factor is applied to all subsequent measurements till the next automatic calibration is performed. The manufacture recommends that an automatic calibration be performed every few hours. This automatic calibration can also be followed by a manual calibration, where the filter paper is measured in measurement mode to check the authenticity of the calibration. This is ensured when measured value, using the same wet filter, is close to 240 mmol $m^{-2}s^{-1}$. However, measuring the same filter paper immediately after the calibration factor is set does not protect against a certain type of systematic error which can occur. It was observed in 2017 that due to falling of the device into multiple hands during field measurements, the auto calibration can lead to higher inaccuracy of the data, as the displayed and saved stomatal conductance is corrected by a factor saved in a place that is not user accessible. Hence the corrections made during calibration are not traceable. The reason for failed automatic calibration can be attributed to dissimilar handling of filter by different users, either wetting it more or less, or touching/dropping the paper and possibly contaminating it. Unfortunately, biased stomatal conductance measurement caused by imperfect auto calibration cannot be corrected, as the correction factors are not saved or traceable. This results in all measurements with a certain calibration number needing to be discarded. Hence, I switched to a model that allowed individual users only to perform a manual measurement on the calibration plate. The dataset of manual measurements was subsequently used to derive a calibration factor, which is a function of temperature and RH. This factor was applied to the measurements. It can be seen that the long-term record of these observations on the calibration plate contains extreme values due to such mishandling of the filter paper. Some individual measurements can be double (~480 mmol $m^{-2}s^{-1}$) or less than half (~90 mmol $m^{-2}s^{-1}$) of the value the calibration plate is supposed to provide because either the filter is so wet that a droplet is sticking out of the orifice or because the filter is too dry. This dataset illustrates how important it is to observe precautions while doing calibration and performing measurements to maintain stability. Precautions include quickly clamping the sensor to avoid the impact of ambient humidity, frequent replacing of desiccant, and maintaining temperature equilibrium while doing calibration, and being cautious when wetting filter.

Figure 2.5 a), shows the variation of measured manual calibration values (spherical markers) from 240 standard, for CALNUM 4002101 in 2018 between 15th May to 4th October and its relationship with temperature and ambient humidity (shown with color scale). Thus, I adopted to follow frequent manual calibration for same CALNUM (for few months to a season) and rectify the noise in the measurements, using relationship equation with leaf temperature and ambient RH as detailed in table 2.2. Figure 2.5b) shows calibration data in red solid markers when correction was applied, resulting in more than 70% data now within the 7.5% uncertainty limit around the average of 240 mmol $m^{-2}s^{-1}$.

Table 2.2 shows the period where data was corrected with respect to calibration during same period and relationship equations applied for correction. The correction equations vary depending on meteorological conditions and depending on the quality of the calibration factor derived during the initial automatic calibration that is applied to all these manual calibrations.

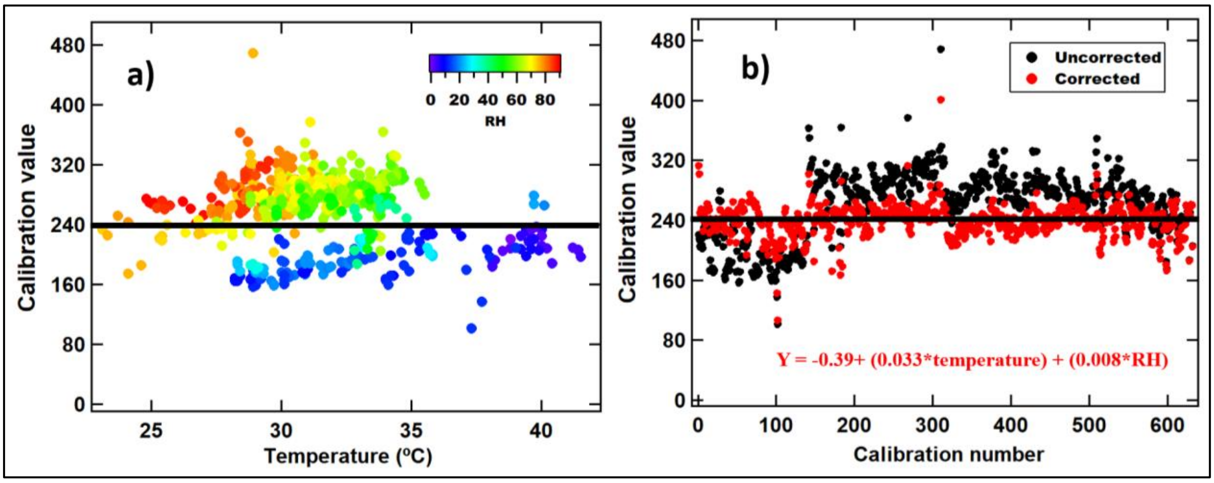

Figure 2.5: a) Calibration values observed for CALNUM 4002101 in 2018 between 15th May to 4th October and its relationship with temperature and ambient humidity (shown as color scale). b) shows uncorrected calibration values (black solid markers) and corrected data with leaf temperature and ambient RH (red solid markers).

Table 2.2: Correction equation used to correct measurement data.

Period of correction	**Correction equations for measured conductance**
7th April to 14th May 2018	Corrected = $\frac{measured}{0.45 + (0.007*\text{temperature}) + (0.002*\text{RH})}$
15th May to 4th October 2018	Corrected = $\frac{measured}{-0.39 + (0.033*\text{temperature}) + (0.008*\text{RH})}$
26th January to 24th February 2021	Corrected = $\frac{measured}{0.703 + (0.005*\text{temperature}) + (0.004*\text{RH})}$
24th February to 9th April 2021	Corrected = $\frac{measured}{0.26 + (0.021*\text{temperature})}$

2.3 Stomatal flux modelling

I adopted DO_3SE (Deposition of Ozone for Stomatal Exchange) model to study impact of various response factors on stomatal conductance and hence stomatal uptake flux of pollutants. It is a dry deposition model developed to investigate tropospheric ozone impact on forest and crops. The model provides stomatal response and thus ozone stomatal flux influenced by factors like temperature, RH, irradiance, vapor pressure deficit, soil moisture, and leaf phenology calculated using the Jarvis algorithm (Jarvis et al., 1976) in the multiplicative mode. It also allows to calculate stomatal conductance in the photosynthetic mode with equations that are based on phenomena of CO_2 gas exchange rate in photosynthesis process (Ball et al., 1987).

Due to the continuous input data requirements of the DO_3SE model, I fill in the gaps left by missing hourly measurements using the approach explained in greater depth in sub-section 2.3.1

2.3.1 Gap filling

2018

Temperature

8320 hours out of 8760 temperature measurements were available from the mobile meteorological station by Decagon Devices Inc. (now Meter group), which was placed next to the tree studied during plant chamber experiments. The remaining 440 hours of measurement were filled in with data from the meteorological station measuring at 18 m height on top of CAF. A reduced major axis regression (RMA) of the hourly data for hours in which both meteorological stations have data a slope of 1.134 ± 0.002 and an intercept of -4.13 ± 0.06 with an $R^2 = 0.97$ indicating that gap filling can result in a slight overestimation of the temperature in particular during night and when soil moisture is high.

Relative humidity

8320 hours out of 8760 RH measurements were available from the mobile meteorological station by Decagon Devices Inc. (now Meter group), which was placed next to the tree studied during plant chamber experiments. The remaining 440 hours of measurement were filled in with data from the meteorological station measuring at 18 m height on top of CAF. A reduced major axis regression (RMA) of the hourly data for hours in which both meteorological stations have data a slope of 0.845 ± 0.003 and an intercept of 18.5 ± 0.2 with an $R^2 = 0.9$ indicating that gap filling can result in a slight underestimation of the RH in particular during night and when soil moisture is high. The humidity near the ground is systematically higher.

Water vapor pressure deficit

Water vapor pressure deficit was calculated with the hourly data after performing gap filling. None of the hours with VPD >7 and only 7 out of 60 hours with VPD > 6 were affected by gap filling. This means that our conclusions about plant behavior at high VPD are robust and not affected by gap filling.

Barometric pressure

8320 out of 8760 barometric pressure measurements were available from the mobile meteorological station by Decagon Devices Inc. (now Meter group), which was placed next to the tree studied during plant chamber experiments. The remaining 440 hours of measurement were filled in using the following procedure. Data gaps exceeding 3 hours (total 440 hours) were filled by averaging the value measured during the same hour of the day on the day before and after the gap.

PAR

8758 hours out of 8760 RH measurements were available from the mobile meteorological station by Decagon Devices Inc. (now Meter group), which was placed next to the tree studied during plant chamber experiments. The remaining 2 hours of measurement were filled in by interpolating the values before and after the gap.

Wind speed

3969 out of 8760 hourly wind speed measurements were available from the MetOne meteorological station with a sampling height of 18 m. The remaining hours were filled in with the 8 years climatological mean wind speed observed for the corresponding hour between 2012-2021. RMA of the measured wind speed against the long-term climatological average revealed a slope of 0.474 ± 0.007 and an intercept of 2.26 ± 0.04 with an $R^2 = 0.21$ indicating that gap filling cannot reproduce storms and periods of extreme calm. Unfortunately, there were no other functional wind speed measurements in 2018 to fill the gap.

Ozone

8422 out of 8760 hourly values were available from the UV photometry ozone monitor Thermo Fisher Model 49i with a sampling height of 18 m. Since no alternative measurements were available in 2018 gap filling was performed following the procedure described in Sinha et al. (2015). Short data gaps of ≤3 hours (total 85 hours) were filled by interpolating the values before and after the gap. Longer data gaps exceeding 3 hours (total 253 hours) were filled by averaging the value measured during the same hour of the day on the day before and after the gap.

NO_2

8051 out of 8760 hourly NO2 values were available from the chemiluminescence NOx monitor Thermo Fisher Model 42i with a sampling height of 18 m. Since no alternative measurements were available in 2018 gap filling was performed following the procedure. Short data gaps of ≤3 hours (total 48 hours) were filled by interpolating the values before and after the gap. Longer data gaps exceeding 3 hours (total 661 hours) were filled by averaging the value measured during the same hour of the day on the day before and after the gap.

SO_2

8314 out of 8760 hourly SO2 values were available from the pulsed UV fluorescence SO2 monitor Thermo Fisher Model 43i with a sampling height of 18 m. Since no alternative measurements were available in 2018 gap filling was performed following the procedure described in Sinha et al. (2015). Short data gaps of ≤3 hours (total 36 hours) were filled by interpolating the values before and after the gap. Longer data gaps exceeding 3 hours (total 410 hours) were filled by averaging the value measured during the same hour of the day on the day before and after the gap.

CO_2

7066 out of 8760 hourly CO_2 values were available from the cavity ring-down spectrometer (Model G2508, Picarro, Santa Clara, USA).with a sampling height of 18 m. Since no alternative measurements were available, gap filling was performed following the procedure. Short data gaps of ≤3 hours (total 25 hours) were filled by interpolating the values before and after the gap. Longer data gaps exceeding 3 hours (total 1669 hours mostly due to plant chamber experiments) were filled by averaging the value measured during the same hour of the day on the day before and after the gap.

2019

Temperature

2986 hours out of 8760 temperature measurements were available from the sensor placed at the top of the canopy during plant chamber measurements which belongs to the mobile meteorological station by Campbell Scientific Inc. The remaining 5774 hours of measurements were filled in from the other mobile station by Decagon Devices Inc. (now Meter group), which was placed next to the tree studied during plant chamber experiments. RMA of the hourly data for hours in which both meteorological stations have data a slope of 1.035 ± 0.002 and an intercept of -0.91 ± 0.04 with an R^2 = 0.99 indicating that gap filling does not bias the temperature measurements.

Relative humidity

2986 hours out of 8760 RH measurements were available from the sensor placed at the top of the canopy during plant chamber measurements which belongs to the mobile meteorological station by Campbell Scientific Inc.. The remaining 5774 hours of measurements were filled in from the other mobile station by Decagon Devices Inc. (now Meter group), which was placed next to the tree studied during plant chamber experiments. RMA of the hourly data for hours in which both meteorological stations have data a slope of 0.623 ± 0.003 and an intercept of 26.2 ± 0.2 with an R^2 = 0.94. The Decagon RH sensor procured in 2017 shows a systematic low bias for high RH measurements (RH > 80%) when compared to the Meatech sensor procured in 2019. RMA of measurements for which the Campbell Scientific sensor shows <70% RH display slope of 0.887 ± 0.008 and an intercept of 11.7 ± 0.4 with an R^2 = 0.95. Overall, the Decagon sensor at 1 m height shows systematically higher values than the Campbell Scientific sensor at 3 m height for RH <70%.

Water vapor pressure deficit

Water vapor pressure deficit was calculated with the hourly data after performing gap filling. All 58 values with VPD >6 are affected by gap filling, because the Meatech sensor only became available in September 2019. Due to the systematically higher RH measurements for RH <70% by the Decagon sensor placed at 1 m height, the calculated VPD values may be underestimated but are certainly not overestimated.

Barometric pressure

2986 hours out of 8760 barometric pressure measurements were available from the sensor placed at the top of the canopy during plant chamber measurements which belongs to the mobile meteorological station by Campbell Scientific Inc. The remaining 5774 hours of measurements were filled in from the other mobile station by Decagon Devices Inc. (now Meter group), which was placed next to the tree studied during plant chamber experiments. RMA of the hourly data for hours in which both meteorological stations have data a slope of 0.977 ± 0.003 and an intercept of 2.3 ± 0.3 with an R^2 = 0.97 indicating that gap filling does not bias the barometric pressure measurements.

PAR

2986 hours out of 8760 PAR measurements were available from the sensor placed at the top of the canopy during plant chamber measurements which belongs to the mobile meteorological station by Campbell Scientific Inc. The remaining 5774 hours of measurements were filled in from the other mobile station by Decagon Devices Inc. (now Meter group), which was placed next to the tree studied during plant chamber experiments. RMA of the hourly data for hours in which both meteorological stations have data a slope of 0.907 ± 0.005 and an intercept of 5 ± 2 with an R^2 = 0.89 indicating that gap filling does not bias the PAR measurements.

Wind speed

7744 hours out of 8760 wind speed measurements were available from the MetOne station at a height of 18 m. The remaining 1016 hours of measurements were filled in from the wind speed measurements at 35 m height. RMA of the hourly data for hours in which both meteorological stations have data a slope of 0.99 ± 0.003 and an intercept of 0.28 ± 0.01 with an R^2 = 0.91 indicating that gap filling does not bias the wind speed measurements.

CO_2

6577 out of 8760 hourly CO_2 values were available from the cavity ring-down spectrometer (Model G2508, Picarro, Santa Clara, USA) with a sampling height of 18 m. Since no alternative measurements were available, gap filling was performed following the procedure. Short data gaps of ≤3 hours (total 7 hours) were filled by interpolating the values before and after the gap. Longer data gaps exceeding 3 hours (total 2176 hours mostly due to plant chamber experiments) were filled by averaging the value measured during the same hour of the day on the day before and after the gap.

2019 till 5th of May

Ozone

2936 out of 3000 hourly values were available from the UV photometry ozone monitor Thermo Fisher Model 49i with a sampling height of 18 m. Since no alternative measurements were available till May 2019 gap filling was performed following the procedure. Short data gaps of ≤3 hours (total 28 hours) were filled by interpolating the values before and after the gap.

Longer data gaps exceeding 3 hours (total 36 hours) were filled by averaging the value measured during the same hour of the day on the day before and after the gap.

NO_2

2681 out of 3000 hourly values were available from the chemiluminescence NOx monitor Thermo Fisher Model 42i with a sampling height of 18 m. Since no alternative measurements were available till May 2019 gap filling was performed following the procedure. Short data gaps of ≤3 hours (total 33 hours) were filled by interpolating the values before and after the gap. Longer data gaps exceeding 3 hours (total 286 hours) were filled by averaging the value measured during the same hour of the day on the day before and after the gap.

SO_2

2989 out of 3000 hourly values were available from the pulsed UV fluorescence SO2 monitor Thermo Fisher Model 43i with a sampling height of 18 m. Since no alternative measurements were available till May 2019 gap filling was performed following the procedure. Short data gaps of ≤3 hours (total 7 hours) were filled by interpolating the values before and after the gap. Longer data gaps exceeding 3 hours (total 4 hours) were filled by averaging the value measured during the same hour of the day on the day before and after the gap.

2019 from 6th of May

Ozone

3909 out of 5760 hourly values were available from the UV photometry ozone monitor Thermo Fisher Model 49i with a sampling height of 18 m. Data for the remaining 1851 hourly values were filled in from the UV photometry ozone Analyzer- Model-Serinus 10 (Make Ecotech) with a sampling height of 35 m. A reduced major axis regression (RMA) of the hourly data for hours in which both analyzers have data reveals a slope of 0.804 ± 0.004 and an intercept of -1.1 ± 0.2 with an $R^2 = 0.85$, indicating that gap filling at most leads to a 20% underestimation of the ozone exposure.

NO_2

4650 out of 5760 hourly values were available from the chemiluminescence NOx monitor Thermo Fisher Model 42i with a sampling height of 18 m. Data for 1081 hourly values were filled in from the chemiluminescence NOx-NO2-Analyzer-Model-Seriuns 40 (Make Ecotech) with a sampling height of 35 m. A reduced major axis regression (RMA) of the hourly data for hours in which both analyzers have data and the end of the year reveals a slope of 0.68 ± 0.004 and an intercept of 3.0 ± 0.1 with an R^2 = 0.84, indicating that gap filling at most leads to a 30% underestimation of the NO_2 exposure. 16 values during hours when both analyzers were not working were filled in with data from the NO_2 Analyzer-Model Serinus 60 (Make Ecotech). A reduced major axis regression (RMA) of the hourly data for hours in which both analyzers have data reveals a slope of 0.876 ± 0.006 and an intercept of 0.9 ± 0.2 with an R^2 = 0.78. The remaining short gaps for which none of the analyzers had data were filled in using the following method: Short data gaps of ≤3 hours (total 2 hours) were filled by interpolating the values before and after the gap. Longer data gaps exceeding 3 hours (total 4 hours) were filled by averaging the value measured during the same hour of the day on the day before and after the gap.

SO_2

4205 out of 5760 hourly values were available from the pulsed UV fluorescence SO2 monitor Thermo Fisher Model 43i with a sampling height of 18 m Data for 1472 hourly values were filled in from the chemiluminescence SO_2 Analyzer-Model Serinus 50 (Make Ecotech) with a sampling height of 35 m. A reduced major axis regression (RMA) of the hourly data for hours in which both analyzers have data a slope of 1.7 ± 0.03 and an intercept of 0.06 ± 0.08 with an R^2 = 0.48, indicating that gap filling may overestimate exposure by 70% for those hours. The remaining gaps for which none of the analyzers had data were filled in using the following method: Longer data gaps exceeding 3 hours (total 83 hours) were filled by averaging the value measured during the same hour of the day on the day before and after the gap.

2020

Ozone

8255 out of 8784 hourly values were available from the UV photometry ozone monitor Thermo Fisher Model 49i with a sampling height of 18 m. Data for the remaining 528 hourly values were filled in from the UV photometry ozone Analyzer- Model-Seriuns 10 (Make Ecotech) with a sampling height of 35 m. A reduced major axis regression (RMA) of the hourly data for hours in which both analyzers have data reveals a slope of 0.91 ± 0.004 and an intercept of -2.5 ± 0.2 with an R^2 = 0.81.

NO_2

8255 out of 8784 hourly values were available from the chemiluminescence NOx monitor Thermo Fisher Model 42i with a sampling height of 18 m. Data for the 504 hourly values were filled in from the chemiluminescence NOx-NO2-Analyzer-Model-Seriuns 40 (Make Ecotech) with a sampling height of 35 m. A reduced major axis regression (RMA) of the hourly data for hours in which both analyzers have data reveals a slope of 0.73 ± 0.004 and an intercept of 1.0 ± 0.1 with an $R^2 = 0.73$, indicating that gap filling at most leads to a 30% underestimation of the NO_2 exposure. The remaining gaps for which none of the analyzers had data were filled in using the following method: Data gaps of >3 hours (total 25 hours) were filled by averaging the value measured during the same hour of the day on the day before and after the gap.

SO_2

7782 out of 8784 hourly values were available from the pulsed UV fluorescence SO2 monitor Thermo Fisher Model 43i with a sampling height of 18 m. Data for988 hourly values were filled in from the chemiluminescence SO2 Analyzer-Model Serinus 50 (Make Ecotech) with a sampling height of 35 m. A reduced major axis regression (RMA) of the hourly data for hours in which both analyzers have data a slope of 0.939 ± 0.06 and an intercept of -0.02 ± 0.04 with an $R^2 = 0.66$, indicating that gap filling does not systematically bias the observations. The remaining gaps for which none of the analyzers had data were filled in using the following method: The remaining short gaps for which none of the analyzers had data were filled in using the following method: Short data gaps of ≤3 hours (total 14 hours) were filled by interpolating the values before and after the gap.

CO_2

6471 out of 8784 hourly CO_2 values were available from the cavity ring-down spectrometer (Model G2508, Picarro, Santa Clara, USA) with a sampling height of 18 m. Since no alternative measurements were available gap filling was performed following the procedure. Short data gaps of ≤3 hours (total 10 hours) were filled by interpolating the values before and after the gap. Longer data gaps exceeding 3 hours to a week (total 465 hours mostly due to maintenance procedure) were filled by averaging the value measured during the same hour of the day on the day before and after the gap. Gaps for the higher days, month or more, were filled by taking average of previous years data of same period (total 1838 hours, for instrument not measuring ambient air due to other experiments or instrument under service.

Temperature

8344 hours out of 8784 temperature measurements were available from the sensor placed at the top of the canopy during plant chamber measurements which belongs to the mobile meteorological station by Campbell Scientific Inc. A total of 336 hours of measurements were filled in from the MetOne sensor at 18 m height. RMA of the hourly data for hours in which both meteorological stations have data a slope of 0.97 ± 0.001 and an intercept of 1.47 ± 0.04 with an $R^2 = 0.98$ indicating that gap filling does not bias the temperature measurements. The remaining 104 hours were filled in with the measurements of the MetOne sensor located at 35 m height. RMA of the hourly data for hours in which both meteorological stations have data a slope of 0.93 ± 0.002 and an intercept of 2.0 ± 0.05 with an $R^2 = 0.96$ indicating that gap filling does not bias the temperature measurements.

Relative humidity

8344 hours out of 8784 RH measurements were available from the sensor placed at the top of the canopy during plant chamber measurements which belongs to the mobile meteorological station by Campbell Scientific Inc. A total of 336 hours of measurements were filled in from the MetOne sensor at 18 m height. RMA of the hourly data for hours in which both meteorological stations have data a slope of 0.9 ± 0.003 and an intercept of -4.1 ± 0.2 with an $R^2 = 0.93$ indicating that gap filling does not bias the RH measurements except at high RH where the sensor at 18 m levels of at 90% RH while the sensor at 3 m shows values till 100% RH. The remaining 104 hours were filled in with the measurements of the MetOne sensor located at 35 m height. RMA of the hourly data for hours in which both meteorological stations have data a slope of 0.92 ± 0.003 and an intercept of 1.6 ± 0.3 with an $R^2 = 0.89$ indicating that gap filling does not bias the RH measurements.

Water vapor pressure deficit

Water vapor pressure deficit was calculated with the hourly data after performing gap filling. None of the values with VPD >6 is affected by gap filling.

Barometric pressure

8340 hours out of 8784 barometric pressure measurements were available from the sensor placed at the top of the canopy during plant chamber measurements which belongs to the mobile meteorological station by Campbell Scientific Inc. A total of 192 hours of measurements were filled in from the MetOne sensor located at a height of 35 m. RMA of the hourly data for hours in which both meteorological stations have data a slope of 1.01 ± 0.002 and an intercept of -1.3 ± 0.2 with an R^2 = 0.98 indicating that gap filling does not bias the barometric pressure measurements. A total of 252 values were filled by the Decagon sensor which from March 2020 onwards was located at a height of 12 m, in Panchkula 15 km NE of our measurement site. RMA of the hourly data for hours in which both meteorological stations have data and the decagon station was in Panchkula reveal a slope of 1.00 ± 0.001 and an intercept of 0.3 ± 0.02 with an R^2 = 0.98 indicating that gap filling does not bias the barometric pressure measurements. The remaining 39 hours of long gaps were filled by averaging the value of the same hour of the day from the day before and after the gap.

PAR

8344 hours out of 8784 PAR measurements were available from the sensor placed at the top of the canopy during plant chamber measurements which belongs to the mobile meteorological station by Campbell Scientific Inc. Out of the remaining hours 401 hours of measurements were filled in from the other mobile station by Decagon Devices Inc. (now Meter group), which from March 2020 onwards was located at a height of 12 m, in Panchkula 15 km NE of our measurement site. RMA of the hourly data for hours in which both meteorological stations have data and the decagon station was in Panchkula reveal a slope of 1.01 ± 0.003 and an intercept of 22 ± 2 with an R^2 = 0.93 indicating that gap filling does not bias the PAR measurements. The remaining 39 hours of measurement were filled in by averaging the value measured during the same hour of the day the day before and after the gap.

Wind speed

8343 hours out of 8784 wind speed measurements were available from the MetOne station at a height of 18 m. The remaining 441 hours of measurements were filled in from the wind speed measurements at 35 m height. RMA of the hourly data for hours in which both meteorological stations have data a slope of 1.04 ± 0.005 and an intercept of 0.23 ± 0.01 with an R^2 = 0.82 indicating that gap filling does not systematically bias the wind speed measurements.

2021

Ozone

8002 out of 8760 hourly values were available from the UV photometry ozone monitor Thermo Fisher Model 49i with a sampling height of 18 m. Data for the remaining 753 hourly values were filled in from the UV photometry ozone Analyzer- Model-Serinus 10 (Make Ecotech) with a sampling height of 35 m. A reduced major axis regression (RMA) of the hourly data for hours in which both analyzers have data reveals a slope of 0.925 ± 0.003 and an intercept of 0.3 ± 0.1 with an $R^2 = 0.9$, indicating that gap filling at most leads to an 8% underestimation of the ozone exposure. For 5 hours, when both stations have not logged data, gap was filled by interpolating the values before and after the gap.

NO_2

8589 out of 8760 hourly values were available from the chemiluminescence NOx monitor Thermo Fisher Model 42i with a sampling height of 18 m. Data for the remaining 171 hourly values were filled in from the chemiluminescence NOx-NO2-Analyzer-Model-Serinus 40 (Make Ecotech) with a sampling height of 35 m. A reduced major axis regression (RMA) of the hourly data for hours in which both analyzers have data reveals a slope of 0.71 ± 0.003 and an intercept of 1.9 ± 0.1 with an $R^2 = 0.84$, indicating that gap filling at most leads to a 30% underestimation of the NO_2 exposure.

SO_2

8557 out of 8760 hourly values were available from the pulsed UV fluorescence SO2 monitor Thermo Fisher Model 43i with a sampling height of 18 m. Data for the 203 hourly values were filled in from the chemiluminescence SO2 Analyzer-Model Serinus 50 (Make Ecotech) with a sampling height of 35 m. A reduced major axis regression (RMA) of the hourly data for hours in which both analyzers have data a slope of 0.91 ± 0.006 and an intercept of 1.1 ± 0.03 with an $R^2 = 0.66$, indicating that gap filling indicating that gap filling does not systematically bias the observations.

CO2

6327 out of 8760 hourly CO_2 values were available from the cavity ring-down spectrometer (Model G2508, Picarro, Santa Clara, USA) with a sampling height of 18 m. Since no alternative measurements were available, gap filling was performed following the procedure. Short data gaps of ≤3 hours (total 10 hours) were filled by interpolating the values before and after the gap. Longer data gaps exceeding 3 hours (total 559 hours) were filled by averaging the value measured during the same hour of the day on the day before and after the gap. Long gaps were filled by averaging previous years data of the same period (total 1864 hours).

Temperature

6100 hours out of 8760 temperature measurements were available from the sensor placed at the top of the canopy during plant chamber measurements which belongs to the mobile meteorological station by Campbell Scientific Inc. A total of 2198 hours of measurements were filled in from the MetOne sensor at 18 m height. RMA of the hourly data for hours in which both meteorological stations have data a slope of 0.93 ± 0.00 and an intercept of 2.53 ± 0.05 with an $R^2 = 0.95$ indicating that gap filling does not bias the temperature measurements. The remaining 462 hours were filled in with the measurements of the MetOne sensor located at 35 m height. RMA of the hourly data for hours in which both meteorological stations have data a slope of 0.91 ± 0.002 and an intercept of 2.8 ± 0.06 with an $R^2 = 0.96$ indicating that gap filling does not bias the temperature measurements.

Relative humidity

6107 hours out of 8760 RH measurements were available from the sensor placed at the top of the canopy during plant chamber measurements which belongs to the mobile meteorological station by Campbell Scientific Inc. The remaining 2653 hours of measurements were filled in from the MetOne sensor at 35 m height. RMA of the hourly data for hours in which both meteorological stations have data has a slope of 0.85 ± 0.003 and an intercept of 5.36 ± 0.28 with an $R^2 = 0.87$. The low slope is caused primarily by the fact that the sensor at 35 m levels off at a lower RH during foggy conditions while the sensor at 3 m shows values till 100% RH. When the sensor at 35 m shows less than 70% RH the slope between the two stations is 0.9 ± 0.003 and the intercept is – 3.6 ± 0.2 and $R^2 = 0.93$. This indicates that RH is at most 10% underestimated.

Water vapor pressure deficit

Water vapor pressure deficit was calculated with the hourly data after performing gap filling. All 7 values with VPD > 6 are affected by gap filling. VPD >7 was not observed in 2021.

Barometric pressure

7619 hours out of 8760 barometric pressure measurements were available from the sensor placed at the top of the canopy during plant chamber measurements which belongs to the mobile meteorological station by Campbell Scientific Inc. All of 1141 hours of measurements were filled in from the MetOne sensor located at a height of 35 m. RMA of the hourly data for hours in which both meteorological stations have data a slope of 0.99 ± 0.002 and an intercept of 0.55 ± 0.10 with an R^2 = 0.99 indicating that gap filling does not bias the barometric pressure measurements.

PAR

7624 hours out of 8760 PAR measurements were available from the sensor of the mobile meteorological station by Campbell Scientific Inc. 4079 hours data belong to a period when the station was deployed under the tree canopy and only 3545 hours when the station was in the open were used in the model input file. A total of 5215 hours of measurements were filled in from the other mobile station by Decagon Devices Inc. (now Meter group), which from March 2020 onwards was located at a height of 12 m, in Panchkula 15 km NE of our measurement site and relocated at site on 16th October 2021. RMA of the hourly data for hours in which both meteorological stations were placed in open sky and the decagon station was in Panchkula reveal a slope of 0.93 ± 0.01 and an intercept of -13.49 ± 4.0 with an R^2 = 0.8 indicating that gap filling does not systematically bias the PAR measurements.

Wind speed

7348 hours out of 8760 wind speed measurements were available from the MetOne station at a height of 18 m. The remaining 1412 hours of measurements were filled in from the wind speed measurements at 35 m height. RMA of the hourly data for hours in which both meteorological stations have data a slope of 1.07 ± 0.004 and an intercept of 0.24 ± 0.01 with an R^2 = 0.87 indicating that gap filling does not systematically bias the wind speed measurements.

2.4 Meteorological measurements

2.4.1 Temperature & humidity measurements

The temperature and relative humidity (RH) at 35 m height were measured using the AIO 2 All in One Weather Station Met One Instruments Inc., Rowlett. The temperature sensor has a resolution of 0.1°C, a range from -40°C to + 60°C, and an accuracy of ± 0.2°C from 0°C to 60°C and ± 0.5°C from -40°C to 0°C. The relative humidity sensor has a dynamic range from 0 to 100%, a resolution of 1% and an accuracy of ± 3% at 25°C.

The temperature and RH at 18 m height were measured using the temperature sensor Model 060A and RH sensor model 083E of Met One Instruments Inc., Rowlett with the 076-radiation shield. The temperature sensor has a range from -50°C to + 50°C, an accuracy of ±0.1°C. The relative humidity sensor has a dynamic range from 0 to 100% within the temperature range of -50°C to 50°C, with an accuracy of ± 2%.

The temperature and RH (relative humidity) at 2 and 3 m height were measured using Campbell Scientific in. CS215-L15-pt with RM Young 6 plate radiation shield. The temperature sensor has a range from -40°C to + 70°C, an accuracy of ±0.4°C between +5°C and +40°C, and an accuracy of ± 0.9°C for the rest of the range. The response time is <120s. The RH sensor has a dynamic range from 0 to 100% within the temperature range of -20°C to 60°C, an accuracy of ±2% in the RH range from 10- 90% RH and an accuracy of ±4% at <10% RH and >90% RH. The temperature response of the RH sensor is within ±2% over the temperature range -20°C to +60°C and the long-term drift is within ±1% per year. The sensor was procured in 2019 and the response time is < 20s.

The RH and temperature at 1 m height were measured with the VP-4 temperature, humidity and barometric pressure sensor of Decagon devices Inc. (now Meter group). The temperature sensor has a dynamic range from -40°C to + 80°C and a resolution of 0.1°C. The accuracy is ± 0.5°C between +0°C and +60°C, and an accuracy of ± 1.0°C for the rest of the range. The response time is <400 s at 1 m/s wind speed. The relative humidity sensor has a range of 0 to 100% RH, a resolution of 0.1% RH and an accuracy of ± 4% or better in the range from 20% to 80% RH at temperatures between + 0°C and + 60°C. At > 80% RH the accuracy over the same temperature range is within ± 4%, while between 5% and 20% RH it is within ± 8%, and at < 5% RH within ± 12%.

2.4.2 Barometric pressure

The barometric pressure at 35 m height was measured using the AIO 2 All In One Weather Station Met One Instruments Inc., Rowlett. The sensor has a dynamic range from 600 to 1100 hPa. The sensor has an accuracy of ±0.5 hPa at 25°C and a resolution of 0.1 hPa.

The barometric pressure at 2 m and 3 m height was measured using Campbell Scientific Inc. CS100 sensor. The sensor has a range of 600 to 1100 hPa, an accuracy of ±1 mb in the temperature range from 0°C to 40°C and ±2 mb in the temperature range from -40 to +60°C. The sensor has a linearity of ±0.4 mb, a long-term stability of ±0.1 mb per year and a response time of <100 ms.

The barometric pressure at 1 m height was measured with the VP-4 temperature, humidity and barometric pressure sensor of Decagon devices Inc. (now Meter group). The instrument has a dynamic range: 490 to 1090 hPa, a resolution of 0.01 kPa and an accuracy of 0.4 kPa.

2.4.3 Soil moisture

Two soil moisture sensors were available to measure soil moisture near the tree and both measured soil moisture in the top 10-15 cm. Care was taken to install the sensor such that there are no major tree roots between the soil moisture sensor rods.

The GS1 sensor of Decagon devices Inc. (now Meter group). The sensor measures soil volumetric water content (VWC) within a range of 0 to 57% VWC, as long as the temperature is within -40°C to 50°C.

The Campbell Scientific Inc. CS655-L40 sensor has a sensing volume of 3600 cm^3, a rod length of 12 cm and a rod spacing of 3.2 cm. It measures soil temperature range of -10° to + 70°C with a ±0.5°C accuracy and soil moisture within a range of 5%-50% with an accuracy of ±3% as long as electrical conductivity (EC) ≤10 dS m^{-1}. The sensor measures soil electrical conductivity within a range of 0-8 dS m^{-1} with an accuracy of ± 5% and relative dielectric permittivity within a range of 1 to 81 and an accuracy of ± 0.8 up to 40 and ± 2 up to 81.

2.4.4 Rainfall

Four independent rainfall sensors are available on campus however, only 3 of them were running continuously. Since the Decagon data logger can only connect to 5 sensors simultaneously, I chose to monitor both PAR and global radiation instead of mounting the rain sensor.

Rainfall at 35 m height was measured using the AIO 2 All In One Weather station Met One Instruments Inc., Rowlett with the model 360 tipping bucket rain gauge with magnetic momentary contact reed switch as plug-in. The system operates in a temperature range of 0°C to 60°C and records 0.01 in (0.25 mm) per tip and has an accuracy of ±1% for less than 30 mm rainfall per hour and ±5% for 30 to 120 mm per hour.

Rainfall at 18m height was measured using model 372 tipping bucket rain gauge with magnetic momentary contact reed switch from Met One Instruments Inc., Rowlett. The system operates in a temperature range of 0°C to 70°C and records 0.5 mm per switch closure and has an accuracy of ±1% at 25 mm rainfall per hour.

Throughfall during periods when plant chamber experiments were ongoing and the sensor was below the canopy and rainfall at other times of the year, was monitored using the TE525-L40 Campbell Scientific Inc. tipping bucket rain gauge with magnetic momentary contact reed switch. The system operates in a temperature range of 0°C to 50°C and records 0.01 in (0.25 mm) per tip and has an accuracy of ±1% for less than 50 mm rainfall per hour.

Rainfall at 1 m height next to the tree was measured using the high-resolution tipping bucket rain gauge ECRN-100 of Decagon devices Inc. (now Meter group). The system operates in a temperature range of 0°C to 60°C and records 0.2 mm.

2.4.5 Global radiation

Global radiation at 35 m height was measured using the pyranometer model 095 as plug-in into the AIO 2 All in One Weather station, Met One Instruments Inc., Rowlett. The sensor measures radiation in the spectral range from 280 to 2800 nm in the range of 0 to 1400 W/m2. The sensor has a 180 ° field of view and is linear within ±1%. The temperature dependence is within ±1.5% from -20°C to +40°C.

Global radiation at 18 m height was measured using the pyranometer model 095 Met One Instruments Inc., Rowlett. The sensor measures radiation in the spectral range from 280 to 2800 nm in the range of 0 to 1400 W/m2. The sensor has a 180 ° field of view and is linear within ±1%. The temperature dependence is within ±1.5% from -20°C to +40°C

Global radiation next to the tree studied was measured at 1 m height using the PYR Sensor of Decagon devices Inc. (now Meter group). The sensor measures radiation in the spectral range from 380 to 1120 nm in the range of 0 to 1750 W/m2 with a ±5% accuracy. The sensor has a 180 ° field of view and can operate in the temperature range -40 °C to +60 °C.

2.4.6 PAR

PAR at the top of the canopy (3 m) was measured using the Kipp & Zonen PQS1 sensor supplied by Campbell Scientific Inc. The sensor has an operational temperature range of -30 °C to +70 °C. It measures radiation in the spectral range 400 to 700 nm ± 4 nm with a 180 ° field of view and a very low temperature sensitivity < -0.12. It can measure in the range 0 to 10,000 µmol $m^{-2}{\cdot}s^{-1}$, provides a high sensitivity of 4 to 10 µV/µmol/$m^2{\cdot}s$ and the response changes < 2 % per year.

PAR next to the tree studied was measured at 1 m height using the SQ-521 PAR sensor of Decagon devices Inc. (now Meter group). The sensor has an operational temperature range of -40 °C to +70 °C, can operate up to 100% humidity and can be submerged in water. It measures radiation in the spectral range 389 to 682 nm ± 5 nm with a 180 ° field of view and a very low temperature sensitivity< -0.11. It can measure in the range 0 to 4,000 µmol $m^{-2}{\cdot}s^{-1}$, has a tilt and azimuth error of less than 0.5%, and the response changes < 2 % per year.

2.4.7 Wind speed and wind direction

Wind speed and wind direction at 35 m height were measured using the AIO 2 All In One Weather Sensor Met One Instruments Inc., Rowlett. The station has a 2D sonic anemometer with a wind speed operating range of 0 to 75 m/s and a wind speed calibrated range 0 to 60 m/s. The wind speed accuracy is ±0.5 m/s or 5% of reading (whichever is greater) and the data is reported with 0.1 m/s resolution. The wind direction is measured from 0° to 359° (no dead band) with an accuracy of ±5° (including Compass) and is reported with a resolution of 1.0°.

Wind speed and wind direction at 18 m height were measured using model 010C winds speed sensor and the model 020C wind direction sensor of Met One Instruments Inc., Rowlett. The Davis cup anemometer has a range of 0.22 to 60 m/s and a wind speed calibrated range 0.22 to 50 m/s. The wind speed accuracy is ±1% of reading and the data is reported with 0.1 m/s resolution. The system can operate within a temperature range of -50°C to +65°C. The wind direction is measured from 0° to 357° with an accuracy of ±3° as long as the wind speed is greater than 0.22 m/s and is reported with a resolution of 0.1°.

Wind speed and wind direction at 2 m height (below canopy during plant chamber experiments) were measured using the Gil 2-D Winsonic sensor. The sensor operates at temperatures between -35°C to + 75°C and measures with a frequency of 40 Hz or better but provides the data as a block average of 1 Hz. It can measure wind speeds from 0 to 60 m/s with an accuracy of ±2 % at 12 m/s and measures wind direction from 0° to 359° (no dead band) with an accuracy of ±3°.

Wind speed and wind direction at 1m height next to the tree studied was measured using the Davis cup anemometer of Decagon devices Inc. (now Meter group). It can measure wind speeds from 0.9 to 78 m/s with an accuracy of ±5 % and measures wind direction from 0° to 359° (no dead band) with an accuracy of ±7°.

Chapter 3

A new index to assess the air quality impact of urban tree plantation

The content of this chapter has been published in the international peer reviewed journal Urban Climate as Datta et al., 2021 with co- authors Sharma, A., Parkar, V., Hakkim, H., Kumar, A., Chauhan, A., Tomar, S. S., and Sinha, B. Sinha B. supervised the investigation, and aided writing – reviewing and editing. I conducted the research, planned field experiments, analyzed the data, optimized and ran the DO_3SE model. Sharma, A. helped in field surveys and with the identification of species. Hakkim, H., and Kumar, A. helped with BVOCs measurements and data analyses. Parkar, V., Chauhan, A., and Tomar, S. S., assisted field surveys, leaf porometer measurements and experiments.

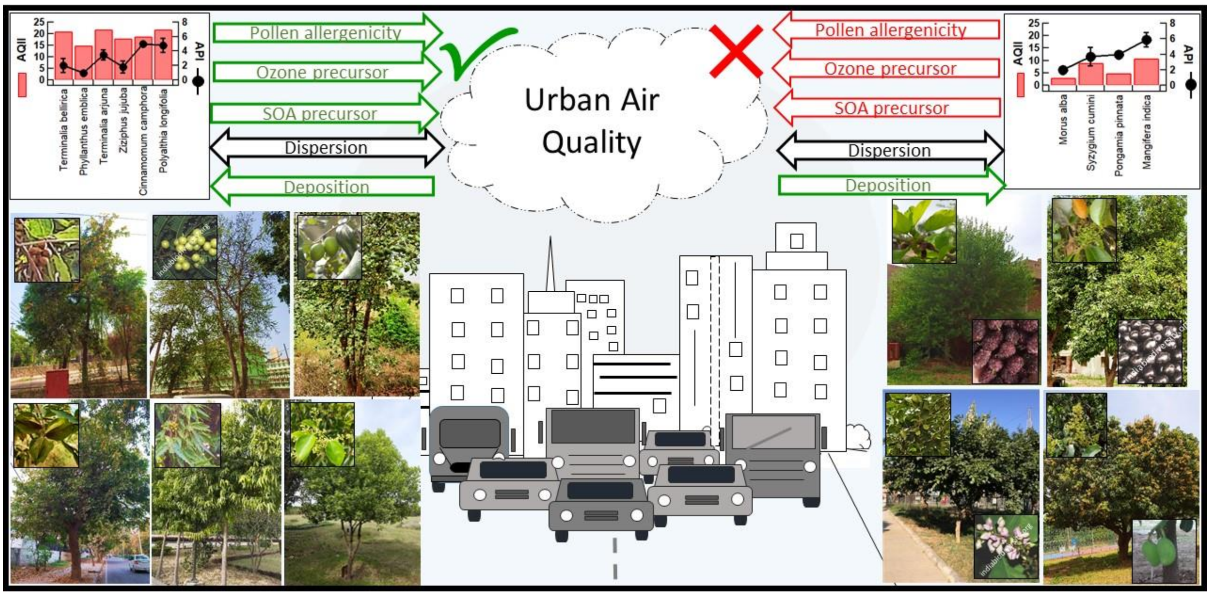

Figure 3.1: Graphical abstract of the chapter

3.1 Abstract

At present, urban planners select tree species for urban plantation based on the size, aerodynamic properties, the aesthetic value of trees and the tree's air pollution tolerance and whether the chosen species will aggravate the pollution by emitting highly reactive ozone or secondary aerosol precursors or allergenic pollen. In this study, I introduce a new Air Quality Impact Index (AQII) which ranks choices in a more holistic manner, by taking 17 aerodynamic properties, leaf structure, pollution uptake potential, pollution tolerance, ozone and aerosol precursor emissions, and the pollen allergy impact into account. I demonstrate the advantage of the AQII ranking by evaluating the impact of two species with equally high API that rank on the opposite ends of the AQII scale on urban air quality during summer season. I review the literature to compile a list of 149 species out of 280 tree species, which are commonly considered for urban plantation, for which VOC emissions have been reported. I also compile the allergy potential (107) and air pollution tolerance and calculate the AQII for 98 species, for which sufficient data is available.

3.2 Introduction

In India, vegetation has always been believed to play a powerful role in cleaning the ambient air (Chaturvedi et al., 2013; Govindarajulu, 2014) The impact of vegetation on secondary pollutant formation, however, has largely been ignored. Plants not only sequester carbon into solid biomass (Karlik, 2012; Grote et al., 2016), they also return carbon back to the atmosphere through the emission of highly reactive biogenic volatile organic compounds (BVOCs). BVOCs play an important role in the lower tropospheric chemistry (Atkinson and Arey, 2003). Globally, BVOCs contribute 90% (~1500TgC/Year) of total volatile organic compounds (VOCs) emitted into the atmosphere (Guenther et al., 1995; Lamarque et al., 2010). Only 10% of atmospheric VOCs are emitted by anthropogenic sources. Most BVOCs are highly reactive and contribute to the formation of secondary pollutants such as secondary organic aerosol (SOA) and tropospheric ozone. According to a recent study using the Model of Emissions of Gases and Aerosols from Nature (MEGAN), isoprene, a highly reactive ozone precursor, contributes 50% to the total emitted BVOCs burden. Monoterpenes, which are known for their high SOA yield contribute 15% (Guenther et al., 2006; Guenther et al., 2012). Emission of isoprene and monoterpenes from the foliage of a plant can occur as a byproduct of photosynthesis, or as part of chemical signaling to attract pollinators (Schiestl and Johnson, 2013) or predators of a pest (Pichersky and Gershenzon, 2002). In addition, BVOC emission can increase under biotic or abiotic stress (Laothawornkitkul et al., 2009), for example, during heat waves (Sharkey et al., 2007). Once emitted, BVOCs in the atmosphere are oxidized by hydroxyl radicals (OH radicals) (Lelieveld et al., 2004) in a process which yields peroxy radicals which in the presence of NOx fuel tropospheric ozone (Calfapietra et al., 2013) and secondary organic aerosol formation (Carlton et al., 2009).

Urban greening is now promoted not just in India, but around the world, as a tool to combat the urban heat island (Chun and Guldmann, 2018) and improve urban air quality (Alcock et al., 2017). It is known to enhance the dry deposition sink of particulate matter (Abhijith et al., 2017; Viippola et al., 2018) and NOx. While the potentially detrimental effect of urban trees on urban air quality (Churkina et al., 2015; Churkina et al., 2017) and human health (Cariñanos and Casares-Porcel, 2011; Eisenman et al., 2019) has been flagged by a number of authors, urban authorities generally fail to consider these impacts while selecting trees for plantation. In most countries, urban planners are more concerned about the root structures, which potentially interferes with urban infrastructure, than they are about the air pollution impact. They spend more time minimizing leaf litter generation and inconvenient fruit formation, than they do in assessing the allergy potential. Allergic ailments from mild to severe are increasing globally (Toh et al., 2012), as well as in India, where pollen allergy has been reported to affect 30% of the population (Singh and Shahi, 2008). Pollen grains are major aeroallergens (Bhattacharya et al., 2018). Symptoms of allergy during peak pollen season cause an increase in hospital visits (Behbehani et al., 2004). In India urban planners typically consider the Air pollution tolerance index (APTI) and the Anticipated Performance Index (API) (Shannigrahi et al., 2004; Prajapati and Tripathi, 2008; Sahu et al., 2020) as a metrics for choosing the right tree. Unfortunately, the APTI only quantifies whether a tree will be able to survive in a given environment. It does not quantify whether the chosen tree species will aggravate or improve air pollution in the target locality. Hence, a good APTI score presents a necessary, but not a sufficient criterion for selecting the right trees for urban plantation. The API considers the APTI score, and some of the criteria which are important for parameterizing the capability of trees to sequester pollutants in an atmospheric model (Abhijith et al., 2017). These criteria include the tree habit, crown structure, the type of tree (evergreen or deciduous), 76 the leaf texture and the impact of the tree on the aerodynamic flows in the street canyon. However, the API also awards positive or negative marks based on the economic value of the tree, without considering, that the lack or presence of a sellable product should play no role while evaluating the impact of trees on urban air quality and human wellbeing.

In this study, I demonstrate the shortcomings of the current API by contrasting the impact of two species with a high API rating, namely *Mangifera indica* and *Polyalthia longifolia*, with an API of 5.9 ± 0.9 and 4.8 ± 1.0, respectively. The former is a high isoprene and moderate monoterpene emitter, while the latter is a non-isoprene emitter and a low monoterpene emitter. Both species are currently considered to be highly suitable for urban plantation, and are among the seven most abundant tree species found in Bangalore (Jaganmohan et al., 2018) and New Delhi (Khera et al., 2009). I study these two as the most frequently planted representatives of two groups of species occupying the opposite ends of the possible BVOC emission scale. I show that when species from opposite ends of the emission scale are considered for plantation in a NOx surplus roadside environment, their impact on downwind ozone formation will differ by more than an order of magnitude. Hence, it is clearly unwarranted to consider them to be equally suitable for urban plantations. Therefore, I propose a new Air Quality Impact Index (AQII), which considers the APTI and the impact of vegetation characteristics on the aerodynamic flow, but removes economic consideration from the equation. Instead, I propose to incorporate the ozone formation potential, secondary organic aerosol formation, and the potential to cause allergic reactions and asthma related hospitalizations into the new AQII.

3.3 Material and Methods

3.3.1 Literature review

To calculate the new AQII score and suggest suitable trees for urban plantation, I review the literature on previous BVOC measurements and measure the BVOC emissions of several tree species which have never been studied. I demonstrate that the ranking assessing the suitability of species for plantation in the urban context can change dramatically when the API is replaced by the AQII. In India, urban planners choose avenue trees from a list of ~250 tropical evergreen and deciduous species. Contrary to this, urban planner in the Northern latitudes often chose their avenue species from a much smaller list of <30 species. BVOC emission fluxes are required for calculating the AQII for all species. After screening the literature on all 280 species for isoprene emission flux measurements, I compiled a list of 149 species (Table 3.1). Isoprene emission fluxes for 142 species in this list have been reported in the peer reviewed literature prior to this study. Isoprene emission fluxes for 7 species are reported for the first time in this study. Out of the 149 species identified above, 125 species had known monoterpene emission fluxes. For 6 species I report monoterpene emission fluxes for the first time in this study. The APTI was available for 82 species, the API - for 62 species, and the leaf area index - for 65 species. Stomatal conductance, an important parameter for estimating the pollution uptake potential of plants (Emberson et al., 2000; Chaparro-Suarez et al., 2011), was available only for 12 species. In this study, I report the maximum stomatal conductance for an additional 15 species, which include some of the most frequently planted species. Data for tree habit, canopy structure, leaf texture, and type of tree was compiled from the literature for 60 species for which it had been reported previously, and the missing data for the remaining 89 species was compiled from the other work (Barwise et al., 2020) or the information available at https://indiabiodiversity.org, http://www.worldagroforestry.org, https://www.cabi.org, http://www.missouribotanicalgarden.org, http://www.flowersofindia.net, and https://plants.jstor.org. I compiled allergy potential of 107 species from literature and classify species based on their allergy potential and pollen spread using parameters such as aeropollen counts (Chakraborty et al., 2016), pollen allergy tests (Mandal et al., 2008) and pollen morphology.

Table 3.1: Lists 149 trees and shrubs frequently planted in India and around the world for which either the isoprene emission potential, monoterpene emission potential, ozone uptake potential, allergy potential of pollen, and the APTI has been reported in the peer reviewed literature or studied in the present study. Species highlighted in green are those for which the final AQII or lower limit to the AQII can be calculated with the available data. Abbreviations are as follow: IEP = isoprene emission potential; MEP = monoterpene emission potential; NE = non emitter; LAI = leaf area index; g_{max} = maximum stomatal conductance; PI = pollen impact; APTI = air pollution tolerance index; API = anticipated performance index; AQII = Air quality impact index; ET = evergreen tree; EC = evergreen conifer; DT = deciduous tree; ES = evergreen shrub; DS = deciduous shrub; DDT = dry deciduous tree. A/W= known allergen and pollen windblown to large area; A/NW = known allergen but pollen hardly spread to a large area; NA/W = not known allergen but pollen windblown to large area; NA/NW = not known allergen and pollen hardly spread to a large area. * denotes properties which have no negative impact on the AQII for which values have not been reported in the literature, but for which a lower limit of the AQII can be calculated by awarding lowest possible score. The AQII value of species with an * needs to be revised once more data becomes available. Deviation in APTI was accounted for anticipated variability in reported AQII with variation in parenthesis.

Family	**Botanical name**	**Common name**	**Type of tree**	**Drought tolerance**	**IEP**	**MEP**	**LAI**	**g_{max}**	**PI**	**APTI**	**API grade (0-7)**	**AQII**
Acanthaceae	*Justicia adhatoda/ Adhatoda vasica*	Bansa	ES	Tolerant	Moderate[1]	Moderate[1]						
Aceraceae	*Acer platanoides*	Norway maple	DT	Moderately tolerant	Low[2]	Low[2]	>6 [3]		A/W [4,5]			10*
Aceraceae	*Acer pseudoplatanus*	Sycamore maple	DT	Sensitive	Low[2,6] NE [7]	Low[2,6] Moderate [7]	~4.4±2.3[3,8]	200-400 [9]	A/W [4,5]			11*
Aceraceae	*Aesculus hippocastanum*	Horse chestnut	DT	Sensitive	NE[2]	NE[2]	~5.8±0.3[3,8]		A/W [4]			13*
Altingiaceae	*Liquidamba styraciflua*	Sweetgum	DT	Moderately tolerant	High[10] Moderate[11]	Moderate[11]	3.6 [8]		A/W [5]			1*

Anacardiaceae	*Mangifera indica*	Mango, Aam	ET	Tolerant	High[PS,12-14] Low[1]	Moderate[PS,1] Low[12] High[14,15]	3.3±0.6 [16,17]	960±90[PS]	A/W[18-20]	15.6±4.1[21-31]	5.9±0.9[21,22,25,27-30]	11(-2)
Anacardiaceae	*Buchanania cochinchinensis / Buchanania lanzan /Buchanania latifolia*	Chironji, Chirauli-nut	DDT	Tolerant	High[14]	Moderate[14]						
Anacardiaceae	*Spondias pinnata*	Wild mango	DT	Moderately tolerant	High[32]	Moderate[15]						
Annonaceae	*Polyalthia longifolia*	False Ashoka	ET	Tolerant	NE[PS,1,32]	Moderate[PS] NE[1]	0.79 [33]	860±80[PS]	NA/W[18,34,35]	16.8±6.2[25-27,29,30,31,36]	4.8±1.0[25,27,29,30]	22(-2)
Annonaceae	*Annona squamosa*	Sugar apple, Custard apple, Sitaphal	ET	Moderately tolerant	NE[14,32]	Low[14] NE[15]		200-400[37]	NA/NW[35]	13.4±8.5 [26,31,38]		20(±1) *
Apocynaceae	*Plumeria alba*	Frangipani, Champa	DS	Tolerant	Low[PS]	Low[PS]	0.31 [33]			3.9 [26]		
Apocynaceae	*Alstonia scholaris*	Saptparni, Devil's tree	ET		NE[1,14,32]	Low[1,14] NE[15]	~1.6 [39]		A/W[18,40,41]	16.2±10.3[23,27,30,31,42]	4.6±1.0 [27,30,42]	14(-2) *
Apocynaceae	*Carissa carandus*	Karonda	ES	Tolerant	NE[32]					4.0 [31]		
Apocynaceae	*Nerium indicum/Nerium oleander*	Kaner (pink)	ES	Tolerant	NE[1] Low[32]	NE[1]			A/W[4,19]	16.4±12.1[22,25-27,31,42]	1.5±1.9[22,25,27,42]	15(-2) *

Apocynaceae	*Tabernaemontana divaricate / Tabernaemontana coronaria*	Crape jasmine	ES	Moderately tolerant	NE[32]	NE[32]				21.0±17.8[23,36,42]	3.0 [42]	
Apocynaceae	*Cascabela thevetia/ Thevetia peruviana*	Peeli kaner	ES	Tolerant	NE[1]	NE[1]				18.6±10.5[23,29,30,42]	1.2±1.1[28,29,42]	
Arecaceae	*Cocos nucifera*	Coconut	ET	Tolerant	Moderate[14]	NE[14]			A/W[18,20,41,43]			9*
Betulaceae	*Betula Pendula*	Silver birch	DT	Sensitive	NE[6]	Moderate[6]		>400 [44]	A/W [45]	19.5 [46]		12*
Bignoniaceae	*Kigelia pinnata/ Kigelia africana*	Kigelia, Balam kheera	ET	Tolerant	NE[PS,1] Low[13]	NE[PS] Low[1]			A/W[19,47]	19.9 [27]	3.0 [27]	16*
Bignoniaceae	*Tecoma stans*	Yellow bell, Piliya	ES	Tolerant	NE[PS] Low[1]	Low[PS,1]			NA/W[34]	8.2 [26]		12*
Bignoniaceae	*Fernandoa adenophylla / Heterophragma adenophyllum*	Marodphali	ET		NE[1,13]	NE[1]						
Bignoniaceae	*Millingtonia hortensis*	Akashneem, Tree Jasmine	ET	Tolerant	NE[32]	Moderate[15]	0.95 [48]			17.6 [27]	4.0 [27]	
Boraginaceae	*Cordia dichotoma/Cordia obliqua*	Challe, Clammy cherry	DT	Tolerant	NE[1] Low[13]	NE[14]						
Cannabaceae	*Celtis occidentalis*	Common hackberry	DT	Moderately tolerant	Low[2]	Low[2]			A/W [5]	11.6±1.9 [49]		8*
Casuarinaceae	*Casuarina equisetifolia*	Vilaayati jhaau,	ET	Tolerant	Moderate[1,13]	Low[1]	1.09 [50]		A/W[18,20,41,43]	6.9±2.5[21,26,31]	2.0 [21]	6*

		she-oak										
Combretaceae	*Anogeissus latifolia*	Dhaura	DDT	Tolerant	NE[14]	Low[14]						
Combretaceae	*Terminalia arjuna*	Arjun	DT	Tolerant	NE[1,13,14]	NE[1,14]	2.19 [51]	910±90[PS]	NA/W[18]	14.9±6.1[21,27,31]	3.5±0.7[21,27]	22(±1)
Combretaceae	*Terminalia bellirica*	Bahera, Bedda nut tree	DT	Moderately tolerant	NE[1,13]	NE[1]	0.97 [33]	270±46[52]	NA/NW[53]	11.7±0.3[22,25,27]	2.0±1.0[22,25,27]	21(1)
Combretaceae	*Terminalia chebula*	Harara, Gallnut	DT	Moderately tolerant	NE[14]	Low[14]	0.72 [33]		NA/NW[53]			20*
Combretaceae	*Terminalia tomentosa*	Asan	DT		Low[14] High[32]	Moderate[14]						
Dipterocarpaceae	*Shorea robusta*	Sal tree	DT		NE[14]	NE[14]						
Ebenaceae	*Diospyros blancoi*	Velvet apple	ET		NE[PS]	NE[PS]	3.04 [54]					
Ebenaceae	*Diospyros melanoxylon*	Kendu, malabar ebony	DT	Tolerant	NE[14]	Moderate[14]				12.5 [19]	5.0 [19]	
Euphorbiaceae	*Ricinus communis*	Castor oil plant	ES	Tolerant	Low[PS]	Low[PS]	1.38 [55]		A/W[18,20,34,43]	17.4±5.1 [25,31]	3.0 [25]	12(-1) *
Euphorbiaceae	*Jatropha gossypiifolia*	Ratanjoti, bellyache bush	ES		NE[32]							
Fabaceae	*Bauhinia tomentosa*	Yellow bauhinia	ES	Moderately tolerant	High[32]	Low[15]						

Fabaceae	*Bauhinia variegata*	Kachnar, Pink bauhinia	DT	Tolerant	Low[1] High[14,32]	NE[1,14]	1.46 [56]		A/W [19,43]	11.6±3.5[21,23,27]	1.5±0.7[21,27]	8(2)*
Fabaceae	*Peltophorum pterocarpum*	Pilmohar, Yellow flametree	DT	Tolerant	High[14]	NE[14]	2.75 [33]		A/W[18,20,41]	19.2±4.1[29,30]	3.5±0.7[29,30]	12*
Fabaceae	*Senna floribunda /Cassia floribunda*	Golden showy cassia	ES	Tolerant	NE[1]	NE[1]			A/W[18,20,43,47]			12*
Fabaceae	*Cassia renigera*	Burmese pink cassia	ET	Tolerant	NE[32]				A/W[18,20,43,47]	12.1 [21]	2.0 [21]	
Fabaceae	*Delonix regia*	Gulmohar, Flame tree	DDT	Tolerant	NE[14,32]	Moderate[14]	4.23 [17]		A/W[18,20,41]	22.4±12.5 [27,31,38,57]	3.0 [27]	10(-2)*
Fabaceae	*Tamarindus indica*	Imli, Tamarind	ET	Tolerant	NE[1,14]	NE[1,14]			A/W[18]	9.0±4.6[26,29,31,38]	2.0 [29]	16(1)*
Fabaceae	*Senna siamea / Cassia siamea*	Kassod	ET	Tolerant	NE[1,14,32]	Low[1,14]	1.24 [33]		A/W[18,20,43,47]	12.2±2.1[21,23,25,27]	3.0 [21,25,27]	14(-1)*
Fabaceae	*Cassia fistula*	Amaltas, Golden shower tree	DDT	Tolerant	NE[1,14,32]	Low[1] Moderate[14]	1.24 [33]	800±80[PS]	A/W[17,41,54]	16.3±6.7[20,21,24-26,29,35,48]	2.6±1.1[20,21,24,26,29]	14(-2)
Fabaceae	*Acacia auriculiformis*	Australian babhool	ET	Tolerant	NE[1]	NE[1]	1.5±0.7 [33,51]		A/W[20,58]	10.8 [21]	4.0 [21]	14*
Fabaceae	*Acacia nilotica / Acacia Arabica*	Babhool	ET	Tolerant	Low[1] NE[13,14]	Low[1,14]		730±70[PS]	A/W[34,35,59]	14.8±0.4 [31,36]		16(1) *
Fabaceae	*Acacia catechu*	Khair	DT	Tolerant	NE[14]	NE[14]	0.44 [33]		A/W[34,59]	7.0 [60]	1.0 [60]	12*
Fabaceae	*Acacia leucophloea*	Safed babool	DT	Tolerant	Low[1]	Low[1]			A/W[34,59]			11*

Fabaceae	*Acacia farnesiana*	Sweet acacia, Needle bush	ES	Tolerant	NE[32]	NE[15]			A/W[34,59]			12*
Fabaceae	*Acacia melanoxylon*	Australian blackwood	ET	Moderately tolerant	NE[32]		12.9 [61]		A/W[34,59]			
Fabaceae	*Acacia pycnantha*	Golden wattle	ET	Tolerant	Low[14]	NE[14]			A/W[34,59]			11*
Fabaceae	*Leucaena leucocephala*	Safed babool	ET	Tolerant	NE[14]	NE[14]	2.8±1.5[17,62]			19.0 [31]		
Fabaceae	*Albizia lebbeck*	Siris	DT	Tolerant	NE[1,14]	Low[1] Moderate[14]	1.72 [51]		A/W[43]	20.7±7.9[23,27,30,31]	2.0 [27,30]	10(-1) *
Fabaceae	*Albizia odoratissima*	Kali siris	DT	Moderately tolerant	Low[13,32]	Moderate[15]						
Fabaceae	*Pithecellobium dulce*	Jangal Jalebi, Madras thorn	ET	Tolerant	Moderate[13,14]	Low[14]			NA/NW[59]	14.6±8.2[22,25,31]	0.0 [22,25]	14(±1) *
Fabaceae	*Prosopis juliflora*	Vilaiti keekar, Velvet mesquite	DS	Tolerant	Low[32]				A/W[43,47]			
Fabaceae	*Butea monosperma*	Palash, Flame of forest	DT	Tolerant	Moderate[13,14]	NE[14]	1.31 [33]		NA/W [35,63]	11.7±1.8[21,22,25,29,30]	3.4±0.9[21,22,25,29,30]	10(1) *
Fabaceae	*Dalbergia sissoo*	Shisham, Indian rosewood	DT	Tolerant	Low[1] High[13,14]	Low[1] NE[14]	1.32±0.5 [33,51,56]	690±70[PS]	A/W[64]	12.3±4.7[21,22,25,27,29,60]	3.8±1.5[21,22,25,27,29,60]	12(±1)

Fabaceae	*Pongamia pinnata / Pongamia glabra*	Pongam tree, Indian beech tree, Karanj	ET	Tolerant	Low[1] High[13,14]	Low[1] Moderate[14]	0.25 [33]	620±60[PS]	A/NW[20,65]	11.9±0.6[23,26,29]	4.0 [29]	5(1)
Fabaceae	*Pterocarpus marsupium*	East Indian kino, Bigasal	DT		High[14]	Moderate[14]						
Fabaceae	*Millettia peguensis / Millettia ovalifolia*	Moulmein rosewood	DT		NE[1]	Low[1]						
Fabaceae	*Robinia pseudoacacia*	False acacia	DT	Tolerant	Moderate[7,66]	Low[7,66]			A/W [4,5]	23.4 ± 12.9 [46,67]		9(-2) *
Fagaceae	*Quercus alba*	White oak	DT	Moderately tolerant	High[10]				A/W [68]			
Fagaceae	*Quercus cerris*	Turkey oak	DT	Tolerant	NE[66]	NE[66]			A/W [5]			13*
Fagaceae	*Quercus coccinea*	Scarlet oak	DT	Tolerant	High[10]				A/W [5]			
Fagaceae	*Quercus petraea*	Sessile oak	DT	Moderately tolerant	Moderate[66] High[69]	NE[66]			A/W [5]			5*
Fagaceae	*Quercus robur*	European oak	DT	Moderately tolerant	High[69]			>400 [9]	A/W [4,5]			
Fagaceae	*Quercus rubra*	Red oak	DT	Sensitive	High[10]				A/W [4,5]			
Ginkgoaceae	*Ginkgo biloba*	Ginkgo	DT	Tolerant	High[11,70]	Moderate[11]			A/W [4,5]			2*
Lamiaceae	*Gmelina arborea*	White teak, Coomb teak, Gumbar	DT		Low[14]	NE[14]	1.51 [56]			12.9±1.5 [29,57]	4.0 [29]	

Lamiaceae	*Tectona grandis*	Sagwan, Teak	DT		Moderate[1,32]	NE[1]	2.2± 0.9[33,51]	200-400[71]	NA/W[18,35]	10.9±3.1[22,25-27,29,31]	2.3±1.0[22,25,27,29]	11(1)
Lauraceae	*Cinnamomum camphora*	Kapoor, Camphor	ET	Tolerant	NE[32]	NE[15]			NA/W[33,72,73]	18.4 [74]	5.0 [74]	19*
Lauraceae	*Cinnamomum tamala*	Tej patta, Bay leaf	ET		High[32]							
Lauraceae	*Cinnamomum zeylanicum*	Cinnamon, Dalchini	ET		NE[13]							
Lythraceae	*Lagerstroemia parviflora*	Crepe myrtle, Pride of India	ES	Tolerant	NE[14]	Low[14]				12.0 [31]		
Lythraceae	*Punica granatum*	Anaar, Pomegranate	DS	Tolerant	Low[32]		2.04 [56]		A/W[4,34]	3.7 [60]	0.0 [60]	
Magnoliaceae	*Magnolia grandiflora*	Him champa	ET	Moderately tolerant	NE[PS]	NE[PS] High[75]	2.19 [76]	890±40[75]	NA/NW[77,78]			15*
Malvaceae	*Bombax ceiba / Bombax malabaricum / Salmalia malabarica*	Sembal, Kapok, Red silk cotton tree	DT	Tolerant	Moderate[13] Low[1,14]	Moderate[1,14,15]	~1.9 [39]	570±60[PS]	A/W[18]	13.2±4.0[29,31,60]	4.5±0.7[29,60]	12(±1)
Malvaceae	*Ceiba petandra*	Silk cotton tree, Kapok	DT	Tolerant	NE[32]	Moderate[15]			A/W[59]			8*
Malvaceae	*Ceiba speciose / Chorisia speciosa*	Kapok, pink flower	DT	Tolerant	NE[1,13]	Low[1] Moderate[15]						

Malvaceae	*Hibiscus rosa-sinensis*	Gurhal	ES	Moderately tolerant	Low[1]	Low[1]	1.26 [79]		A/W[19,20]	15.9±6.6[25,36]	3.0 [25]	11(-2) *
Malvaceae	*Pterospermum acerifolium*	Karnikara, Dinnerplate tree, Kanak champa	DT		Low[1,13]	Low[1]			NA/NW[34]			17*
Malvaceae	*Firmiana simplex / Sterculia urens*	Katira, Gum karaya	DT	Tolerant	NE[32]	NE[15]						
Meliaceae	*Swietenia macrophylla*	Big leaf mahogany	ET	Tolerant	NE[PS]	Moderate[PS]	2.93 [80]	530±50[PS]	NA/NW[81]	13.59 [57]		20
Meliaceae	*Azadirachta indica*	Neem	ET	Tolerant	NE[1,13,14]	Low[1] Moderate[14]	2.3±2.2 [17,33]	960±90[PS]	A/W[18-20,34,41]	16.0±3.4[22-27,29,31]	4.3±1.3[22,25,27,29]	16(-1)
Meliaceae	*Cedrela toona*	Red cedar, Toon	ET	Moderately tolerant	NE[32]	Moderate[15]	1.61 [56]		NA/W[34]	8.2 [60]	4.0 [60]	8*
Meliaceae	*Chukrasia tabularis*	Indian mahogany	DT	Tolerant	NE[13]	Low[15]	~1.7 [39]					
Meliaceae	*Melia azedarach*	Dek, Bakain	DT	Tolerant	NE[13] Low[1]	Low[1]	2.23 [80]		A/W[73]	8.4±2.7[21,60]	3.0±1.4[21,60]	13*
Moraceae	*Artocarpus heterophyllus*	Jack fruit, Kathal	ET	Sensitive	Moderate[14]	Low[15]		449±44 [52]		12.0±2.5[26,27,29,30,31]	4.7±1.2[27,29,30]	
Moraceae	*Artocarpus lacucha*	Monkey jack, Dahu	DT	Moderately tolerant	High[32]					9.3±0.2[22,25]	2.0 [22,25]	
Moraceae	*Ficus benjamina*	Weeping fig	ET	Tolerant	NE[PS] Low[82]	Low[PS] NE[82]	3.6 [83]	287 [84]	A/NW [73,85]	13.7 [74]	3.0 [74]	17
Moraceae	*Ficus aurea*	Strangler fig	ET	Tolerant	Low[1]	Low[1]			NA/NW [85]			20*
Moraceae	*Ficus elastica*	Rubber tree	ET	Tolerant	NE[1]	Low[1]	<2 [86]		A/NW [73,85]	17.4 [74]	5.0 [74]	17*

					Low[32]							
Moraceae	*Ficus retusa*	Chilkan	ET	Tolerant	Low[1]	Low[1]			NA/NW [85]			20*
Moraceae	*Ficus racemosa /Ficus glomerata*	Gular fig	ET	Moderately tolerant	High[1,13]	Low[1]	0.35 [33]		NA/NW [85]	18.6±0.8[27,31]	5.0 [27]	13*
Moraceae	*Ficus religiosa*	Peepal	DDT	Tolerant	High[1,13]	Low[1]		1160±120 [PS]	NA/NW [85]	18.0±5.2[21,22,25-27,29,31,36,38]	5.6±1.1[21,22,25,27,29]	13(-1) *
Moraceae	*Ficus benghalensis*	Banyan, Bargad	ET	Tolerant	Low[1] High[13,14]	Low[1] Moderate[14]	0.78 [33]		NA/NW [85]	18.1±5.9[21,22,25,27,29,31,36,38]	5.6±0.5[21,22,25,27,29]	12(-1) *
Moraceae	*Ficus infectoria*	Pilkhan	ET		High[13,14]	NE[1] Moderate[14]			NA/NW [85]	17.6±6.0[21,22,25,31]	6.0 [21,22,25]	9(-2) *
Moraceae	*Morus alba*	Shahtoot, Mullberry	DT	Tolerant	High[13,14]	Moderate[14]	2.06 [56]		A/W[4,19,34]	8.6±4.9 [31,60]	2.0 [60]	3(1) *
Moraceae	*Streblus asper*	Sewra, Toothbrush tree	ET		High[12] Moderate[32]	Low[12]						
Moringaceae	*Moringa oleifera*	Drumstick tree, Moringa	DT	Tolerant	NE[32]				A/W[18,20,41,63]	15.0±4.2[31,36]		
Myrtacea	*Psidium guajava*	Amrood, Guava	ET	Tolerant	High[1,13,14]	Low[1,14]	0.89 [87]	721 [88]	NA/W[34,41]	16.2±3.9[22,25-27,31,36]	3.7±0.6[22,25,27]	13(-1)
Myrtaceae	*Eucalyptus species*	Eucalyptus	ET		Moderate[1]	Low[1]	1.6 [51]	640 ± 80[75]	A/W[20,43]	13.6±4.6[24,26,89]		9(±1)
Myrtaceae	*Eucalyptus globulus*	Blue gum, Safeda	ET	Tolerant	High[13,14]	Moderate[14]	4.51 [17]		A/W[20,43]	19.0 [36]		6*
Myrtaceae	*Syzygium cumini / syzygium jambolana*	Jamun, Java plum	ET	Tolerant	High[1,13,14]	Moderate[1,14,15]	0.67 [33]	780±80[PS]	A/W[20,34]	12.7±3.0[22,23,25,27,29,30,36,74]	3.7±1.2[22,25,27,29,30,74]	9(±1)

Myrtaceae	*Callistemon lanceolatus*	Bottlebrush	ET	Tolerant	NE[1,32]	Low[1]				5.8 [26]		
Oleaceae	*Nyctanthes arbor-tristis*	Parijat, Harshingar, Night flowering jasmine	ES		NE[PS]	NE[PS]			NA/NW[34]	8.0 [31]		15*
Oleaceae	*Fraxinus excelsior*	European ash	DT	Moderately tolerant	NE[6,66]	NE[6,66]			A/W [4]			10*
Phyllanthaceae	*Phyllanthus emblica/Emblica officinalis*	Indian gooseberry, Amla	DT	Tolerant	NE[1,14]	NE[1,14,15]	0.47 [33]		NA/W[34,47]	10.8±3.4[21,30,31,89]	1.0 [21,30]	15(1) *
Pinaceae	*Abies alba*	Silver European fir	EC	Sensitive	NE [69] Moderate[90]	Moderate[69,90]			NA/W[4,91]			2*
Pinaceae	*Pinus nigra*	Black pine	EC	Tolerant	NE[66]	Moderate[66]	>6 [3]		NA/W[5,91]			13*
Pinaceae	*Pinus pinaster*	Maritime pine	EC	Moderately tolerant	NE[66]	Low [66]	>6 [3]		NA/W[4,5,91]			14*
Pinaceae	*Pinus pinea*	Stone pine	EC	Tolerant	NE[66]	Moderate [66]	>6 [3]		NA/W[4,5,91]			13*
Pinaceae	*Pinus radiata*	Monterey pine	EC	Moderately tolerant	NE[66]	Low [66]	>6 [3]		NA/W[5,91]			14*
Pinaceae	*Pinus sylvestris*	Scots pine	EC	Tolerant	NE[66] Low[69]	Moderate[66,69]			NA/W[5,91]			11*
Platanaceae	*Platanus acerifolia*	London plane	DT	Moderately tolerant	High[2]	NE[2]			A/W[92]			4*
Platanaceae	*Platanus orientalis*	Oriental plane	DT	Moderately tolerant	High[66]	NE[66]			A/W[92,93]	14.9 [94]	5 [94]	5*

Proteaceae	*Grevillea robusta*	Khajur, Silver oak	ET	Moderately tolerant	Moderate[13] NE[1]	NE[1]	5.6±0.4 [17,61]		A/NW [4,73,95]	16.4±6.2[21,23,60]	4.5±0.7[21,60]	13(-2) *
Putranjivaceae	*Putranjiva roxburghii*	Putranjiva, Putijia	ET		NE[PS]	Moderate[PS]	2.17 [96]	940±90[PS]	A/W[20,34,43]	12.4±4.5[21,22,25]	4.0 [21,22,25]	11(±1)
Rhamnaceae	*Ziziphus jujuba*	Ber	DT	Tolerant	Low[13] NE[1,14]	NE[1,14]	2.4 [97]		NA/W[4,18,35]	17.6±6.2[22,23,25,27,29,30,31]	1.8±0.8[22,25,27,29,30]	18(-2) *
Rhamnaceae	*Ziziphus nummularia*	Jhar-beri	S	Tolerant	Low[32]							
Rhamnaceae	*Ziziphus xylopyrus*	Kathber	S	Tolerant	Low[14]	Moderate[14]						
Rosaceae	*Prunus persica*	Aaru, Peach	DT		NE[1]	NE[1]			A/W[98]			9*
Rosaceae	*Crataegus monogyna*	Common hawthorn	DT	Tolerant	NE[6]	Low[6]	>6 [3]		NA/W[5]			15*
Rubiaceae	*Neolamarckia cadamba / Anthocephalus cadamba*	Kadamb	ET	Sensitive	NE[14]	NE[14]	~1.75 [99]	200-400[71]		14.4±4.0[21,23,27,31]	4.5±0.7[21,26]	
Rubiaceae	*Mitragyna parviflora*	Kaim	DT		Low[14]	Low[14]						
Rutaceae	*Aegle marmelos*	Bel	DDT	Tolerant	NE[13,14]	NE[14]			A/W[18,34,43]	13.4±3.1[21,24,29,30]	3.0±1.0[21,29,30]	11(±1) *
Rutaceae	*Citrus limon*	Nimboo, Lemon	ES	Sensitive	Low[1] NE[13]	Low[1]			NA/NW[34,47]	12.3±2.4[24,26,31,89]		14(-1) *
Rutaceae	*Citrus reticulata*	Santara, Mandarin orange	ES	Tolerant	NE[13]	Low[100]			NA/NW[34,43]			17*

Rutaceae	*Citrus sinensis*	Sweet orange	ET	Tolerant	NE[13]	Moderate[15]	4.5±0.4 [17,101]		NA/NW[34,47]	8.8 [28]	1.0 [28]	16*
Rutaceae	*Murraya koenigii*	Curry leaves, Meethi neem	DS	Tolerant	NE[13,14]	High[14]			NA/NW[34]	8.4±1.3[36,60,89]	2.0 [60]	13*
Rutaceae	*Murraya paniculata*	Orange jasmine	ES	Tolerant	NE[14]	Moderate[14]	1.69 [33]		A/W[64]	14.3±4.3[25,27]	3.0 [25,27]	9(±1) *
Salicaceae	*Populus deltoides*	Poplar	DT	Tolerant	High[PS,32,102]	NE[PS,102]	2.89 [103]	520±50[PS]	A/W[20,43]	7.5 [60]	3.0 [60]	10
Salicaceae	*Populus nigra*	Black poplar	DT	Sensitive	High[6,10,104]	Moderate[6,10,104]			A/W [4, 5]			-1*
Salicaceae	*Salix spp.*	White willow	DT	Sensitive	High[6,104]	Low[6,104]			A/W [4]			3*
Sapindaceae	*Dodonaea viscosa*	Vilayti-menhdi, Hopseed bush	ES	Tolerant	NE[1]	Low[1]			A/W[59]			11*
Sapindaceae	*Schleichera oleosa*	Macassar oil tree, Kusam	DT		Low[1]	Low[1]						
Sapindaceae	*Schleichera trijuga*	Macassar oil tree, Kusam	DT		Moderate[32]							
Sapindaceae	*Sapindus emarginatus*	Reetha, Soapnut tree	ET		Low[32]							
Sapotaceae	*Mimusops elengi*	Maulsari	ET		NE[PS,105] High[32]	Low[PS] NE[15]	1.17 [33]	240±20[PS]	A/W[18,41,59]	15.1±3.3[21,26,29,30,57]	4.7±1.2[21,29,30]	14(-2)

Sapotaceae	*Manilkara zapota / Achras zapota*	Chikoo	ET	Tolerant	High[13]					11.5 [26]		
Sapotaceae	*Madhuca longifolia / Madhuca latifolia*	Mahua	ET	Tolerant	High[14,32]	NE[14] Low[15]	2.50 [54]		A/W[20,34]	12.2±3.5[21,22,23,27,29,30,31,89]	3.5±1.8[21,22,25,27,29,30]	11(±1) *
Sapotaceae	*Manilkara hexandra*	Rayan, Khirni, Ceylon ironwood	ET	Tolerant	NE[13]	Moderate[15]						
Simaroubaceae	*Ailanthus altissima*	Tree of heaven	DT	Tolerant	NE[14]	Low[14]			A/W [4,20]	14.4 [94]	3.0 [94]	12*
Simaroubaceae	*Ailanthus excelsa*	Tree of heaven	DDT	Tolerant	NE[32]	Moderate[15]	1.73 [106]		A/W [4,20,34,64]	11.0 [21]	4.0 [11]	6*
Sterculiaceae	*Pterygota alata / Sterculia alata*	Pahari odal	ET		NE[13]	NE[15]						
Tiliaceae	*Tilia cordata*	Small-leaved lime	DT	Sensitive	NE[2]	NE[2]	3.9 [8]		A/W [4,5]			11*
Ulmaceae	*Ulmus pumila*	Siberian elm	DT	Tolerant	NE[7]	NE[7]			A/W [4,5]	21.7±1.3 [67]		16*
Verbenaceae	*Lantana camara*	Lantana weed, Raimuniya	ES	Tolerant	High[1]	Moderate[1]			A/W[18,34,41,43]	9.4±2.1[23,89]		1*

References are as follow:

PS stands for present study, [1](Padhy and Varshney, 2005), [2](Fitzky et al., 2019), [3](Hirons and Sjöman, 2019), [4](Cariñanos and Casares-Porcel, 2011), [5](Barwise et al., 2020), [6](Owen et al., 2003), [7](Jing et al., 2020), [8](Grote et al., 2016), [9](Morecroft and Roberts, 1999), [10](Geron et al., 2001), [11](Corchnoy et al., 1992), [12](Klinger et al., 2002), [13](Varshney and Singh, 2003), [14](Malik et al., 2018), [15](Singh et al., 2011), [16](Rajan et al., 2001), [17](Koricho et al., 2020), [18](Chakraborty et al., 2016), [19](Chauhan and Goyal, 2006), [20](Bhattacharya et al., 2018), [21](Shannigrahi et al., 2004), [22](Prajapati and Tripathi, 2008), [23](Das and Prasad, 2010), [24](Mohammed et al., 2011), [25](Pathak et al., 2011), [26](Krishnaveni et al., 2014), [27](Pandey et al., 2015), [28](Anake et al., 2018), [29](Sahu et al., 2020), [30](Karmakar et al., 2021), [31](Singh et al., 1991), [32](Singh et al., 2008), , [33](Rane et al., 2017), [34](Sahney and Chaurasia, 2008), [35](Pohekar and Kalkar, 2016), , [36](Bharti et al., 2017), [37](Endres, 2007), [38](Kamble et al., 2021), [39](Mo et al., 2014), [40](Hussain et al., 2014), [41](Mandal et al., 2008), [42](Kaur and Nagpal, 2017), [43](Singh and Shahi, 2008), [44](Mäenpää et al., 2011), [45](Ziemianin et al., 2021), [46](Nadgórska–Socha et al., 2017), [47](Satheeshkumar and Vittal, 1998), [48](Tor-ngern and Leksungnoen, 2020), [49](Molnár et al., 2020), [50](Liu et al., 2015), [51](Biswas et al., 2014), [52](Song et al., 2020), [53](Gargi and Sinha, 2017), [54](Darmayanti and Fiqa, 2017), [55](Hu et al., 2016), [56](Thakur and Kaur, 2001), [57](Sulistijorini et al., 2008), [58](Boral et al., 2004), [59](Mishra et al., 2002), [60](Kashyap et al., 2018), [61](Erskine et al., 2005), [62](Wolfe and Van Bloem, 2012), [63](Sermin et al., 2019), [64](Mondal et al., 1998), [65](Raju and Rao, 2006), [66](Aydin et al., 2014),[67](Liu et al., 2008), [68](Loria et al., 1989), [69](Moukhtar et al., 2006), [70](Guenther et al., 1996), [71](Chaturvedi et al., 2013), [72](Wu et al., 2006), [73](Yang et al., 2015), [74](Rai and Mandal, 2020), [75](Noe et al., 2008), [76](Li et al., 2017), [77](Thien, 1974), [78](Cariñanos et al., 2019), [79](Baille et al., 1994), [80](Jhou et al., 2017), [81](Novick et al., 2003), [82](Wang et al., 2005), [83](Neinavaz et al., 2016), [84](Hao et al., 2010), [85](Eisikowitch and Ghara, 2017), [86](Koedsin and Yasen, 2016), [87](Mushtaq et al., 2019), [88](Assis et al., 2015),[89](Bakiyaraj and Ayyappan, 2014), [90](Pokorska et al., 2012), [91](Szczepanek et al., 2017), [92](Vrinceanu et al., 2021), [93](Pazouki et al., 2008), [94](Hatamimanesh et al., 2021), [95](Kalinganire et al., 2001), [96](Wahala et al., 2013), [97](Chen et al., 2014), [98](Jiang et al., 2015), [99](Shukla and Ramakrishnan, 1984), [100](Fares et al., 2011), [101](Nirgude et al., 2016), [102](Evans et al., 1982), [103](Murthy et al., 2005), [104](Owen et al., 1998), [105](Geron et al., 2006), [106](Jat et al., 2010)

3.3.2 Selection criteria of plant species

In this study, conducted between April 2018 and February 2020, I screened 14 plant species commonly planted along roads in India for their VOC potential in different seasons. All plants were growing under open environment conditions and were aged between 5 to 7 years. Six of the selected species, namely *Putranjiva roxburghii*, *Diospyros blancoi*, *Swietenia macrophylla, Nyctanthes arbor-tristis, Plumeria alba,* and *Ricinus communis,* have never been screened for BVOC emission prior to our study, but are frequently planted in urban India, while contradictory results have been reported for the emission potential *Mimusops elengi* in prior screening studies (Geron et al., 2006; Singh et al., 2008). For *Magnolia grandiflora* the monoterpene emission potential had been reported previously (Noe et al., 2008) but our study is the first to report isoprene emission potential. *Ficus benjamina* (Wang et al., 2005) had previously been studied only under static sampling. Five species reported in this study, namely *Mangifera indica, Polyalthia longifolia, Kigelia pinnata, Populus deltois* and *Tecoma stans,* have been studied by other authors (Varshney and Singh, 2003; Padhy and Varshney, 2005; Singh et al., 2008; Singh et al., 2011; Malik et al., 2018), but I studied their emissions under a larger range of environmental variables to record the diurnal profile of emission fluxes and the seasonality of emissions.

Trees were identified with the help of taxonomic keys, and all the herbarium samples were verified with the herbarium samples present in the herbarium of the Department of Botany, Panjab University Chandigarh.

Vegetation sequesters ozone (Emberson et al., 2000) and certain ozone precursors such as NO_2 (Chaparro-Suarez et al., 2011) through stomata and, therefore, acts as a sink for atmospheric ozone and ozone precursors. This ozone uptake potential of urban vegetation is governed by leaf stomatal conductance. To include this parameter into the AQII, stomatal conductance measurements are required. Prior to our study, the stomatal conductance of only 12 out of 149 species had been reported and this lack of observations severely restricts our ability to calculate AQII. In this study, I screen 15 species accounting for some of the most frequently planted species for their stomatal conductance. These include *Mangifera indica*, *Putranjiva roxburghii, Swietenia macrophylla, Populus deltoids, Polyalthia longifolia, Mimusops elengi, Acacia arabica, Azadirachta indica, Bombax ceiba, Cassia fistula, Dalbergia sissoo, Ficus religiosa, Pongamia pinnata, Syzygium cuminii* and *Terminalia arjuna.*

3.3.3 Sampling methodology and flux calculation

To measure BVOC emission flux rate of plant individuals, I adopted a dynamic branch cuvette method, considered suitable for highly reactive and volatile compounds. I used the same setup as used by others (Ortega et al., 2008; Vettikkat et al., 2020). Briefly, I used polyvinyl fluoride bags (Tedlar® bags) as enclosure of effective volume 54L. The system is designed as dynamic cuvette and supplied with dry, ozone and VOC free zero air at a flow rate of 30 L min^{-1} using mass flow controller and a high-capacity vacuum pump (ModelN145.1.2AT.18, KNF, Germany). Ozone values below detection limits were measured and the proper functioning of the ozone trap was validated using a portable ozone monitoring sensor (PO3M; 2BTechnologies, Colorado, US). For continuous temperature and relative humidity recording within the cuvette, I used a portable temperature humidity sensor (HTC Easylog, India). Ambient temperature, humidity, PAR, and soil moisture (SM) next to the tree were measured with a portable meteorological station by Decagon (a portable setup equipped with VP-RH and temperature sensor, QSO-S PAR sensor, and GS1 soil moisture sensor, Decagon Devices, USA) and Campbell Scientific (portable sensors equipped with CS215 RH and temperature sensor, PQS1 PAR sensor, CS655 soil moisture sensor, Campbell Scientific Inc.).

Furthermore, above canopy temperature, relative humidity, wind speed, wind direction, global radiation, tropospheric ozone mixing ratios and $PM_{2.5}$ were monitored 20m above ground level at the IISER Mohali atmospheric chemistry facility (30.667◦N–76.729◦E, 310 m.a.s.l.) in Punjab, India (Sinha et al., 2014) using MetOne meteorological sensors, UV photometry (Thermo Fisher Model 49i) and beta attenuation technique (Thermo Fisher Model 5014i Beta), respectively.

Online measurement of isoprene and monoterpene was performed wherever feasible. Online measurements were supplemented by offline sampling to increase the number of species covered and the number of replicates of each species. For online sampling, output air from the cuvette was introduced into the high-sensitivity proton transfer reaction mass spectrometer (PTR-MS) (HS Model 11-07HS-088; Ionicon Analytik Gesellschaft, Austria), a detailed description can be read elsewhere (Sinha et al., 2014). For offline measurements, samples were collected into a passivated 6 L steel canisters (SilcoCan Restek, USA) and later analyzed. A more detailed explanation of setup and measurement can be found in previously published work (Vettikkat et al.,2020). At the end of each experiment set, I plucked the leaves from sampled branch to measure total leaf area and dry leaf weight.

Leaf level emission flux was calculated in μg m^{-2} s^{-1} using equation (1) (Sinha et al., 2007)

$$`\mathrm{Flux} = \frac{Q}{A} * \left(m_{in,VOC} - m_{out,VOC}\right) * \frac{M_V}{V_m} \tag{1}$$

Where, Q is the flow rate of input air in m^3s^{-1}, A is the area of leaves, $m_{in,\ voc}$ and $m_{out,\ voc}$ are VOC mixing ratio in background air and output air, Mv is the molecular weight of the VOC in g mol^{-1} and Vm is the molar gas volume in m^3mol^{-1}. To compare values with already reported, I normalized the hourly emission rate to dry leaf weight.

I classify species based on their isoprene emission potential and consider a species to be a high isoprene emitter, if the normalized flux is ≥25 μg g^{-1}(dry leaf weight) h^{-1}, a moderate emitter, if it is between 10 ≤ to < 25 μg g^{-1} h^{-1}, a low emitter, if it is between 1 ≤ to < 10 μg g^{-1} h^{-1}, and a non-emitter, if the flux is < 1 μg g^{-1} h^{-1}. For monoterpene, ≥ 10 μg g^{-1} h^{-1} is considered as high, 1 ≤ to < 10 μg g^{-1} h^{-1} moderate, <1 μg g^{-1} h^{-1} low and non-monoterpene emitting species, if flux is negligible or below detection limit (BDL).

I conducted leaf porometer measurements of stomatal conductance using SC-1 leaf porometer from Decagon Devices, USA (accuracy: ± 10%, resolution: 0.1 $mmolm^{-2}s^{-1}$). A total of 23194 individual leaf porometer measurements spanning all seasons were taken between December 2016 and March 2021 on 15 different species. I classify species based on their capacity to sequester air pollutants through stomatal uptake. I use the maximum stomatal conductance for water vapor (g_{stomax} in $mmolm^{-2}s^{-1}$) of each species as a proxy for air pollution uptake potential, and classify them into species having a high (g_{stomax} > 400 $mmolm^{-2}s^{-1}$), medium (g_{stomax} 200 - 400 $mmolm^{-2}s^{-1}$), and low (g_{stomax} < 200 $mmolm^{-2}s^{-1}$) capacity to sequester air pollutants.

3.3.4 Calculation of the SOA formation potential, ozone formation potential, ozone uptake potential and $PM_{2.5}$ dry deposition flux to the leaf surface

Stomatal ozone uptake for the year 2018 was modelled using the DO_3SE model (Emberson et al., 2000) by means of the photosynthetic equation (2) (Ball J.T. et al., 1987; Nikolov et al., 1995), in which G_{sto} is stomatal ozone flux ($mmolm^{-2}s^{-1}$), G_{min} is the measured daytime minimum stomatal conductance to ozone ($mmolm^{-2}s^{-1}$), A_n is net assimilation rate ($\mu molm^{-2}s^{-1}$), m defines species-specific sensitivity of stomatal conductance to net assimilation, h_b is leaf surface relative humidity in decimal fraction, C_b represents leaf surface CO_2 concentration ($\mu molmol^{-1}$) and f_{phen} phenology function.

$$G_{sto} = (G_{min} + m * A_n * \frac{h_b}{c_b}) * f_{phen} \quad (2)$$

The DO_3SE model was initialized with hourly meteorological observations and ozone mixing rations measured during the year 2018 at the IISER Mohali atmospheric chemistry facility. Ozone formation potential (OFP) was calculated using equation (3). In this equation, E_{iso} and E_{mono} stand for the measured foliage level emission fluxes of isoprene and monoterpene, respectively, and MIR_{iso} and MIR_{mono} represent the maximum incremental reactivity under high NO_x conditions, considered to be 10.61 for isoprene and 4.04 for monoterpene (Carter, 1994, 2010).

$$\mathrm{OFP}_{(\mathrm{iso+mono})} = (\mathrm{E}_{\mathrm{iso}} * \mathrm{MIR}_{\mathrm{iso}}) + (\mathrm{E}_{\mathrm{mono}} * \mathrm{MIR}_{\mathrm{mono}}) \quad (3)$$

Secondary organic aerosol formation potential (SOAFP) in $\mu gm^{-2}s^{-1}$ was calculated using equation (4) in terms of average SOA yield. I consider the percentage SOA yield of 5.3% for isoprene (Chan et al., 2010) and 11% for monoterpene (α pinene) under high NOx conditions (Ng et al., 2007) for our calculations.

$$\mathrm{SOAFP}_{(\mathrm{iso+mono})} = (\mathrm{E}_{\mathrm{iso}} * \%\mathrm{yield}_{\mathrm{iso}}) + (\mathrm{E}_{\mathrm{mono}} * \%\mathrm{yield}_{\mathrm{mono}}) \quad (4)$$

The PM2.5 dry deposition flux in $\mu gm^{-2}s^{-1}$ was calculated using equation (5), wherein ($MC_{PM2.5}$) stands for the measured ambient mass concentration of $PM_{2.5}$, and V_d - for the dry deposition rate of $PM_{2.5}$ particulate matter. To calculate V_d, I followed equation (6) (Zhang and He, 2014).

$$PM_{2.5}\ dry\ deposition\ rate = \mathrm{MC}_{PM_{2.5}} * V_d \quad (5)$$

$$V_d = V_g + \frac{1}{R_a + \frac{1}{V_{ds}}} \quad (6)$$

$$V_{ds} = a * u_*$$

Herein, V_g, is gravitational settling velocity, R_a represents canopy aerodynamic resistance, and a is empirical constant for different land use categories. I use the value 4.3 x 10^{-3} for constant 'a'. This parameterization has been recommended for evergreen needleleaf trees, evergreen broadleaf trees, deciduous needleleaf trees, deciduous broadleaf trees, drought deciduous trees, mixed wood forests, and urban landscapes (Zhang and He, 2014). u^* is friction velocity of the wind. R_a and u^* are taken from the output of the DO_3SE model run for *Mangifera indica* and *Polyalthia longifolia.*

3.4 Results and Discussion

3.4.1 Evaluation of the suitability of tree species for urban plantations using the new AQII

Table 3.1 lists a total of 149 trees and shrubs for which either the isoprene emission potential, monoterpene emission potential, ozone uptake potential, allergy potential of pollen, the API or APTI have been reported in the peer reviewed literature or studied in the present study. 119 of these are native and exotic species frequently planted in India. The list also includes 30 species from other parts of the world for which the APTI has been reported in the literature. Till date the tree species for any urban plantation programs in India are selected on the basis of two indices: the APTI quantifies how well a tree will survive in a polluted environment, and the API (Prajapati and Tripathi, 2008; Sahu et al., 2020; Shannigrahi et al., 2004) evaluates how desirable the tree is for urban plantation. The API considers factors such as survival in the polluted environment and how much pollution a tree potentially sequesters through dry deposition based on canopy structure, height, leaf surface texture, and leaf area index. Unfortunately, the index also considers the economic value of products that can be obtained from the tree and fails to consider BVOC emissions.

Two types of species stand out in this table and are discussed in detail in this manuscript. The first type includes species with a high API score but high ozone and SOA precursor emissions. Such species are currently considered to be highly suitable for urban plantation, but are likely to fuel secondary pollution formation. *Mangifera indica*, *Ficus benghalensis* and *Ficus infectoria* have an API >5 (Anake et al., 2018; Karmakar et al., 2021; Pandey et al., 2015; Pathak et al., 2011; Prajapati and Tripathi, 2008; Sahu et al., 2020; Shannigrahi et al., 2004) and have been identified as both prolific isoprene and monoterpene emitters (Klinger et al., 2002; Malik et al., 2018; Padhy and Varshney, 2005; Singh et al., 2011; Varshney and Singh, 2003). *Mangifera indica* is consistently among the most frequently planted species across Indian cities. This is why I chose it as illustrative example for this group of high BVOC emitters in the current study (Khera et al., 2009; Jaganmohan et al., 2018), 2009).

The second group is much larger and comprises of species which have low isoprene and monoterpene emission fluxes (Malik et al., 2018; Padhy and Varshney, 2005; Singh et al., 2011; Singh et al., 2008; Varshney and Singh, 2003; Wang et al., 2005). It can be subdivided into two sub-groups, namely species with low BVOC emissions that have a below average API score of ≤ 3 (Hatamimanesh et al., 2021; Karmakar et al., 2021; Kashyap et al., 2018; Kaur and Nagpal, 2017; Krishnaveni et al., 2014; Mohammed et al., 2011; Pandey et al., 2015; Pathak et al., 2011; Prajapati and Tripathi, 2008; Sahu et al., 2020; Shannigrahi et al., 2004), and species with low BVOC emissions that have an above average API score of ≥ 4 (Karmakar et al., 2021; Kaur and Nagpal, 2017; Pandey et al., 2015; Pathak et al., 2011; Prajapati and Tripathi, 2008; Rai and Mandal, 2020; Sahu et al., 2020; Shannigrahi et al., 2004). Species with low BVOC emissions and below average API score are often avoided during plantation drives, but are likely to have a positive air quality impact. *Terminalia bellirica*, *Nerium indicum*, *Kigelia pinnata DC*, *Ricinus communis*, *Tamarindus indica*, *Senna siamea*, *Cassia fistula*, *Acacia catechu*, *Albizia lebbeck*, *Hibiscus rosasinensis*, *Melia azedarach*, *Ficus benjamina*, *Phyllanthus emblica*, *Ziziphus jujube*, *Aegle marmelos* and *Ailanthus altissima* belong to this group. These species should be considered for plantation more frequently. Species with low BVOC emission and above average API score of ≥ 4 are already favored during planation drives. *Polyalthia longifolia*, *Alstonia scholaris*, *Acacia auriculiformis*, *Cinnamomum camphora*, *Azadirachta indica*, and *Ficus elastica* belong to this group. *Polyalthia longifolia* happens to be one of the most abundant trees found in many Indian cities (Jaganmohan et al., 2018; Khera et al., 2009). Hence, I chose *Polyalthia longifolia* as illustrative example for this group in the current study.

In this study, I contrast the impact of two species from opposite ends of the BVOC emission scale, namely *Mangifera indica* and *Polyalthia longifolia*, with an API of 5.9 ± 0.9 and 4.8 ± 1.0, on urban air quality during summer season. I chose summer because at our site the air quality standard for ozone (Kumar et al., 2016) and particulate matter (Pawar et al., 2015) is exceeded on > 90% and ~80%, respectively, for all summer days. *Polyalthia longifolia*, is a non isoprene emitter and a low monoterpene emitter during most seasons, while *Mangifera indica* is a high isoprene and moderate monoterpene emitter throughout the year. *Polyalthia longifolia* has moderate monoterpene emissions in early summer, when the old leaves turn yellow and fall, while the new leaves emerge (data for this period included in Figure 3.),

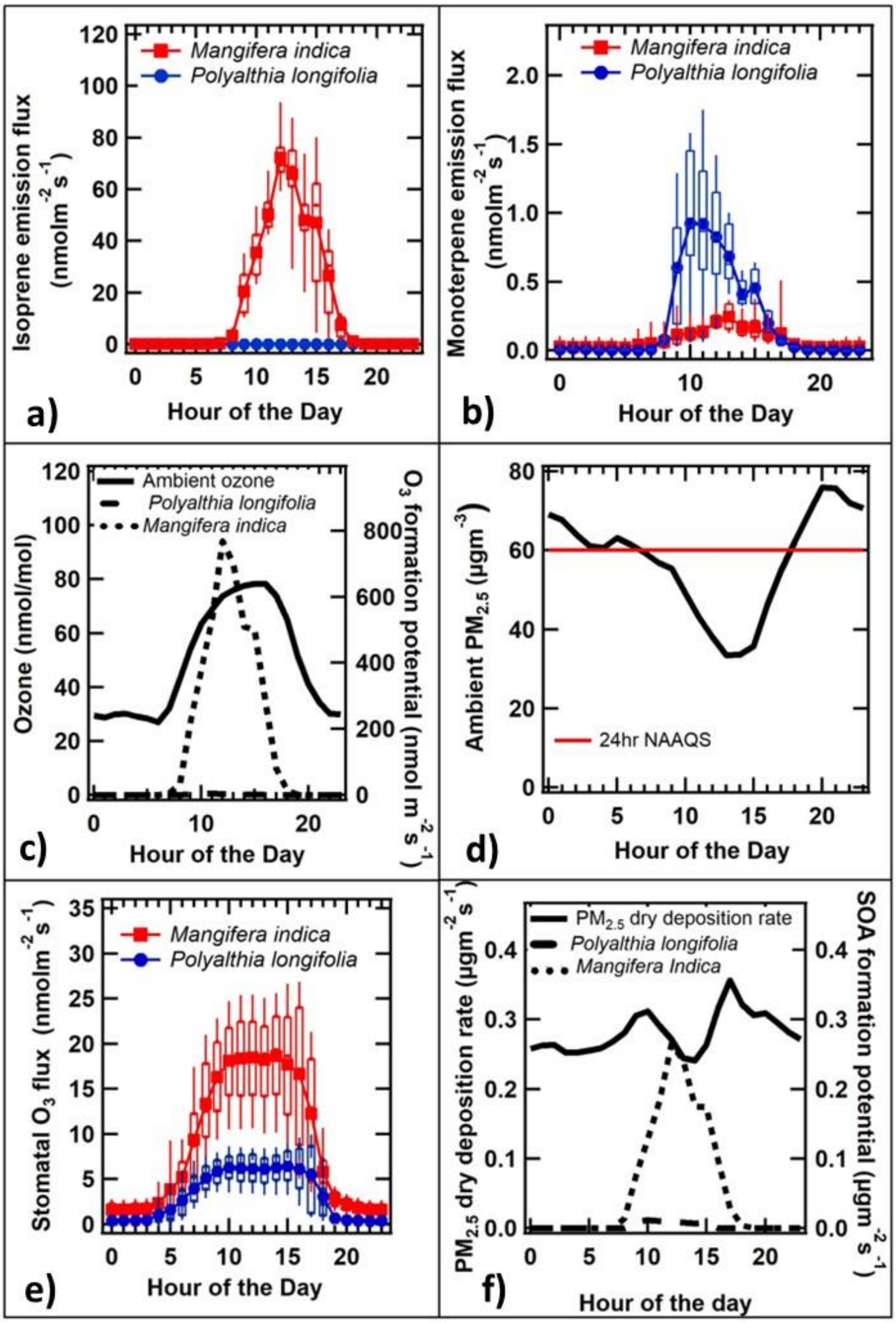

Figure 3.2:a) and b) Isoprene and monoterpene emission flux of *Mangifera indica* and *Polyalthia longifolia*. Figures c) and d) show the seasonal average diurnal profile of the tropospheric ozone mixing ratios and $PM_{2.5}$ mass loading, respectively, during summer season (March to June 2018) at our experimental site. The 24-h air quality standard for $PM_{2.5}$ is marked with a red line in Figure d). Figure c) also shows the ozone formation potential of the BVOC emissions from the summer time ozone precursor emissions of these two species in a NOx rich environment in nmol m^{-2} s^{-1}. Figures e) and f) show the stomatal uptake of tropospheric ozone and potential dry deposition loss rate of $PM_{2.5}$ to the leaf surface (solid lines) for the same two species. Figure f) also shows the SOA formation potential for both species in a NOx rich environment (dashed lines).

but continues to be a non isoprene emitter throughout the year. Both have a high API and are equally recommended for urban plantation at present.

Figure 3.2a shows the isoprene emission flux of both species during summer season in nmol per square meter of active leaf surface area per second, while Figure 3.2b shows their monoterpene emission flux in the same units. Figure 3.2c show the seasonal (March-June) average diurnal profile of the tropospheric ozone mixing ratios, and the ozone formation potential of the VOC emissions. It is clear that the impact of both species on ozone formation differs by two orders of magnitude when these species are planted in a NOx surplus roadside environment. *Polyalthia longifolia* sequesters more ozone through its stomata (Figure 3.2e) than can be formed from its precursor emissions (Figure 3.2c) even in summer. *Mangifera indica* VOC emissions, on the other hand, contribute to tropospheric ozone formation, as the ozone formation potential of its precursor emission flux is 4 times larger than the stomatal uptake during peak daytime. Figure 3.2d shows the seasonal (March-June) average PM2.5 mass loadings and the 24-hr average ambient air quality standard for $PM_{2.5}$. Figure 3.2f shows the dry deposition flux of $PM_{2.5}$ to the leaf surface and the SOA formation potential of the VOC emissions. It is clear that currently particulate matter mass loadings at our site are so high, that plant precursor emissions hardly add to the overall burden. At present, the dry deposition flux of particulate matter to the leaf surface (Figure 3.2f) is larger than the SOA formation potential for both species. However, equation 5 shows that this dry deposition flux depends on the particulate matter mass loadings and deposition velocity. In a relatively clean environment with $< 10 \mu gm^{-3}$ $PM_{2.5}$, the net impact of *Mangifera indica* on ambient particulate matter calculated with identical emission fluxes and meteorological parameters, using the same set of equations (equation 4 to equation 6), would switch towards being dominated by its SOA precursor emissions, rather than the leaves dust uptake. In India at present, PM pollution is high and most urban planners are aware about the adverse impact of particulate matter pollution, but know little about the adverse impact of trace gasses such as ozone and about pollen allergies. Hence, urban tree plantation is currently optimized towards maximizing particulate matter dry deposition fluxes only.

I believe that this traditional index has outlived its suitability for evaluation trees within the context of urban plantation programs and should be replaced by an index, which captures the air quality impact more holistically and neglects economic considerations. Hence, I propose the following modifications to the existing API index and introduce a new AQII. Table 3.2 lists the parameters accounted for in the new AQII. It includes the grading criteria. For each parameter a species can score at most three positives (+++) or three negatives (---) based on how its properties will impact air quality. The total score is calculated by adding one to the species score for each + sign and subtracting one from the species score for each – sign. The maximum possible AQII value is 29 and a minimum possible score is -7.

1) I propose to remove economic criteria from the consideration and base our assessment purely on the air pollution impact of the tree under study.

2) The original API considers deciduous trees as undesirable, because of the inconvenience leaf litter causes to municipal authorities. However, in some urban locations, peak pollution events are driven by wintertime fog (Hakkim et al., 2019) and heating related biomass burning emissions. In such locations, winter deciduous trees, which allow better sunlight penetration during cold season, have the potential to reduce heating related emissions and fogginess. At the same time, winter deciduous trees will reduce the urban heat island and sequester pollutants during the hot and dry season. Hence, they should not be considered as a-priory undesirable in all locations and I remove the negative score for winter deciduous trees from our new AQII.

3) Dry deciduous trees which shed their foliage in summer, are undesirable in all locations, as both ozone and particulate matter pollution tends to be higher during the hot and dry season of the year (Kumar et al., 2016; Pawar et al., 2015). Trees which lose their leaves during this season fail to reduce both pollution and the urban heat island when it matters most, and increase summertime fire risk through the production of dry biomass. I, therefore, introduce a negative score for dry deciduous trees only.

4) The present API awards negative marks to short trees and shrubs with small canopies without considering that these may be the only choice for certain locations (e.g., under electricity lines). This negative score is not warranted, as recent research has shown, that short vegetation elements such as green walls and hedges between the road and the sidewalk reduce the particulate matter exposure of pedestrians more efficiently than tall alley trees (Vos et al., 2013). Alley trees tend to reduce wind speeds and, therefore, the ventilation within the street canyon, which results in hyperlocal pollution accumulation (Vos et al., 2013). In our new index, I remove the negative score for short vegetation.

5) Leaves with smooth surfaces, which generally record lower PM removal rates (Zhang et al., 2018) are awarded a negative rating in the API index without considering that they still provide

a surface for dry deposition (Ottelé et al., 2010). In our new index I remove the negative score for smooth leaves but award a positive rating to leaf surface roughness.

6) Isoprene is a highly reactive ozone precursor (Churkina et al., 2015; Churkina et al., 2017). Hence, the isoprene emission potential must be included in any air quality related performance index to evaluate the impact of the selected tree species on the secondary ozone formation. I consider high (---) and moderate (--) isoprene emitters to be detrimental to urban air quality, while I consider low emitters (++) and non-emitters (+++) to be beneficial.

7) Monoterpene emissions have an impact on secondary aerosol formation and need to be included to quantify the impact of the proposed tree selection on secondary particulate matter pollution formation (Carlton et al., 2009). I consider high (---) and moderate (--) monoterpene emitters are to be detrimental to urban air quality, while I consider low emitters (++) and non-emitters (+++) to be beneficial.

8) Trees can release primary biological particles in the form of pollen and some pollen particles are wind borne and highly allergenic. Such emissions significantly influence human wellbeing and need to be considered while evaluating the suitability of trees for urban plantation. I consider species with pollen that are known allergens to have a large negative impact (---), if they are air pollinated and windblown and affect a substantial area (Toh et al., 2012). Trees, whose pollen are known allergens but which are insect or bird pollinated, are considered to have only a localized negative impact (--). Trees whose pollen grains are not known allergen are considered to have a negative impact on air quality (-), only if they are air pollinated and windblown over a large area, as the pollen contributes to $PM_{2.5}$ and PM_{10} mass loadings directly. Trees, whose pollen grains are not known allergen, and which are insect, bat or bird pollinated, are considered to have a positive pollen impact score (+++).

9) Pollution uptake of gaseous pollutants such as tropospheric ozone (Emberson et al., 2000) and nitrogen dioxide by vegetation is governed by stomatal uptake (Gessler et al., 2000; Chaparro-Suarez et al., 2011). The maximum stomatal conductance for water vapor is considered to be a good proxy for the pollution sequestration potential through stomatal uptake. Species with a high (++) and moderate (+) stomatal conductance are considered to be beneficial to urban air quality, while species with a low stomatal conductance are not helpful in sequestering gaseous pollution. A high stomatal conductance during the hot and dry season is

particularly beneficial for combatting the urban heat island effect (+++) and sequestering ozone and its precursor during a time of the year when photochemical ozone formation is highest (Churkina et al., 2015; Churkina et al., 2017).

10) Climate change, increasing air temperature, and thus drought conditions are emerging threats to forests (Peng et al., 2011). Where urban forests planted to mitigate urban air pollution, an arid environment can impose constraints. Drought and heat stress limit tree growth, can increase BVOC emissions (Peñuelas and Staudt, 2010) and can result in tree death (Anderegg et al., 2012). Hence, drought sensitive trees can add to the potential fire burden and may contribute little towards alleviating the urban heat island when it is most required. Drought tolerant species should, therefore, be preferred for urban plantation and are awarded three positive scores (+++) in our AQII. In well planned urban plantation schemes irrigation with tertiary treated water could be considered to reduce drought impact and permit plantation of drought sensitive species.

Table 3.2: Grading character and grading criteria considered for species air pollution tolerance efficiency, air quality improving efficiency and air quality impact.

Grading character	Pattern of assessment	Grade allotted
Air pollution tolerance index	< 12 12 to 15 >15	+ ++ +++
Tree habit	Small Medium Large	+ ++ +++
Canopy structure	Sparse/Irregular/Globular Spreading crown/open/semi dense Spreading dense	+ ++ +++
Leaf area Index (LAI)	Low (< 2) Medium (2-4) High (>4)	+ ++ +++
Leaf texture (laminar structure)	Smooth Coriaceous	+ ++
Type of tree	Dry deciduous tree	---
OFP ∝ Isoprene emission potential (IEP)	High isoprene emissions ($\geq$25 μg g^{-1} h^{-1}) Medium isoprene emissions (10$\leq$to<25 μg g^{-1} h^{-1}) Low isoprene emissions (1$\leq$to<10 μg g^{-1} h^{-1}) Non-isoprene emitting species (<1 μg g^{-1} h^{-1})	--- -- ++ +++
SOAFP ∝ monoterpene emission potential (MEP)	High monoterpene emissions ($\geq$10 μg g^{-1} h^{-1}) Medium monoterpene emissions (1$\leq$to<10 μg g^{-1} h^{-1}) Low monoterpene emissions (<1 μg g^{-1} h^{-1}) Non-monoterpene emitting species (<0.1 μg g^{-1} h^{-1} or below detection limit (BDL))	--- -- ++ +++
OUP ∝ maximum stomatal conductance (MSC)	High stomatal conductance during hot and dry season High Medium Low	+++ ++ +
Pollen impact on allergic and asthmatic patients (PI)	Known allergen & windblown over large area Known allergen & pollen hardly spread No known allergies & windblown over large area No known allergies & pollen hardly spread	--- -- - +++

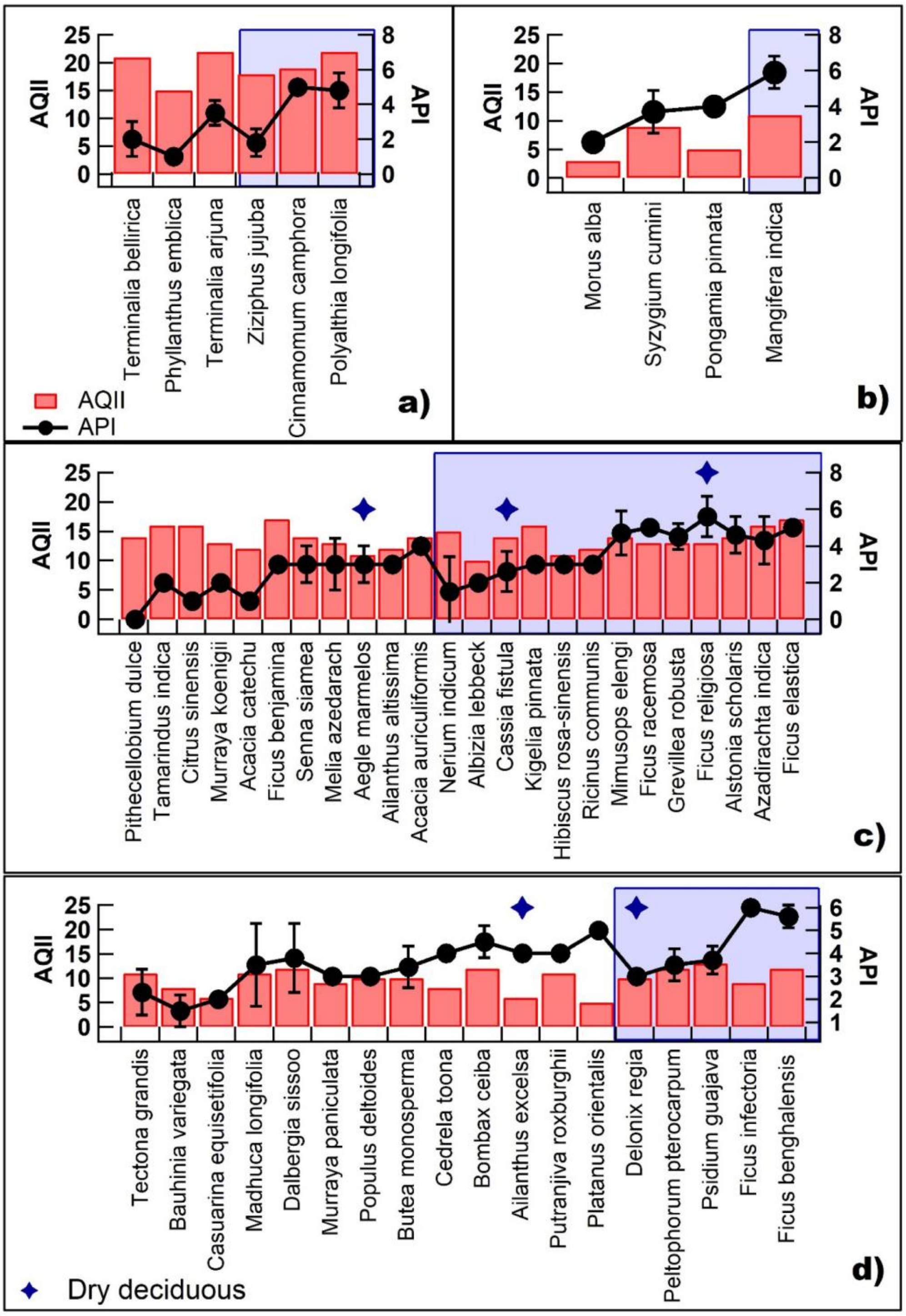

Figure 3.3**:** Comparison between new air quality impact index (AQII) and reviewed anticipated performance index (API). Total of 52 species were divided into four categories: a) Species which are non or low isoprene emitters and non or low monoterpene emitters with non-allergenic pollen. b) Species which are moderate to high isoprene and moderate to high monoterpene emitters, with allergenic pollen. c) Species with a negative score for either one of the three, isoprene emission potential or monoterpene emission potential or pollen impact c) Species with a negative score for two of the three, isoprene emission potential, monoterpene emission potential or pollen impact. The blue shaded part represents the species with a high APTI >15 under polluted conditions, which are highly pollution tolerant.

3.4.2 Comparison of the new AQII and old API scores

Table 3.1 includes 98 species, for which a complete (18) or partial (80) AQII score can be calculated. Unfortunately, the API score is only available for 52 of these species. For species with known isoprene emission potential, monoterpene emission potential, and allergy impact, for which only APTI, the maximum stomatal conductance (g_{stomax}), or the leaf area index LAI have not been reported, I compute a partial score marked with an *. Since neither stomatal conductance nor leaf area index nor APTI can negatively impact air quality, a lower limit to the AQII score of species for which only these parameters are missing can be calculated by assuming a low APTI, low LAI and low g_{stomax}. Their true AQII score could be higher and their score should be updated as soon as more data becomes available. Overall, there are 62 species for which API score has been reported in the peer reviewed literature. However, I compare the old API and the new AQII score in Figure 3.3 only for 52 species, for which both are available. Figure 3.3a shows that the AQII score and the API assessment agree for *Polyalthia longifolia*, and *Cinnamomum camphora*, with AQII value of 22 and > 19 respectively and API assessment of good to very good (score ≥ 4). A good agreement between the two indices is generally observed for species with a high APTI which are low or non-emitters of isoprene and monoterpenes, when their pollen impact is low and their economic value is high. Our new AQII is generally lower than the API for species with a high APTI which are prolific isoprene and moderate to high monoterpene emitters (Figure 3.3b and 3.3d) such as *Mangifera indica, Pongamia pinnata, Ficus benghalensis, Ficus infectoria*, and *Syzygium cumini*. Their AQII values range between 5 and 12 and stand in stark contrast to the high API score (≥ 3.7) which is linked to the high economic value of products and their high APTI score. The reverse effect of a good or very good AQII score (≥ 15), but moderate to poor API score (< 3) can be seen for species with a low isoprene and monoterpene emission potential and low pollen impact which do not produce products of high economic value or have a low APTI score or unfavorable crown/leaf structure such as *Phyllanthus emblica*, *Zizyphus jujuba*, and *Terminalia bellirica* (Figure 3.3a).

It can be seen in Figure 3.3 that the API score of many species carries a large uncertainty. Unfortunately, the same species (e.g., *Cassia fistula*) has been awarded contradicting API grades from 1 to 4 with an assessment of very poor to good by different authors (Karmakar et al., 2021; Pandey et al., 2015; Pathak et al., 2011; Prajapati and Tripathi, 2008; Shannigrahi et al., 2004). Similar discrepancies in the API assessment by different authors have been observed for *Terminalia bellirica*, *Terminalia arjuna*, *Senna siamea*, *Butea monosperma*, *Dalbergia* *sissoo*, *Tectona grandis*, *Azadirachta indica*, *Melia azedarach*, *Ficus religiosa*, *Syzygium cumini*, *Ziziphus jujuba*, *Aegle marmelos*, *Madhuca longifolia*, *Mangifera indica*, *Psidium guajava*, *Nerium indicum*, *Peltophorum pterocarpum* (Anake et al., 2018; Karmakar et al., 2021; Kashyap et al., 2018; Pandey et al., 2015; Pathak et al., 2011; Prajapati and Tripathi, 2008; Rai and Mandal, 2020; Sahu et al., 2020; Shannigrahi et al., 2004). At times, a large range of APTI is reported for the same species by various authors (e.g., 10 to 28) for *Cassia fistula* (Karmakar et al., 2021; Pandey et al., 2015; Pathak et al., 2011; Prajapati and Tripathi, 2008; Shannigrahi et al., 2004; Singh et al., 1991). Several authors have flagged that the APTI of the same species can differ between clean and polluted sites (Kashyap et al., 2018) and I recommend that the AQII assessment should be performed using only the APTI measured at polluted sites, which reflect the plants' ability to handle pollution more accurately. In addition, however, the same APTI value (e.g., 12), for the same species, has been converted to between one plus (Pandey et al., 2015) and five pluses (Shannigrahi et al., 2004) contributing towards the API score by different authors (Table 3.3).

Overall, the APTI which awards up to 6 pluses totally dominates the old API score (with API $\geq$4 representing good (4), very good (5), excellent (6) and best (7) score) at the expense of other parameters which affect the air quality. Hence, in our new AQII I reduce the impact of the APTI on the final AQII score (Table 3.2) by ensuring all parameters with an impact on the air quality are awarded a maximum of 3 pluses and up to a maximum of 3 minuses 461 and, therefore, carry equal weightage. I also propose a new set of cut offs of APTI < 12 for a low (+) 12 - 15 for a medium (++) and APTI > 15 for a high (+++) APTI score under polluted conditions. This approach splits the 82 species with known APTI into 3 roughly equal sized groups and provides the highest discerning power.

Table 3.3: Grading criteria for converting the measured APTI range to an API score by different authors.

Grades	APTI Range in different studies					
	[1]	[2]	[3]	[4, 5, 6, 7, 8]	[9]	[10]
+	≤6	≤8	≤9	≤12	≤14	≤20
++	6-10	8-10	9-11	12-15	14-17	20-30
+++	10-14	10-11	11-13	15-18	17-20	30-40
++++	14-18	11-12	13-15	18-21	20-23	40-50
+++++	≥18	≥12	15-17	≥21	≥23	≥50
++++++			≥17			

[1] Kashyap et al., 2018, [2] Shannigrahi et al., 2004, [3] Sahu et al., 2020, [4] Anake et al., 2018, [5] Prajapati and Tripathi, 2008, [6] Rai and Mandal, 2020, [7] Karmakar et al., 2021, [8] Pathak et al., 2011 [9] Pandey et al., 2015 [10] Kaur and Nagpal, 2017

3.4.3 Selection of species suitable for urban plantation

Figure 3.3a shows all species which have low isoprene and monoterpene emissions, and do not have allergenic pollen. Their AQII ranges between 15 and 22. All species in Figure 3.3a are highly suited for urban plantation. In general, tree species with an AQII ≥ 17 are usually a good choice. The list includes *Terminalia arjuna*, *Terminalia bellirica.*, *Terminalia chebula*, *Polyalthia longifolia*, *Swietenia macrophylla*, *Pterospermum acerifolium*, *Zizyphus jujuba*., *Citrus reticulata*, *Cinnamomum camphora*, *Annona squamosa*, *Nyctanthes arbor-tristis*, *Ficus aurea*, *Ficus elastica*, *Ficus retusa*, and *Ficus benjamina. Swietenia macrophylla* is not included in Figure 3.3a because it is a moderate monoterpene emitter, while *Ficus benjamina*, and *Ficus elastic* have pollen that is allergic, but not windblown. For all three the benefits of the plantation may outweigh its adverse impacts in most locations. For the remaining missing species, the API is not known.

Figure 3.3b shows species with moderate or high isoprene and monoterpene emissions, and allergenic, windblown pollen. Such species are best avoided in urban locations and generally have an AQII of ≤11 even when their APTI is high. *Mangifera indica*, *Pongamia pinnata*, *Morus alba, Syzygium cumini, Eucalyptus globulus, Liquidambar styraciflua, Ginkgo biloba, Populus nigra* and *Lantana camara* are best avoided for urban planation. The lowest AQII scores (≤ 1) of all the species studied were observed for *Lantana camara,* an invasive weed, which is a high isoprene emission potential, moderate monoterpene emission potential and highly allergenic windblown seeds, *Liquidamba styraciflua* and *Populus nigra*.

Figure 3.3c shows species with a negative score on one of the three parameters. Either on account of ozone precursor emissions, or on account of SOA precursor emissions or due the allergy potential of their pollen. Their AQII score ranges from 8 to 16. For species with a moderate AQII from ≥ 8 to ≤16 I recommend a site-specific impact assessment. *Phyllanthus emblica* owes its low AQII score to its low APTI score, while *Citrus limon, Magnolia grandiflora, Nyctanthes arbor-tristis, Tecoma stans, Pinus pinaster, Pinus radiata* and *Crataegus monogyna* owe it to their unknown APTI. All these can be planted in residential neighborhoods, but may be unsuitable for plantation along major roads. *Acer platanoides, Acer pseudoplatanus, Aesculus hippocastanum, Ricinus communis, Alstonia scholaris, Nerium indicum, Kigelia pinnata, Casia floribunda, Casia siamea, Cassia fistula, Azadirachta indica, Albizia lebbeck, Tamarindus indica, Acacia auriculiformis, Acacia nilotica, Acacia catechu, Acacia farnesiana, Acacia leucophloea, Acacia pycnantha, Aegle marmelos, Dodonaea viscosa, Ailanthus altissima, Hibiscus rosa-sinensis, Melia azedarach, Prunus persica, Quercus cerris, Fraxinus excelsior, Tilia cordata, Ulmus pumila, Celtis occidentalis a*nd *Mimusops elengi* owe their moderate score primarily to the fact that their pollens are known allergens and windblown. Hence, their plantation should only be considered far away from residential neighborhoods. However, their low isoprene and monoterpene emissions make them suitable for roadside plantations along highways. *Psidium guajava, Pithecellobium dulce, Tectona grandis, Butea monosperma, Ficus racemose* and *Ficus religiosa* can be considered in parks, far away from busy roads and industrial areas. Their pollen does not cause allergic reactions, but they are known to be prolific isoprene emitters. *Swietenia macrophylla, Citrus sinensis, Cedrela toona, Pinus nigra, Pinus pinea, Pinus sylvestris,* and *Murraya koenigii* are prolific monoterpene emitters, but their pollen does not cause allergic reactions. *Tecoma stans, Nyctanthes arbor-tristis, Crataegus monogyna, Pinus radiata* and *Pinus pinaster* only have windblown, but non-allergenic pollen, and owe their low score to the fact that several parameters have not been measured yet. Species that emit SOA precursors or windblown pollen are best avoided in locations where additional PM emissions will trigger exceedances of the air quality index for particulate matter. This consideration only applies to relatively clean locations where the air pollution impact of emissions is likely to exceed dry deposition loss of PM. Our calculations in Figure 3.2 show that in heavily polluted environment the dry deposition loss of particulate matter to the leaf surface dominates the vegetation impact on aerosol mass loadings even for species with high SOA precursor emissions.

Figure 3.3d shows species with a negative score on two of the three parameters. Their AQII score ranges from 3 to 13 and only one parameter (either ozone precursor emissions, or SOA precursor emissions or pollen allergy potential), does not contribute negatively to the score. I recommend that for species with an AQII score ≤ 13 the site-specific impact assessment should be conducted even more carefully. *Grevillea robusta* has a score <13, due to its crown structure and allergenic pollen which are not windblown, but low BVOC emissions and can be considered in parks. *Tectona grandis, Abies alba, Ficus benghalensis,* and *Ficus infectoria* are prolific isoprene and monoterpene emitting species, but their pollen is not allergenic. They can be planted in parks provided the site will not exceed the air quality index for particulate matter just because to the additional emissions. *Betula Pendula, Delonix regia, Bombax ceiba, Ceiba petandra, Putranjiva roxburghii*, *Murraya paniculata*, and *Ailanthus excelsa* have windblown allergic pollen and moderate to high monoterpene emissions. They can be considered for roadside plantation along highways. *Platanus acerifolia, Platanus orientalis, Bauhinia variegate*, *Cocos nucifera*, *Peltophorum pterocarpum, Casuarina equisetifolia, Dalbergia sissoo*, *Robinia pseudoacacia, Quercus petraea, Populus deltoids, Eucalyptus species*, *Salix spp.* and *Madhuca longifolia* have allergenic windblown pollen which makes them unsuitable for residential areas and are isoprene emitters, which makes them unsuitable for roadside planation. These species are, therefore, only suitable for rural background sites.

I note that discrepancies between the traditional evaluation of species and our new AQII are not restricted to Asian species. *Platanus* species are used as avenue trees in many parts of Europe (Grote et al., 2016) and *Platanus orientalis* is considered a very good option for avenue plantation based on its API assessment (Hatamimanesh et al., 2021). However, *Platanus* species have a poor drought tolerance, are prolific isoprene emitters and have allergenic, windblown pollen. Consequently, their AQII score is low (≤ 5).

3.5 Conclusion

At present, urban planners selecting trees for urban plantation based on criteria, which are heavily biased towards aesthetics, convenience of the municipal authorities, and the trees APTI, which quantifies how well the tree can survive in a polluted environment. So far, most urban planners fail to evaluate whether the species selected for plantation will improve air quality or cause air quality deteriorations at the targeted plantation site. In this study, I are introducing a new AQII which allows to evaluate the impact of planned tree plantation drives in the urban environment in a more holistic manner. Our index provides urban planners with a new quantitative tool for assessing the air quality impact of urban plantations. I take aerodynamic properties, leaf structure, pollution tolerance, ozone and SOA precursor emissions, and the pollen allergy impact into account and give all these species equal weightage. I conduct a literature review for 149 species and calculate the newly proposed AQII for 98 species, for which sufficient data is available.

Chapter 4

Nocturnal pollutant uptake contributes significantly to the total stomatal uptake of *Mangifera indica*

The content of this chapter has been published in the international peer reviewed journal Environmental Pollution as Datta et al., 2022 with co-authors Sharma, A., and Sinha, B. Sinha B. supervised investigation, and aided writing – reviewing and editing. I conducted the research, planned and conducted field experiments, analyzed the data, optimized and ran the DO_3SE model. Sharma, A. helped in field experiments and with leaf porometer measurements.

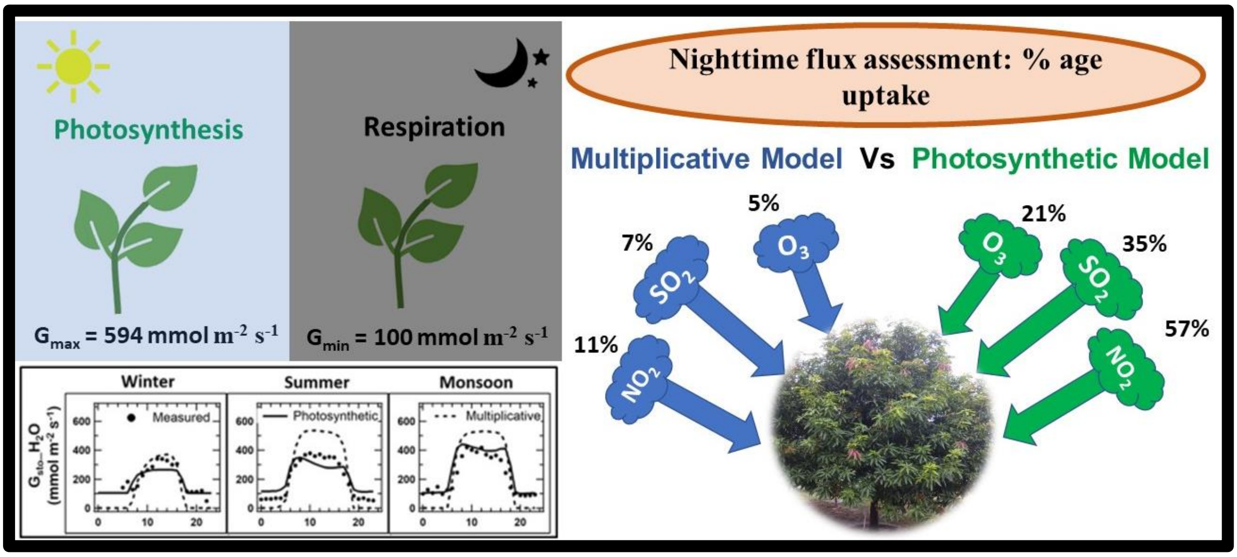

Figure 4.1: Graphical abstract of the chapter

4.1 Abstract

DO_3SE (Deposition of Ozone for Stomatal Exchange), is a dry deposition model, designed to assess tropospheric ozone risk to vegetation, and is based on two alternative algorithms to estimate stomatal conductance: multiplicative and photosynthetic. The multiplicative model has been argued to perform better for leaf-level and regional level application. In this study, I demonstrate that the photosynthetic model is superior to the multiplicative model even for leaf-level studies using measurements performed on *Mangifera indica*. I find that the multiplicative model overestimates the daytime stomatal conductance, when compared with measured stomatal conductance and prescribes zero conductance at night while measurements show an average conductance of 100 mmol(H_2O)$m^{-2}s^{-1}$ between 9 p.m. and 4 a.m. The daytime overestimation of the multiplicative model can be significantly reduced when the model is modified to include a response function for ozone-induced stomatal closure. However, nighttime pollutant uptake fluxes can only be accurately assessed with the photosynthetic model which includes the stomatal opening at night during respiration and is capable of reproducing the measured nighttime stomatal conductance. At our site the nocturnal flux contributes 64%, 39%, 46%, and 88% of the total for NO_2 uptake in winter, summer, monsoon, and post-monsoon, respectively. For SO_2, nocturnal uptake amounts to 35%, 28%, 28%, and 44% in winter, summer, monsoon, and post-monsoon, respectively while for ozone the nighttime uptake contributes 30%, 17%, 18%, and 29% of the total stomatal uptake in winter, summer, monsoon, and post-monsoon respectively.

4.2 Introduction

The leaves of vegetation provide a conduit to reduce pollutants in the air. They serve as surface for dry deposition (Cabaraban et al., 2013; Datta et al., 2021) but also sequester trace gases including ozone (O_3) and O_3 precursors through stomatal uptake (Emberson et al., 2000). These trace gases are taken up into internal tissues of leaves through stomata, small pores on the epidermis of leaves, through the process of diffusion. The foliar process of gas exchange is determined by the opening of stomata, and stomatal conductance is generally measured using sensors that assess the water vapor exchange between the leaf and the environment. Flux-based models have become the state of the art in assessing stomatal uptake of air pollutants (Nowak et al., 2006; Cabaraban et al., 2013; Selmi et al., 2016) by vegetation in recent years. The evaluation of stomatal uptake flux depends on stomatal response and there are two fundamental approaches used in modelling stomatal behavior, namely the more widely used multiplicative approach or Jarvis algorithm (Jarvis et al., 1976), which assumes that stomatal conductance for a species is influenced by temperature, irradiance, vapor pressure deficit (VPD), phenology, and soil moisture (SM). The second approach is called Ball-Berry, and is a photosynthesis-based algorithm (Ball et al., 1987), that postulates dependency of stomatal conductance on CO_2 exchange rate and is linked to the photosynthesis model of (Farquhar et al., 1980).

In the past, the multiplicative model has been argued to be a better performer for regional level and leaf-level applications (Büker et al., 2007). Its main advantage is that it incorporates the response of stomata to environmental stimuli through functions that can be experimentally determined, and tuned for each species and location (Emberson et al., 2000). The disadvantage of this model is that it is empirical and based on the statistical correlation between environmental factors and stomatal conductance. The photosynthetic model has the advantage that it is based on a mechanistic view of the photosynthesis process. Optimization theory can be used to link the carbon and water cycle, but also the nutrient, carbon and water cycles by expressing the marginal water cost per unit carbon gain or nutrient gain (Damour et al., 2010; Bonan et al., 2014; Haverd et al., 2018). One of the basic disadvantages of the photosynthetic model is that these optimization functions and the environmental response functions of various rate constants are not accessible and tunable (Bonan, 1995; Sellers and Collelo, 1996; Cox et al., 1998; Emberson et al., 2000; Bonan et al., 2014; De Kauwe et al., 2015; Haverd et al., 2018). Instead, they are hidden in the model code and for the DO_3SE model (Emberson et al., 2000), they are also poorly documented.

The land surface module in Earth System Models (ESMs) can be modified to incorporate photosynthesis based stomatal uptake flux estimates for other trace gases such as O_3, by scaling to the stomatal water vapor flux, which is already computed by this module. ESMs are used to predict future carbon uptake for different climate change scenarios. Nutrient limitations, water limitations, photosynthetic CO_2 uptake and respiration are the primary drivers of the terrestrial carbon cycle (Körner, 2003; Flato, 2011; Körner, 2015; Riley et al., 2018; Huang et al., 2021; Wei et al., 2022), and part of these models. Thus, photosynthesis-based flux models have the advantage over multiplicative models, that they can be integrated into the land surface module of climate models, which currently couples the carbon cycle, nutrient cycling and the water cycle.

In the present study, I compare both the models and evaluate their suitability to model the air pollutant uptake of the tropical tree species, *Mangifera indica*. The phenology of tropical trees is different from that of temperate trees as they possess a lower number of photo-periodic and thermo periodic adaptations (Reich, 1995). Tropical trees drop some of their leaves throughout the year (5-13% per month). Leaf shedding in tropical dry forests tends to peak during the dry season and flushing (the emergence of new leaves), which peaks during the wet season (Reich, 1995). Leaves in tropical dry biomes are typically retained 2 years. So far, stomatal conductance and environmental response functions of very few tropical trees have been studied (Assis et al., 2015; Cassimiro et al., 2016; Moura et al., 2021).

I use the well-known DO_3SE (Deposition of Ozone for Stomatal Exchange) model, which is a dry deposition model for our investigations (Emberson et al., 2000). This model is widely used for example under the Convention on Long-Range Transboundary Air Pollution European Monitoring and Evaluation Programme (CLTRAP-EMEP). DO_3SE as a dry deposition model, allows parameterization of environmental variables, based on Jarvis' multiplicative algorithm or the photosynthetic algorithm (Emberson et al., 2000), to obtain stomatal response and O_3 flux. Primarily, it is designed to assess tropospheric O_3 deposition risk to European land-cover types, crops and forest trees (Emberson et al., 2007; Büker et al., 2015), but it has been parameterized for applicability to tropical species (Assis et al., 2015; Cassimiro et al., 2016; Moura et al., 2021) also. Most studies in the past have used the model only in the multiplicative mode (Alonso et al., 2008; Fares et al., 2013; Assis et al., 2015; Cassimiro et al., 2016; Moura et al., 2021), despite the fact that the model has the option of using the photosynthetic approach for the simulation of stomatal conductance.

In the present study, I evaluate the hypothesis that the multiplicative model is more suitable for local, regional and leaf-level applications. I parameterized the model for both the multiplicative and the photosynthetic algorithms and subsequently compared the model output with the measured stomatal conductance to water vapor, and measured CO_2 assimilation observed in the field experiments on *Mangifera indica*. In particular, I evaluate both models with respect to how well they are able to reproduce not just the daytime, but also the nighttime stomatal conductance. I also evaluate how these differences between the models affect the annual pollution uptake estimates for different pollutants. So far, most prior studies have compared the accumulated exposure to a threshold above 40 ppb (AOT40) metric and the stomatal uptake modelled with the multiplicative DO_3SE model (Matyssek et al., 2004; Assis et al., 2015). Very few studies have previously compared the photosynthetic and multiplicative uptake mechanism for the same site (Fares et al., 2013; Hoshika et al., 2017) and none have compared the models for nighttime uptake.

4.3 Material and methods

4.3.1 Site description

Our research was conducted in IISER Mohali (30.667°N, 76.729°E, 310 m a.m.s.l.), Punjab, in the north-west Indo-Gangetic plain. The region is a part of the Tricity - Chandigarh, Mohali, and Panchkula. The region experiences four seasons – summer (MAMJ), monsoon (JAS), post-monsoon (ON) and winter (DJ). As can be seen in Figure 4.2, the hourly averaged ambient temperature at the top of the canopy during the study period ranged from 2.7°C in winter up to 44.1°C during the arid-dry summer. The site receives winds from north-west direction during most of the year and from the south-east during monsoon season (Pawar et al., 2015; Kumar et al., 2016). Monsoon starts from late June to early July and extends till September.

The experimental site is located within a residential campus where *Mangifera indica* trees are present both as part of the original agricultural landscape (>20 years old) and due to more recent plantation (2008-2012). *Mangifera indica* is a broadleaf evergreen tree that usually maintains leaves for 2-3 years. It belongs to the genus *Mangifera* which originates in tropical Asia, an area where plants are known to go through irregular mass flowering triggered by drought (Sakai et al., 2006). More details on the biology of *Mangifera indica* and the meteorology of the site can be found in the sub-section 4.3.1.1.

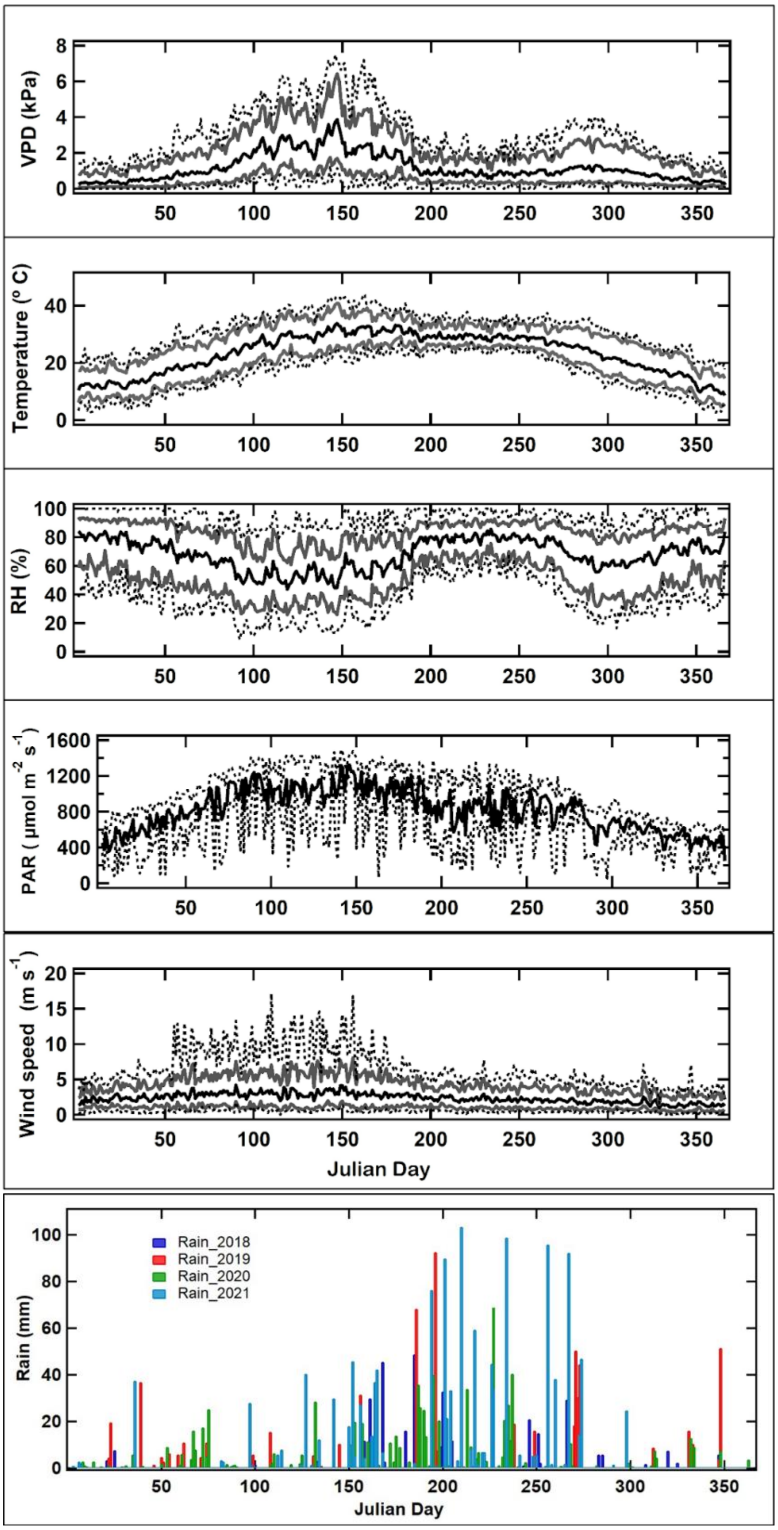

Figure 4.2: Seasonal cycle of meteorological parameters at our study site. The solid black line shows the average 24-hr average of the four years studied. The grey solid lines show the average 24-hr maximum and average 24-hr minimum of the parameter under consideration. The dashed lines show the highest 24-hr maximum and the lowest 24-hr minimum observed on that Julian day during the study period. For PAR the black solid line shows the 7-hour average PAR for the time window 9 am to 4 pm and the highest and lowest 7-hour average PAR recorded on that day. The transition from the hot dry summer to the summer monsoon is usually completed by Julian day 180 but can happen as early as Julian day 150 or as late as Julian day 190 in some years.

4.3.1.1 Detailed description of the *Mangifera indica* biology and measurement site

Mangifera indica is a broadleaf evergreen tree that usually maintains leaves for 2-3 years. It belongs to the genus Mangifera which originates in tropical Asia, an area where plants are known to go through irregular mass flowering triggered by drought (Sakai et al. 2006).

When *Mangifera indica* is grown in tropical or temperate dry regions, flowering and fruiting occurs in dry season, because drought stress suppresses vegetative flushing (Tahir et al., 2003), and time since last flushing is the variable that drives flowering (Ramírez and Davenport, 2010). Mango trees grow 13-30 m tall and can live for more than 100 years. At our site *Mangifera indica* flowering occurs at the end of winter (February March) and the fruits are harvested in late summer (June) and throughout the first month of the monsoon season (July). *Mangifera indica* has between two and four major anchoring tap roots that can reach 6 m depth and often reach down to the water table. The finer fibrous feeder roots are found close to the surface extending at most up to 1 m depth and usually cover an area as large as the crown. *Mangifera indica* is drought tolerant. It has been documented that drought stress suppresses flushing (Tahir et al., 2003), and results in a shrinkage of the surface root network (Zaharah and Razi, 2009) in *Mangifera indica*. However, it appears that low surface soil moisture has a limited impact on the stomatal conductance of leaves unless there is prolonged drying (Elsheery and Cao, 2008). It has been documented that fruits continue to develop under drought stress, albeit in lesser numbers, even when soil moisture stays below 15% till the onset of the monsoon. *Mangifera indica* is drought adapted. Deficit irrigation schemes in which the soil moisture is maintained between 10 - 20% show better fruit quality than complete irrigation (Spreer et al., 2009).

Irrigation of gardens and roadside vegetation at our site was done regularly and the trees studied do receive irrigation, hence the surface root network is usually well developed, and soil moisture did not drop below 10% for more than a few hours during most years (2019-2021). Irrigation failed between the end of March and end of May 2018 due to a tubewell failure. The same period also saw very little pre-monsoon rain. The resulting drought stress likely affected the surface root network, and it is possible that the tap root lost access to its usual moisture sources towards the end of the period. Our recorded soil moisture response functions are based on observations in this period. However, for our model runs I had to switch the influence of soil moisture on the stomatal conductance off, so that the model is able to reproduce observations outside this 2 - month period. The soil at the study site is alluvial, with a clay hardpan with poor hydraulic conductivity in the top 40 cm, but several other layers including sand and gravel layers with better hydraulic conductivity beneath. Soil moisture was measured in the topmost clay layer. A cross section of the soil sequence photographed within campus at a location where a river intersects the floodplain is shown in Figure 4.3. The unconfined aquifer is located approximately 10 m below the surface and its depth varies with season.

Figure 4.3: Photograph of the soil structure at the study site. The top layer contains a clay hardpan approximately 40 cm below the surface and has poor hydraulic conductivity. Soil moisture measurements were performed in this top layer 10 cm below the surface, which contains most of the fibrous roots of *Mangifera indica*. However, tap roots have access to several sand and gravel layers with better hydraulic located below the surface.

4.3.2 Measurements of stomatal conductance to water vapor and meteorological measurements

Stomatal conductance to water vapor measurements were taken at different hours of the day, in different seasons, from April 2018 to February 2022, with SC-1 leaf porometer, Meter group, USA (steady state measurement approach, accuracy ±10%, resolution 0.1 mmol (H_2O) $m^{-2}s^{-1}$) on 5 different mature *Mangifera Indica* (Mango) trees. The leaf porometer was regularly calibrated with a calibration plate that yields a stomatal conductance of 240 mmol (H_2O) $m^{-2}s^{-1}$. During plant chamber experiments, conductance measurements were performed 24/7 unless leaves were wet. Stomatal conductance readings were taken on a branch adjacent to the plant chamber on the same tree (typically 5 readings on different leaves of the same tree per hour). In addition, stomatal conductance readings were taken on up to 4 others additional *Mangifera indica* trees on campus if they had sunlit leaves during that hour. Throughout the rest of the 4 years, measurements were usually taken at midday (11 a.m. – 3 p.m.) and the timing depended on the leaf porometer availability and site access. The original dataset included 7657 measurements. Outliers (N = 27) were removed by assuming values that were more than 3σ above the seasonal average can be treated as outliers.

Two air quality stations (AQS) have been deployed in the campus – the first stationed at Central Analytical Facility (CAF) having height around 18 m above ground level and the second at around 35 m height at academic block-2 (AB2) building. Both the stations measure temperature, RH, solar radiation, rain, wind direction, wind speed, O_3, sulphur dioxide (SO_2), and nitrogen dioxide (NO_2) continuously. Data is available since May 2019 from AB2 station and since August 2011 from CAF station. Alongside, two portable meteorological stations by Decagon and Campbell Scientific Inc. are available for near tree measurements of temperature, relative humidity (RH), pressure, wind speed, wind direction, photosynthetic active radiation (PAR), and SM at 10 cm below surface, and rainfall. More details on all the sensors used for meteorological measurements are available in the section 2.4 of chapter 2. VPD was calculated from temperature and RH measurements as described in the sub-section 4.3.2.1.

4.3.2.1 VPD calculations

Vapor Pressure Deficit (VPD) was calculated from temperature and RH measurements using the following equation of Campbell and Norman (2000)

$$VPD = e_s(T)(1 - h) \qquad (1)$$

and the equation

$$e_s(T)[Pa] = (1.0007 + 3.46 * 10^{-6} * P) * 6.1121 * \exp\left(\frac{17.502\,T}{240.97+T}\right) \qquad (2)$$

by Buck (1981)

Wherein h stands for relative humidity expressed as a fraction, T for the temperature in º C, and P for the pressure in Pascal (Pa) (Buck, 1981; Campbell and Norman, 2000). VDP was calculated with the temperature and humidity sensor at the canopy height (3 m), which was placed next to the plant chamber during plant chamber experiments, whenever data was available. Gaps were filled in decreasing order of preference with data from the sensors at 1 m height and the sensor at 18m height and the sensor at 35m height as detailed in the sub-section 2.3.1 of the chapter 2. Figure 4.4 shows a few days of temperature, RH and VDP data from all sensors.

For this study, I primarily use the meteorological observations from our mobile temperature, RH and PAR sensors located next to the trees studied. However, windspeed, rain and air pollutant measurements were taken from CAF station, which is located at 18 m height and hence above the tree canopy to avoid biases. In this study, I use data acquired during the 2018, 2019, 2020 and 2021. The average diurnal profile of meteorological observations during each season restricted to the hours during which stomatal conductance measurements were performed has been shown in Figure 4.5. Ambient data for tropospheric O_3, SO_2, and NO_2 was measured using UV photometry (Thermo Fisher Model 49i), pulsed UV fluorescence (Thermo Fisher Model 43i), and chemiluminescence (Thermo Fisher Model 42i), respectively. Detailed description and information on maintenance and calibration of instruments in AQS, CAF is available in the earlier publications (Sinha et al., 2014; Kumar et al., 2016). Since the DO_3SE model requires continuous input data, I perform gap filling for missing hourly measurements using the methodology described in greater detail in the section 2.3.1 of the chapter 2.

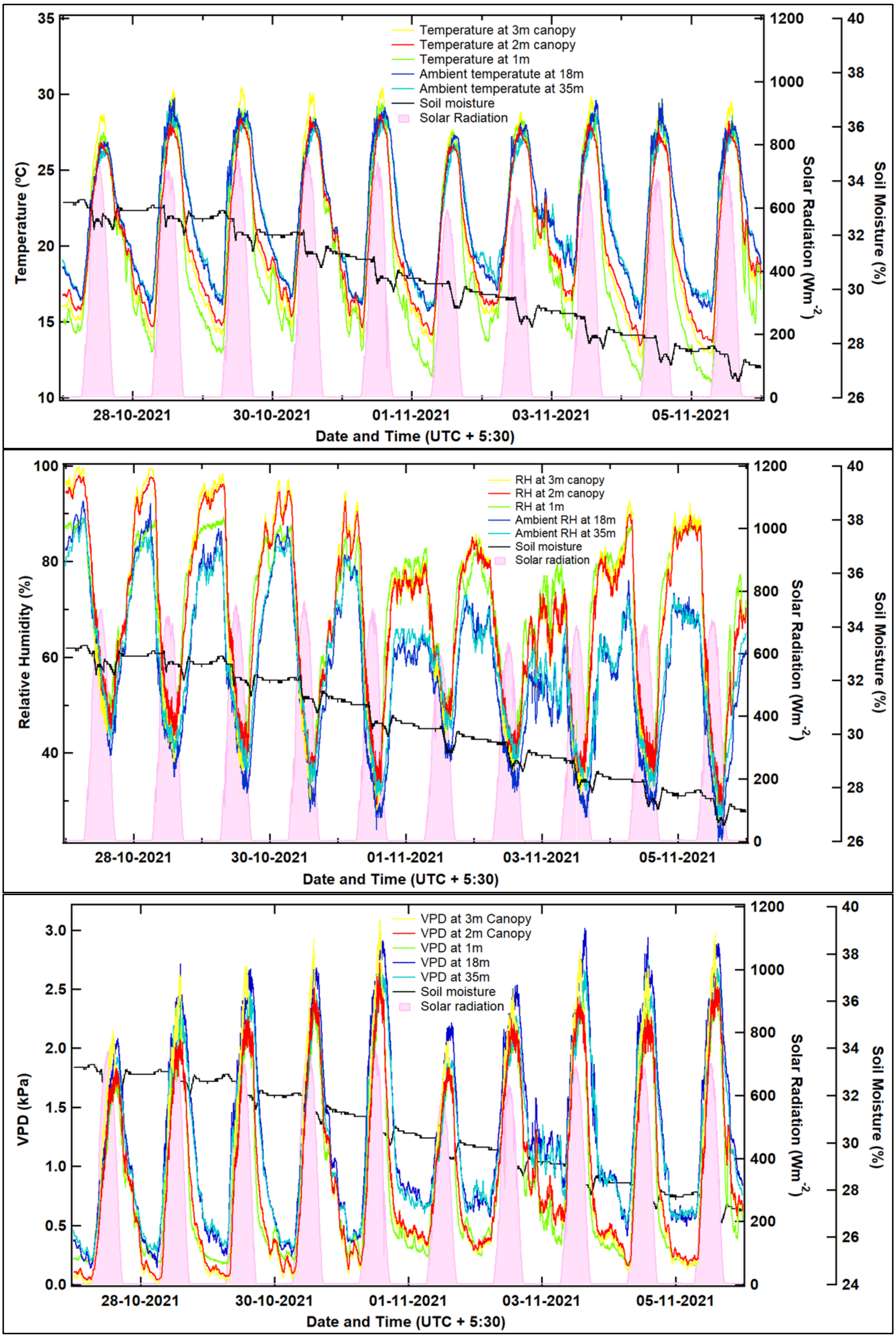

Figure 4.4: Temperature, RH and VPD profile at the study site. The sensor at 3 m height is located at the top of the canopy. The sensor at 2 m height is located near the trunk below the canopy. The sensor at 1 m height is located in an open area next to the tree.

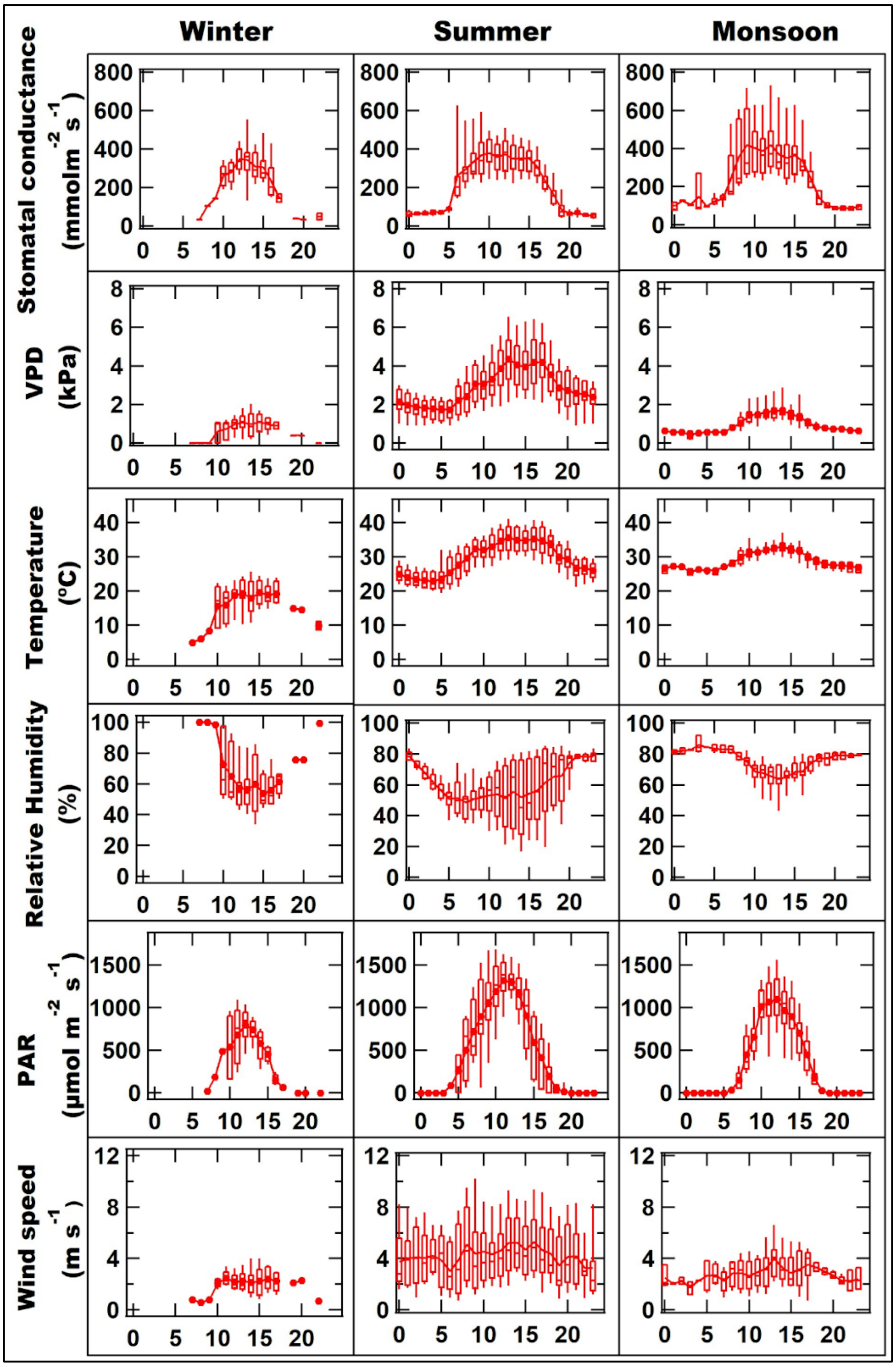

Figure 4.5: Average diurnal profile of Stomatal conductance, VDP, Temperature, Relative humidity, PAR and wind speed. Only hours in 2018, 2019, 2020, and 2021 in which stomatal conductance measurements were available are included in this figure. The box indicates the 25th and 75th percentile of the hourly observations in each hour, while the whiskers extend from the 10th to the 90th percentile. The median is indicated by a solid bar inside the box while the average is marked by round markers connected with a line.

4.3.3 Measurements of CO_2 assimilation and ambient CO_2 mixing ratios

The branch cuvette method, adopted and explained by other publications (Ortega et al., 2008; Vettikkat et al., 2020), was deployed on 2 different mango trees to measure carbon dioxide (CO_2) assimilation. While this type of plant cuvette system is typically used to measure VOC fluxes, it can also be used to measure CO_2 fluxes (Vettikkat et al., 2020). The input and output of the cuvette was connected to a cavity ring-down spectrometer (CRDS, Model G2508, Picarro, Santa Clara, USA) for the measurements of dry CO_2 mixing ratios. The instrument switched between measuring the plant chamber input and output air. The instrument is deployed at CAF. Net carbon assimilation was calculated using equation (3) (Vettikkat et al., 2020) in µmol (CO_2)$m^{-2}s^{-1}$.

$$`A_{net} = \left(M_{in,CO2} - M_{out,CO2}\right) * \frac{1}{V_m} * \frac{Q}{A} \quad (3)$$

Here, Q (m^3s^{-1}) is input air flow rate, A_{net} the net carbon assimilation, A the total leaf area enclosed in the cuvette, $M_{in,CO2}$ and $M_{out,CO2}$ are measured CO_2 mixing ratios in background air and output air, and V_m (m^3mol^{-1}) is the molar gas volume. Our work includes three measurement studies, from 28th August to 4th September 2018, the second from 17th to 21st January 2019, and the third from 26th June to 1st July 2021. The plant chamber was mounted on a branch and contained 25-55 leaves. After each plant chamber experiment, the leaves inside the plant chamber were collected and scanned together with a scale bar to determine the total leaf area in an image processing software (ImageJ) to express the fluxes per m^2 of leaf area.

4.3.4 Stomatal conductance modelling using the photosynthetic and multiplicative version of the DO_3SE model

The model was tuned for both multiplicative and photosynthetic modes that are based on two algorithms: The multiplicative algorithm (Jarvis et al., 1976) shown in equation (4) and the photosynthetic algorithm (Ball et al., 1987) shown in equation (5). In equation (4) the multiplicative stomatal conductance ($g_{sto-multi}$) is the maximum stomatal conductance (g_{max}) multiplied with environmental functions (f_{light}, f_{temp}, f_{VPD}, f_{SM} and, f_{phen}) that describe stomatal conductance, relative to g_{max}, for PAR, temperature, VPD, SM, and phenology (Mills et al., 2017).

$$g_{sto\_multi} = g_{max} \times f_{phen} \times f_{light} \times max\,(f_{min}, (f_{VPD} \times f_{temp} \times f_{SM}))$$

(4)

$$g_{sto\_photo} = \left(g_{min} + m \times A_n \times \frac{h_b}{C_b}\right) * f_{phen}$$

(5)

4.3.4.1 Environmental response function of the multiplicative DO_3SE

The environmental response functions are calculated using equations (6) to (9) which we have taken from the chapter 3 of the Mapping Manual for modelling and mapping critical loads & levels (Mills et al., 2017). The parameters were derived using the boundary line method which has been extensively used and discussed in previous works (Alonso et al., 2008; Assis et al., 2015; Cassimiro et al., 2016; Hoshika et al., 2017; Moura et al., 2021). All function values used in model are listed in Table 4.1

$$f_{light} = 1 - \exp((-\text{light}_a) * PAR) \tag{6}$$

$$f_{temp} = \max(f_{min}, ((T - T_{min}) / (T_{opt} - T_{min})) * ((T_{max} - T) / (T_{max} - T_{opt}))^{bt}) \tag{7}$$

$$bt = (Tmax - Topt) / (Topt - Tmin)$$

$$f_{VPD} = \min(1, \max(f_{min}, ((1-f_{min}) * (VPD_{min} - VPD) / (VPD_{min} - VPD_{max})) + f_{min})) \tag{8}$$

$$f_{SW} = \min(1, \max(f_{min}, ((1-f_{min}) * (SM_{min} - SM) / (SM_{min} - SM_{max})) + f_{min})) \tag{9}$$

The maximum conductance to water vapor (g_{max}) was determined to be 594 mmol(H_2O)m^{-2} s^{-1} based on the average of 303 values above the 90th percentile of stomatal conductance values observed in summer and monsoon seasons. The minimum stomatal conductance was determined to be 100 mmol(H_2O)$m^{-2}s^{-1}$ as average of 1558 nighttime stomatal conductance measurements taken between 9 p.m. and 4 a.m.

Equation (5) is the basic equation used in the photosynthetic model to calculate stomatal conductance (g_{sto_photo}). g_{min} is daytime minimum stomatal conductance (mmol(H_2O)$m^{-2}s^{-1}$), *m* defines species- specific sensitivity of stomatal conductance to net assimilation, A_n is net assimilation rate (μmol(CO_2)m^{-2} s^{-1}), h_b, represents RH at leaf surface as decimal fraction, and C_b represents CO_2 concentration (μmol/mol) at leaf surface. Net photosynthesis rate depends on the rate of carboxylation and electron transport (Farquhar et al., 1980), and, in the model, is tuned by parameters V_{cmax} and J_{max}. Literature reported values for *Mangifera indica* vary widely between 10 and 79 μmolm^{-2}s^{-1} for V_{cmax} and 20-164 J_{max} (Allan et al., 2000; Urban et al., 2003; Urban et al., 2004). While V_{cmax}, J_{max} and m have been shown to vary seasonally, in response to environmental parameters such as drought stress and across leaves on the same tree (Urban et al., 2003; Urban et al., 2004; Wolf et al., 2006; Hoshika et al., 2017), the formulation of the photosynthetic DO_3SE allows only for one set of these parameters that remains fixed throughout the year and applies to all leaves sunlit and shade alike. Hence the parameters need to be constrained empirically as described in sub-section 4.3.4.2.

4.3.4.2 Empirical optimization of the photosynthetic model

To constrain our model, I adopted the inverse estimation of Vc_{max} and m from carbon and moisture fluxes (Wolf et al., 2006). To optimize the model, I started from the values presented in (Urban et al., 2004) for *Mangifera indica* and then changed the J_{max} Vc_{max} used in the DO_3SE to minimize the sum of the Euclidean distance between the vector of the model predicted carbon flux values (Fc_{model}) and the vector of observed carbon flux values ($Fc_{measured}$).

$$min \sum (F_{C-model} - F_{C-measured})^2 \tag{10}$$

This was done for all hours with simultaneous measurements of carbon fluxes and stomatal conductance (N=127). I ran this optimization in multiple iterations progressively lowering the J_{max}/Vc_{max} ratio from 2.3 to 0.8. The former represents the highest ratio observed in *Mangifera indica* (Urban et al. 2003) while the latter represents the lowest ratio reported in the literature for heat stressed *Triticum aestivum* (Stasik and Jones, 2007).

Table 4.1: Parameter values for tuning DO3SE multiplicative and photosynthetic model, for *Mangifera indica*, in the present study and compared to DO3SE multiplicative studies from literature for *Psidium guajava* (Assis et al., 2015), *Astronium graveolens* (Cassimiro et al., 2016), and *Moringa oleifera* (Moura et al., 2021). *gsto0 (µmol (H2O) m-2s-1) represents the minimum stomatal conductance observed when leaf stomata are supposed to be closed. It is taken as average of stomatal conductance measurements at nighttime from 20:00 hour to 04:00 hour. #fO3 is the included O3 function assumed for estimating impact of O3 on the multiplicative flux output.

Function	Parameters	Units	Values				
			Multiplicative				Photosynthetic
			Mangifera indica	*Psidium guajava*	*Astronium graveolens*	*Moringa oleifera*	*Mangifera indica*
	g_{max}	mmol (H_2O) $m^{-2}s^{-1}$	594	721	152	559	
	*g_{sto0}	µmol (H_2O)$m^{-2}s^{-1}$					100000
f_{min}		Fraction	0.13	0.026	0.059	0.2	
f_{phen}	Start day	Julian day	1	0	0		
	End day	Julian day	365	365	365		
	a	Fraction	0.55	1	1		0.55
	b	Fraction	0.85	1	1		0.85
	c	Fraction	1.0	0.4	0.7		1.0
	d	Fraction	0.65	1	1		0.65
	e	Fraction	0.55				0.55
f_{light}	α	Constant	0.01	0.014	0.035	0.0032	
f_{temp}	T_{min}	˚C	0	15	13	9	
	T_{opt}	˚C	30	28	27	26	
	T_{max}	˚C	50	43	40	38	
f_{VPD}	VPD_{max}	kPa	8.0	1.2	1.1	0.9	
	VPD_{min}	kPa	9.0	5.5	3.9	3.3	
f_{SM}	SM_{max}	%	6	22			
	SM_{min}	%	0	3			
	m	Dimensionless					25
	V_{cmax}	µmol$m^{-2}s^{-1}$					30
	J_{max}	µmol$m^{-2}s^{-1}$					24
#f_{O3}	$O3_{max}$	ppbv	30				
	$O3_{min}$		160				

The best year around model measurement match was found for the lowest J_{max}/Vc_{max} ratio (0.8) for V_{cmax} =30 µmolm^{-2}s^{-1} and J_{max} 24 µmolm^{-2}s^{-1}.

This provided the best compromise for model measurement agreement during both vegetative and reproductive growth and minimized the model measurement disagreement in the early morning hours without compromising the model performance during midday too much. Figure 4.6 shows that the increase in measured stomatal conductance above the nighttime average conductance, and the switch from net respiration to net carbon assimilation occurs when PAR crosses a threshold of 300 µmol m^{-2}s^{-1}. Yet the model calculates the highest conductance and assimilation in the early morning hours when PAR is between 100-300 µmol m^{-2}s^{-1}, and again calculates carbon and moisture fluxes that exceed measured fluxes in the evening when PAR falls below 300 µmol m^{-2}s^{-1}. This points towards problems with the light response function in the photosynthetic model. A low J_{max} helps suppress this behavior, while a high Vc_{max} mitigates the impact of the low J_{max} on the midday model measurement disagreement.

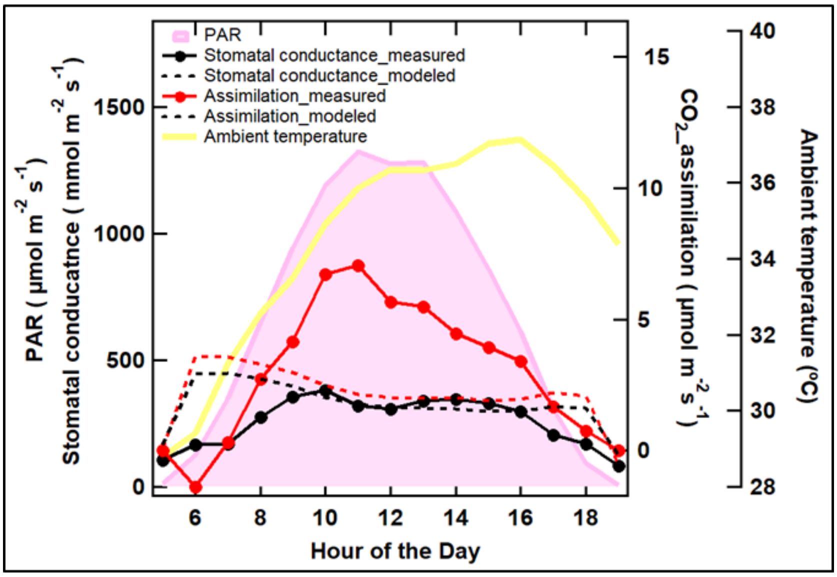

Figure 4.6: Average diurnal cycle of measured stomatal conductance and carbon assimilation (dots connected by lines), modelled stomatal conductance and carbon assimilation (dashed lines), temperature and PAR for the plant chamber experiment in April 2021.

Our Vc_{max} is very close to the Vc_{max} currently implemented for tropical tree (non-oxisols) in the Biosphere Energy Transfer Hydrology (BETHY) model, broadleaf evergreen trees in Canadian Terrestrial Ecosystem Model (CTEM), and broadleaf trees in Joint UK Land

Environment Simulator (JULES) model (Rogers, 2014). Species-specific sensitivity of stomatal conductance to net CO_2 assimilation, m, is calculated to lie between 8 and 16 for C3 type plants (Nikolov et al., 1995). It has been noted earlier that ecosystem level derivations of m are typically higher (15-25) than leaf level measurements. Our plant chamber measurements yield an "m" parameter that is in line with ecosystem observations (25±2) while regressing the Ball index against the measured stomatal conductance with the help of equation (5), possibly because some leaves in the plant chamber are shaded, and their carbon fluxes are limited by light availability, yet they contribute to transpiration. Experiments on bean plants showed that plants switched to respiration immediately when being introduced into 24/7 complete darkness, yet the circadian rhythm of stomatal conductance continued, initially unaltered, and tapered off over the course of 3 days (Hennessey et al., 1993). For our study, I have disabled SM influence on stomatal conductance in the model. I do, however, provide the measured SM response function in Table 4.1. The model calculates SM based on only rain input and thus does not correctly represent SM in the case of irrigated trees.

To set maximum stomatal conductance to O_3 in the model, the measured maximum stomatal conductance to water (594 mmol (H_2O) $m^{-2}s^{-1}$) is multiplied with a conversion factor of 0.663 (Massman, 1998), to account for the difference in the diffusion constant between H_2O and O_3. I also used the model to quantify SO_2, and nitrogen NO_2 stomatal uptake. To employ the model for this, , I used the ambient hourly NO_2, and SO_2 data from 2018 to 2021 and set g_{sto_max} to NO_2, and SO_2 instead of O_3 , by multiplying maximum stomatal conductance to water with a conversion factor of 0.625 and 0.5, respectively, based on the difference in the diffusion constants of NO_2 and SO_2 to water vapor (Wesely, 1989; Selmi et al., 2016). The annual stomatal uptake was calculated as described in the sub-section 4.3.4.3 with the leaf area index (LAI) of *Mangifera indica* (3.3) and the crown area of a mature tree (100 m^2) (Rajan et al., 2001; Datta et al., 2021).

4.3.4.3 Calculation of the annual stomatal uptake

The stomatal flux is calculated from the stomatal conductance via equation (11)

$$F_{st-x} = c_x(z_i) * g_{sto-x} * \frac{r_c}{r_b+r_c} \tag{11}$$

wherein F_{st-x} is the stomatal flux of the pollutant x, c_x is the concentration of the pollutant x at the top of the canopy of height i (m), g_{sto-x} is the stomatal conductance of the compound x and

r_c and r_b represent the leaf surface and quasi linear resistance, respectively. The derivation of r_c and r_b as a function of wind speed and leaf dimensions is described in detail in the Mapping Manual (Mills et al., 2017).

I calculated the total uptake per tree by multiplying the leaf area index (LAI) of *Mangifera indica* (3.3) (Datta et al., 2021) with the crown area of a mature tree (100 m^2) (Rajan et al., 2001).

4.4 Results and Discussion

4.4.1 Calibration of the multiplicative and photosynthetic DO_3SE model

Table 4.1 lists the parameter values used to calibrate the multiplicative DO_3SE model for stomatal conductance derived from the plots in Figure 4.7. I calibrated both multiplicative and photosynthetic models for *Mangifera indica* and ran the model without SM influence on g_{sto} and with measured CO_2 mixing ratios. While comparing the environmental response functions of *Mangifera indica* recorded at our site with those of other tropical tree species such as *Psidium guajava* (Assis et al., 2015), *Astronium graveolens* (Cassimiro et al., 2016), and *Moringa oleifera* (Moura et al., 2021), one unique feature stands out. *Mangifera indica* has an exceptional tolerance to hot and dry air and is capable of maintaining maximum stomatal conductance till a VPD_{max} of 8 kPa. This is more than double the highest VPD_{max} observed for any other tropical tree species so far studied and may be a peculiar adaptation of plant species that evolved to flower and fruit during the drought that precedes the onset of the rainy season in tropical winter dry climates (Sakai et al., 2006).

At our site, the wet season starts in late June to early July and lasts till September. *Mangifera indica* enters reproductive growth towards the end of March and fruits during the hottest time of the dry season when natural SM is lowest and the region is often exposed to Loo winds from desert regions in the middle East (Pawar et al., 2015). The trees also show high conductance even in drying soil when irrigation is withdrawn (SM_{max}=6%), possibly because the tap roots retain access to some deeper moisture sources.

Figure 4.7 shows the relationship of relative stomatal conductance with ambient temperature, PAR, VPD, SM, and tree phenology. *Mangifera indica* is an evergreen tree. Hence the phenology function f_{phen} has to cover the full 365 days of the year. The individual functions (f_{light}, f_{temp}, f_{VPD}, f_{phen} and f_{SM}) represented by a solid line in Figure 4.7, describe the maximum stomatal conductance observed for a given light intensity, temperature, VPD, time of the year and SM.

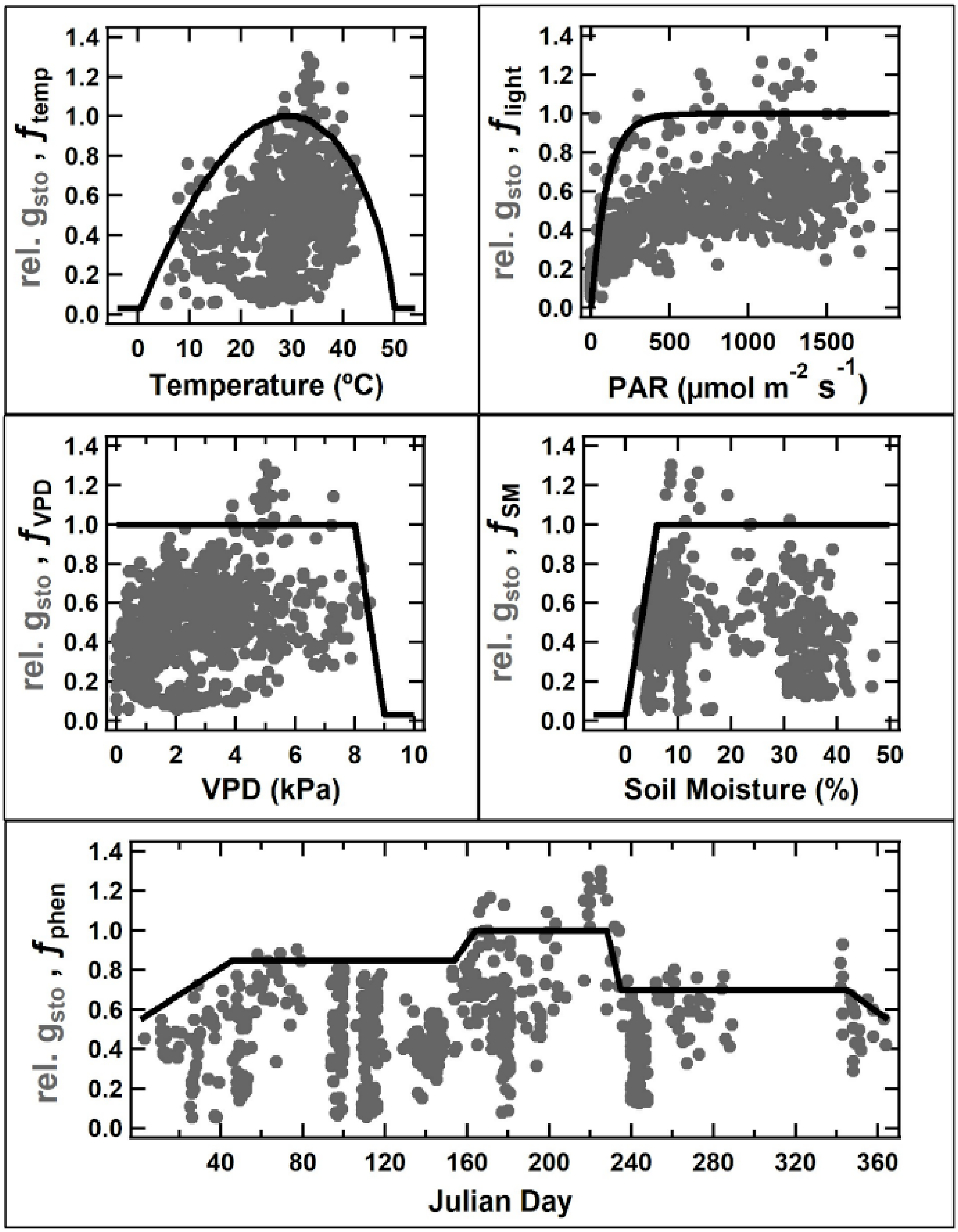

Figure 4.7: Plot shows the relationship of the hourly averaged relative stomatal conductance (rel. g_{sto}) with temperature, PAR, VPD, SM, and Julian day, respectively. The solid line represents the boundary line function for each variable.

4.4.2 Comparison between the multiplicative and photosynthetic DO$_3$SE model

In Figure 4.8, the top panel shows the comparison of stomatal conductance for water vapor, G_{sto}_H_2O (mmol (H_2O) $m^{-2}s^{-1}$), between measured values, the photosynthetic DO$_3$SE, and the multiplicative DO$_3$SE. The diel profile represents the average conductance in winter, summer, and monsoon seasons for four consecutive years (2018 - 2021). In summer and monsoon season, the seasonal average stomatal conductance of the multiplicative model is overestimated in the daytime when compared to measured conductance. This results in a systematic overestimation of stomatal conductance (reduced major axis regression (RMA) slope = 1.49 ± 0.04, intercept = - 40 ± 13, R = 0.73) and daytime pollutant uptake by this model. This overestimation can be reduced, but not fully closed by incorporating a function to account for a reversible O_3-induced stomatal closure (RMA regression slope = 1.24 ± 0.03, intercept = -50 ± 10, R = 0.74), in Figure 4.12. In addition, the multiplicative model writes zero flux values into the output file during night hours, when solar radiation < 50 Wm^{-2}, even when f_{min} is set to the appropriate value (in this case f_{min} = 0.13) in the model. This causes a negative intercept for the model-measurement regression and makes the current version of the multiplicative model poorly suited for assessing the stomatal uptake of trace gases with significant nighttime mixing ratios. While in the original model formulation of the multiplicative model presented by (Emberson et al., 2000), f_{min} could be used to make the model reproduce the average measured nighttime stomatal conductance,

$$g_{sto\_multi} = g_{max} \times f_{phen} \times max\,(f_{min}, (f_{VPD} \times f_{temp} \times f_{SM} \times f_{light})) \quad (12)$$

the same parameter in equation (4) no longer fulfills this function, because f_{light} was moved out of the bracket (Wieser and Emberson, 2004). The corresponding parameter in the photosynthetic model input (g_{sto0}) is used as g_{min} in equation 5 and remains positive even when A is zero.

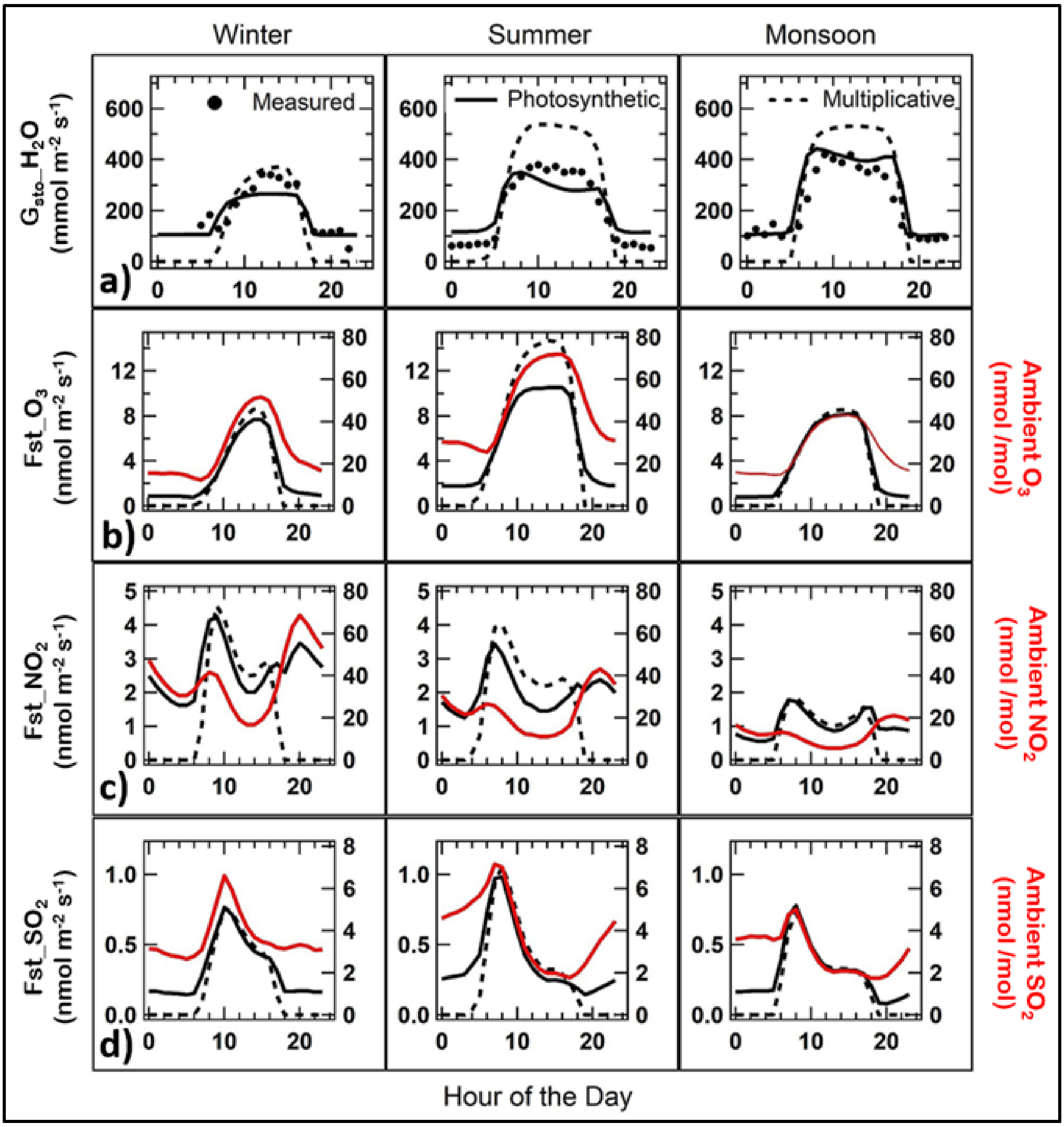

Figure 4.8: Panel a) shows the comparison of measured stomatal conductance of water vapor ($G_{sto}\_H_2O$) in mmol (H_2O) $m^{-2}s^{-1}$, marked with solid black markers, with multiplicative and photosynthetic model output, marked with dotted black line and solid black line respectively. Panels b), c), and d) shows the comparison of both models' output of stomatal O_3 flux, stomatal NO_2 flux, and stomatal SO_2 flux respectively, marked with dotted black line for multiplicative and solid black line for photosynthetic model and red lines for the observed ambient mixing ratios.

The photosynthetic model models the nocturnal stomatal conductance more accurately and is, hence, more suitable for calculating the pollutant uptake for pollutants emitted primarily at night. It slightly underestimates daytime conductance in winter and summer (RMA regression slope 0.71±0.02, intercept 54±7, R=0.61), possibly because Vc_{max} and J_{max} during flowering and fruiting are different from the values seen during dormancy and vegetative growth. Previous work compared both models with the help of flux tower measured ecosystem fluxes, and concluded that the photosynthetic model is superior to the multiplicative model provided it treats “m” as a variable, that exponentially depends on RH and changes in response to SM (Fares et al., 2013; Hoshika et al., 2017).

Figure 4.9 shows that the photosynthetic model is also capable of modelling the observed CO_2 fluxes. It underestimates midday assimilation, specifically during reproductive growth and overestimates assimilation in the early morning hours. The cumulative assimilation from the start of the day till a given hour is reproduced more accurately than the instantaneous assimilation and underestimated to the same degree as conductance (RMA regression slope 0.7 ± 0.04, intercept 7.6 ± 0.9, R = 0.7). The root cause of the mismatch between modelled and observed instantaneous assimilation appears to be that the hour-to-hour variations in assimilation are primarily governed by the environmental response functions of Vc_{max} and J_{max}, which are hidden in the model code and cannot be tuned. Due to these functions the model calculated assimilation during dawn, dusk and on cloudy days (Figure 4.6 and 4.9), exceeds measurements, possibly due to a problematic light response function. In reality, our observed assimilation is always low under twilight conditions and peaks during mid-day. There is evidence that the upper limit on assimilation during any particular hour of the day is imposed by the internal circadian rhythm of the plant. *Mangifera indica* trees transferred into 24/7 light treatment maintained a circadian rhythm with assimilation peaking at the subjective mid-day, and being lowest at the subjective midnight (Allan et al., 2000; Dios de and Gessler, 2018). Accurate modelling of both conductance and assimilation on cloudy days would require a circadian rhythm of stomatal conductance that is independent of carbon assimilation, as the circadian rhythm of stomatal conductance continues for 3 days even when plants are kept in complete darkness (Hennessey et al., 1993).

Our field measurements recorded a stomatal conductance of 100 ± 50 mmol (H_2O) $m^{-2}s^{-1}$ during night hours throughout the year. Nighttime stomatal opening has been observed in a number of species across biomes (Matyssek et al., 2004; Daley and Phillips, 2006; Caird et al., 2007; Dawson et al., 2007; Hoshika et al., 2018). Respiration and nighttime stomatal appear to be correlated, in particular during the first 5 hours after sunset (Wang et al., 2021). It has been hypothesized that nighttime stomatal conductance confers evolutionarily benefits that include a continuation of evaporative leaf cooling till the leaves reach favorable temperatures in hot climates (Wang et al., 2021), a competitive advantage in acquiring nutrients (Snyder et al., 2008), and a competitive advantage in the competition for scarce water resources despite the increased overall water usage (Yu et al., 2019).

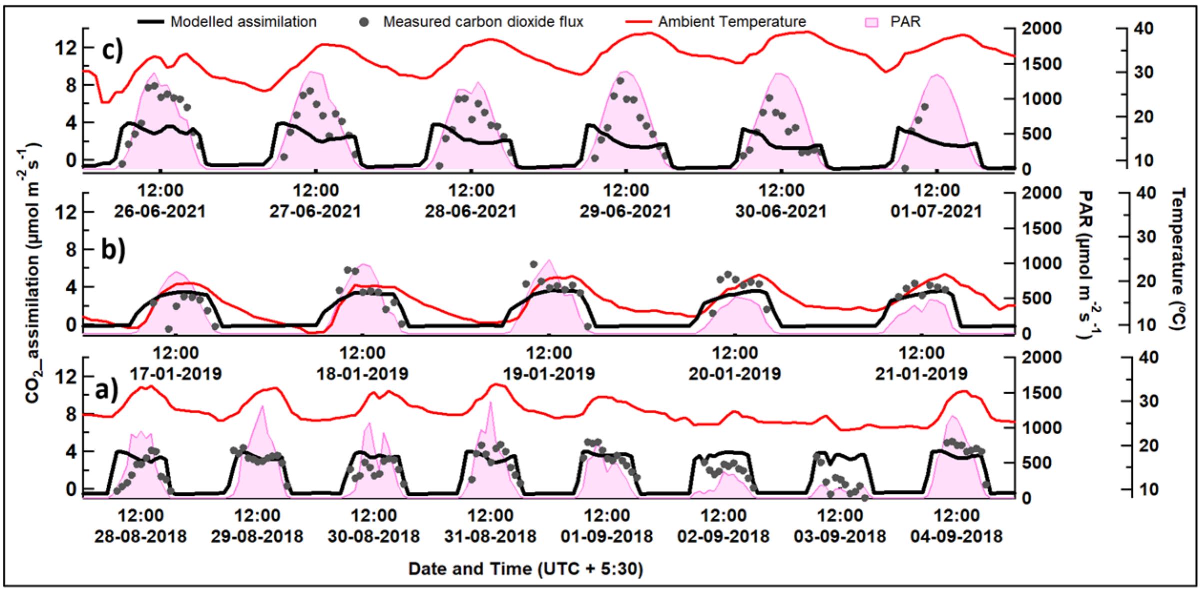

Figure 4.9: Shows net assimilation model output, with a solid line, compared with the periods when CO_2 fluxes were measured, in solid black markers, from field measurements in 2018, 2019, and 2021. PAR (units on the right-hand axis) is shown as a shaded area and Temperature (units on the secondary right-hand axis) is shown as a red line.

The bottom panels of Figure 4.8 show the differences between the modelled stomatal uptake of O_3, NO_2 and SO_2 between the photosynthetic and multiplicative DO3SE run for four years and three seasons (2018 to 2021). DO3SE model is used to assess O_3 risk on vegetation due to O_3 uptake through the diffusion of gases into internal tissues of leaves through stomata in the transpiration process. It can also be used for other gases with low mesophilic resistance and intercellular resistance, such as NO_2 (100 sm^{-1}) and SO_2 (~ 0 sm^{-1}) (Wesely, 1989; Selmi et al., 2016). It can be seen from the Figure 4.8 and Table 4.2, that it is crucial to use the photosynthetic DO3SE model for accurately calculating the stomatal uptake of air pollutants that can have high nighttime mixing ratios such as NO_2, and SO_2. Figure 4.8 shows that NO_2 mixing ratios at our site peak during the evening traffic rush that occurs after sunset. As O_3 is not titrated to 0 ppb at night and our site is downwind of emission sources, tailpipe NO emissions are typically converted to NO_2 by the time they reach our site. SO_2 mixing ratios increase throughout the night as emissions from industrial sources accumulate in the nocturnal boundary layer and peak during the breakup of the nocturnal boundary layer at dawn, when SO_2 emissions from the 275 m stack of a nearby power plant get transported downwards. The multiplicative model has a tendency to overestimate the average daytime stomatal conductance, but neglects the nighttime uptake, which contributes significantly to the total stomatal flux of acidic trace gases.

Table 4.2: Comparison between pollutant uptake per tree (*Mangifera indica*) with the photosynthetic model (Photo) and multiplicative model (Multi) and percentage contribution of nighttime flux in pollutant uptake.

Pollutant uptake in kg/Tree										
Pollutant	Winter		Summer		Monsoon		Post-monsoon		Annual	
	Photo	Multi	Photo	Multi	Photo	Multi	Photo	Multi	Photo	Multi
O_3	0.33	0.27	0.97	1.03	0.47	0.42	0.33	0.31	2.09	2.02
NO_2	0.29	0.14	0.33	0.24	0.12	0.09	0.18	0.09	0.93	0.57
SO_2	0.05	0.03	0.09	0.07	0.05	0.04	0.04	0.03	0.22	0.16
Nighttime percentage contribution in pollutant uptake										
Pollutant	Winter		Summer		Monsoon		Post-monsoon		Annual	
	Photo	Multi	Photo	Multi	Photo	Multi	Photo	Multi	Photo	Multi
O_3	30	06	17	05	18	06	29	05	21	05
NO_2	64	08	39	10	46	12	88	16	57	11
SO_2	38	05	30	09	31	07	48	07	35	07

4.4.3 Comparison of the calculated annual pollutant uptake per tree between the multiplicative and photosynthetic DO$_3$SE model

Table 4.2 shows the calculated annual pollutant uptake per tree for *Mangifera indica* in kg per tree in different seasons. While I show both the results of the photosynthetic and multiplicative model, it should be noted that this is done purely for the purpose of comparison and that the output of the photosynthetic models should be used for air quality impact assessments as the multiplicative model overestimates daytime pollutant uptake and underestimates the nighttime uptake. The O_3 uptake of *Mangifera indica* is highest in summer (0.97 kg/tree), when O_3 levels at our site are highest (Kumar et al., 2016), followed by the monsoon (0.47 kg/tree). During late summer and early monsoon season, the stomatal conductance of *Mangifera indica* is highest as the trees reach the final stages of fruiting at the end of June or beginning of July. The transition from hot and dry conditions to the summer monsoon varies strongly from year to year and occurs between Julian day 150 and 190. Similar enhancements in stomatal conductance during flowering and fruiting have also been documented in other species (Vettikkat et al., 2020). O_3 levels in monsoon season tend to be lower and stomatal conductance declines at the end of the fruiting period despite sufficient SM, as after fruiting, the trees enter a brief period of dormancy before flushing with new leaves. This reduces the overall uptake flux during monsoon season. The O_3 uptake during post-monsoon (0.33 kg/tree), and winter (0.33 kg/tree) season is almost equal. When one compares the annual average, then the multiplicative model underestimates the total O_3 uptake, by ~3%. However, actual differences are larger when one compares nighttime and daytime separately. The multiplicative model overestimates the daytime O_3 uptake by 16%. For O_3, the nighttime stomatal uptake calculated by the photosynthetic model contributes 30%, 17%, 18%, and 29% of the total stomatal uptake in winter, summer, monsoon, and post-monsoon, respectively. This high contribution of the nighttime O_3 uptake to total stomatal O_3 uptake demonstrates that considering nighttime flux in modelling total pollutant uptake by vegetation is important, even for a species that is formed by photochemistry during the day. At our measurement site, night time O_3 episodes with O_3 mixing ratio above 40 ppb during night hours (Figure 4.10) occur relatively frequently, when the site receives aged air masses in which O_3 has not been titrated by fresh NO emissions. In such aged air masses, the daytime peak levels take several hours after sunset to drop below 40 ppb. High nighttime O_3 episodes with the 1-hour average O_3 exceeding 80 ppb at our site are associated with vertical transport during storms or with mountain winds bringing air masses from higher altitudes. About 80 % of such high O_3 events occur in summer and monsoon.

For pollutants, such as NO_2 or SO_2, the ambient mixing ratios peak during the night. Hence, considering the nighttime NO_2 and SO_2 uptake of vegetation is even more important for quantifying their stomatal deposition flux accurately. Table 4.2 displays the net uptake in kg per tree for these pollutants as calculated by both the models as well as the nighttime percentage contribution to total pollutant uptake. The nocturnal flux quantified by the photosynthetic model contributes 64%, 39%, 46%, and 88% of the total for NO_2 uptake in winter, summer, monsoon, and post-monsoon, respectively. NOx emission at our site peaks in the early evening hours. The nocturnal uptake for SO_2 amounts to 38%, 30%, 31%, and 48% in winter, summer, monsoon, and post-monsoon, respectively. Overall, the multiplicative model underestimates the total annual NO_2 uptake by 39 % and the SO_2 uptake by 27 %, despite overestimating day-time uptake.

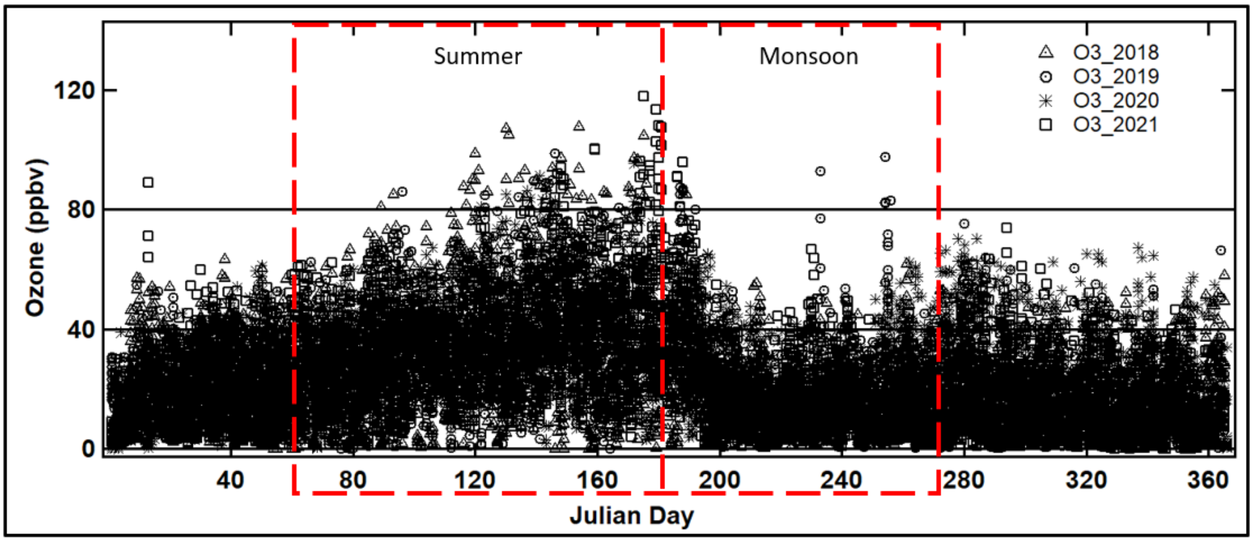

Figure 4.10: Nighttime ozone levels for 2018 to 2021, shows frequently occurring events of ozone above 40ppbv and even higher than 80ppb in summer and monsoon.

4.4.4 Evidence for O_3 - induced stomatal closure in *Mangifera indica*

The presence of high ambient O_3 can suppresses the metabolism of CO_2 and thus stomatal conductance (Wittig et al., 2007). Currently the model only accounts for the impact of O_3 enhanced leaf senescence in wheat and potato (Pleijel et al., 2002; Danielsson et al., 2003; Pleijel et al., 2007; Gonzalez–Fernandez et al., 2010; Osborne et al., 2019). *Mangifera indica* trees in the Indo Gangetic plain, show high conductance during summer when O_3 levels are very high. The multiplicative model overestimates daytime conductance when properly tuned, indicating that stomatal conductance is not modified by meteorological factors alone. Our experimental observations indicate that high ambient O_3 can induce stomatal closure directly (Figure 4.12). Figure 4.11 shows the variation in differences between the multiplicative stomatal flux output and the measured stomatal conductance is largest when ambient O_3 mixing ratios are highest. An instantaneous and reversible stomatal closure has been documented in, *A. thaliana* (Vahisalu et al., 2010; Vainonen and Kangasjärvi, 2015; McAdam et al., 2017) and *Vicia faba* (Guidi et al., 1993), while a delayed but reversible reduction in stomatal conductance in response to chronic O_3 exposure at 80 ppb has been documented in *Populus nigra deltoides*

(Dusart et al., 2019). The model measurement agreement for the multiplicative DO_3SE model improves significantly, with the RMA slope versus measurements decreasing from 1.49 ± 0.04 to 1.24 ± 0.03, when a function to account for a reversible O_3 - induced stomatal closure is included into the calculation (Figure 4.11b).

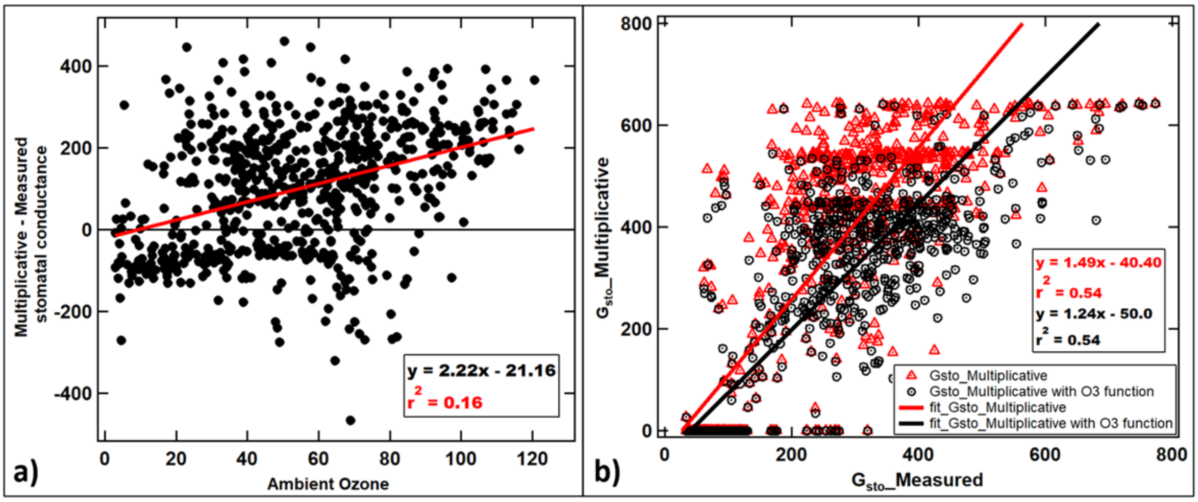

Figure 4.11: Panel a) shows the variation in difference between multiplicative stomatal flux output and measurements (multiplicate –measured). Panel b) shows the relationship of the multiplicative flux with the measured data without ozone function in red markers and multiplicative flux with the ozone function in black markers.

I propose to incorporate a function for reversible O_3-induced stomatal closure (equation 13) that needs to be multiplied with f_{phen} in equation 4.

$$f_{O3} = \min(1,\max(f_{min},((1-f_{min})*(O_{3min} - O)/(O_{3min} - O_{3max})) + f_{min})) \quad (13)$$

with $O_{3min} = 30$ and $O_{3max} = 160$

Figure 4.12 shows that daytime model measurement agreement improves significantly, with the RMA slope versus measurements decreasing from 1.49 to 1.24 when the O_3 function is included, however, nighttime values remain unaltered. Hence, the main conclusion that the photosynthetic model is superior for calculating total pollutant uptake by vegetation, including nighttime uptake, remains unaffected.

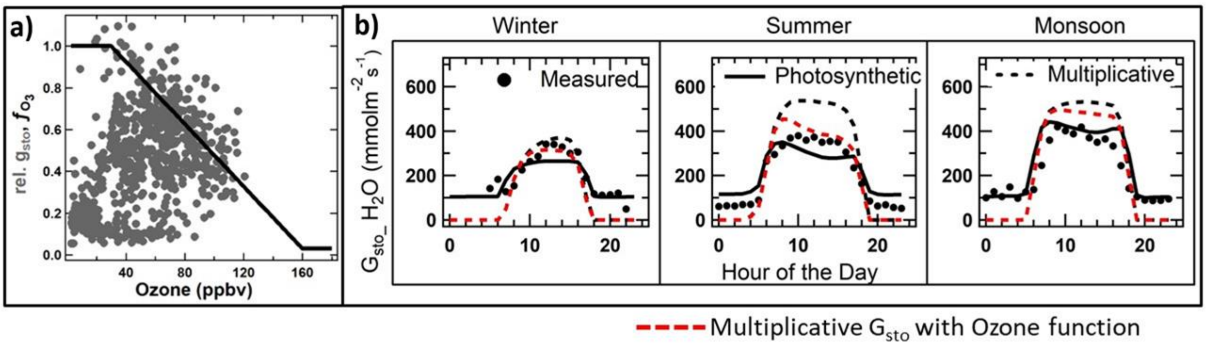

Figure 4.12: Panel a shows dependency of stomatal conductance (rel. g_{sto}) on ambient O_3. The O_3 function (f_{O3}) describing maximum conductance for O_3 and shown in black solid line is computed using the function f_{O3}=min $(1$,max $(f_{min}, ((1–f_{min})*(O_{3min} – O) / (O_{3min} – O_{3max})) + f_{min}))$with O_{3min}=30 and O_{3max}=160. Panel b) shows shift in multiplicative flux after inclusion of the O_3 function (red dotted line), and compares it with multiplicative model output without the O_3 function (dashed black line) and photosynthetic model (solid black line).

4.5 Conclusion

DO_3SE, is a dry deposition model, designed to assess tropospheric O_3 risk to vegetation, and is based on two algorithms: multiplicative and photosynthetic. The multiplicative model has been argued to perform better for leaf-level and regional level application. In this study, I demonstrated that the photosynthetic model is superior to the multiplicative model even for leaf-level studies using measurements performed on *Mangifera indica*. The photosynthetic model has the advantage of already being integrated into the carbon and water cycle module in Earth system models. The corresponding modules can be modified to incorporate photosynthesis based stomatal uptake flux estimates of other trace gasses.

I found that the multiplicative model overestimated the daytime stomatal conductance, when compared with measured stomatal conductance of water, and prescribed zero conductance at night. The following improvements would enable the multiplicative approach to reproduce our *Mangifera indica* data better:

1) A return to the original formulation of the DO_3SE model proposed by (Emberson et al., 2000) which permits the use of the parameter f_{min} to model nighttime fluxes.

2) The ability to load a measured SM function (as is currently the case for measured leaf temperature). This would simplify the use of the model for single - site studies, particularly at locations where part of the moisture influx is through poorly quantified irrigation.

3) A tunable function that can model the reversible ROS induced stomatal closure observed in addition to the currently available function that models the O_3-induced leaf senescence. These two functions describe two different biochemical processes.

The photosynthetic DO_3SE model too, would benefit from further improvements listed below:

1) A shift to the non-linear formulation in which "m" is modulated by RH and SM (Fares et al., 2013; Hoshika et al., 2017).

2) The option to vary Vc_{max} and J_{max} seasonally or at least have different values for the dormancy, reproductive and vegetative growth phases.

3) Inclusion of the circadian rhythm that regulates stomatal conductance independently of assimilation, which persists for several days even if the plant is transferred to an environment with constant light, constant darkness or without CO_2 (Hennessey et al., 1993; Allan et al., 2000; Dodd et al., 2014; Dios de and Gessler, 2018).

4) Our data indicates that the model overestimates carbon assimilation under twilight conditions, possibly because the light response function has been optimized to reproduce stomatal conductance during cloudy days, and stomatal conductance and assimilation are linearly linked. Stomatal conductance on cloudy days needs to be handled via an independent circadian rhythm of stomatal conductance, and the light response function needs to be modified to reduce the overestimation of carbon assimilation under twilight condition.

Chapter 5

Conclusion: results and findings in brief

The present work deals with the importance of assessing green spaces in urban pollutant environments in a more holistic manner to handle the destructive effects of urbanization. In this chapter, I am summarizing briefly the answers to the questions posed at the beginning of my thesis:

What role do trees and vegetation play in an urban environment in the fight against air pollution? Do they improve or deteriorate air quality in Indian cities?

In my thesis I contrasting the impact of two species with a high API rating, namely Mangifera indica and Polyalthia longifolia, with an API of 5.9 ± 0.9 and 4.8 ± 1.0, respectively, on urban air quality. *Polyalthia longifolia,* is a non-isoprene emitter and a low monoterpene emitter during most seasons, while *Mangifera indica* is a high isoprene and moderate monoterpene emitter throughout the year. *Polyalthia longifolia* has moderate monoterpene emissions in early summer, when the old leaves turn yellow and fall, while the new leaves emerge but continues to be a non-isoprene emitter throughout the year. Both are equally recommended for urban plantation at present. The impact of both species on ozone formation differs by two orders of magnitude when these species are planted in a NOx surplus roadside environment. *Polyalthia longifolia* sequesters more ozone through its stomata than can be formed from its precursor emissions even in summer and hence reduces ozone levels both at the site itself and downwind. For *Mangifera indica* the ozone formation potential of its precursor emission flux is 4 times larger than the stomatal uptake during peak daytime. Hence, the plantation of *Mangifera indica* fuels tropospheric ozone production and exceedances both at the plantation site and downwind and can aggravate rather than ameliorate ozone exceedance events. The impact of both species on particulate matter mass loadings at our site are currently dominated by the high anthropogenic PM emissions. PM levels are so high, that plant precursor emissions hardly add to the overall burden. At present, the dry deposition flux of particulate matter to the leaf surface is larger than the SOA formation potential from the emitted aerosol precursors for both species. However, this dry deposition flux depends on the particulate matter mass loadings and deposition velocity. In a relatively clean environment with <10 μg m^{-3} $PM_{2.5}$, the net impact of *Mangifera indica* on ambient particulate matter, would switch towards being dominated by its

SOA precursor emissions, rather than the leaves dust uptake and the same tree would turn into a net aerosol source instead of being a net aerosol sink.

What are the isoprene and monoterpene emission rates and trends of various tree species used for urban plantations in India?

An inventory of isoprene and monoterpene emission factors was prepared for 149 trees and shrubs out of a total of 280 tree species, which are commonly considered for urban plantation around the world. The inventory is based on a review of the peer-reviewed literature and fresh measurements reported in this thesis. Isoprene emission fluxes for 142 species were available in the literature while isoprene emission fluxes for 7 species are reported for the first time in this thesis. For monoterpene emission fluxes data for 125 species were compiled from the literature and data for 6 species was presented or the first time in this thesis. Emission factors varies for different species. Out of 149, isoprene emission flux ranged from high to moderate for 43 species and from low to no emission for 106 species. Similarly, out of 131, monoterpene emission flux ranged from high to moderate for 34 species and from low to no emission for 97 species.

One of the important findings in my thesis is that several species which are currently considered highly suitable for urban plantation namely *Mangifera indica*, *Ficus benghalensis* and *Ficus infectoria* based on the API are both prolific isoprene and monoterpene emitters and, therefore, likely to fuel secondary pollution. At the same time there are several species with low BVOC emissions that are often avoided during plantation drives because of their low API. Yet *Terminalia bellirica, Nerium indicum, Kigelia pinnata DC, Ricinus communis, Tamarindus indica, Senna siamea, Cassia fistula, Acacia catechu, Albizia lebbeck, Hibiscus rosa-sinensis, Melia azedarach, Ficus benjamina, Phyllanthus emblica, Ziziphus jujube, Aegle marmelos* and *Ailanthus altissima* will have a net positive impact on the air quality at the site. These species should be considered for plantation more frequently.

What are the main shortcomings of the current process for selecting trees for urban plantations, and why is there a need for a better index?

The present criteria in India to choose a plant for urban plantation is based on two indices - The air pollution tolerance index (APTI), which evaluates the ability of the tree to survive in a polluted environment. The second is the anticipated performance index (API) which evaluates the overall performance of a tree based on pollution tolerance capacity and pollution mitigation potential via tree morphological traits. API also includes the economic value of a tree while assessing suitability without considering that the existence or absence of a marketable product should have no bearing on the assessment. The anticipated performance index (API) does not consider how the emissions of BVOCs from the tree or the pollen allergy potential will affect the air quality and human well-being. So, most urban planners at present don't consider whether the species chosen for the plantation will enhance air quality or worsen it at the intended plantation location.

The old API score is primarily dominated by the Air pollution tolerance index (APTI) index score of a species which awards up to 6 pluses to the old API score (with API ≥4 representing good (4), very good (5), excellent (6) and best (7) score). This comes at the expense of other parameters which affect the air quality. Sadly, there has been great variation not only between the APTI measurements conducted by different authors for the same species (e.g., APTI 10 to 28) for *Cassia fistula*, but more importantly between how the same APTI score for the same species contributes to the final API when different authors perform the assessment. The same APTI value (e.g. 12), for the same species, *Cassia fistula*, has been converted to between one plus and five pluses contributing towards the API score by different authors, resulting in a situation where the same species is rated to be highly desirable or undesirable depending on who does the assessment. Similar discrepancies in the API assessment by different authors have been observed for *Terminalia bellirica*, *Terminalia arjuna*, *Senna siamea*, *Butea monosperma*, *Dalbergia sissoo*, *Tectona grandis*, *Azadirachta indica*, *Melia azedarach*, *Ficus religiosa*, *Syzygium cumini*, *Ziziphus jujuba*, *Aegle marmelos*, *Madhuca longifolia*, *Mangifera indica*, *Psidium guajava*, *Nerium indicum*, and *Peltophorum pterocarpum.*

In my thesis I propose to standardize the cut offs of related to the APTI and reduce the impact of the APTI on the final score so that different parameters receive equal weightage. I propose APTI<12 should be considered a low (+) 12–15 a medium (++) and APTI >15 a high (+++) APTI score under polluted conditions. This approach splits the 82 species with known APTI into 3 roughly equal sized groups and provides the highest discerning power.

What is the best approach towards quantifying the impact of urban trees and plants on air quality and towards ranking species according to their ability to both tolerate the stress of pollution, and reduce pollution levels at a plantation site and downwind?

In this thesis I propose a new assessment index, called the air quality impact index (AQII), which incorporates the impact of ozone and aerosol precursor emission, stomatal conductance or pollution uptake potential as well as the pollen allergy potential and drought tolerance of the proposed species in the decision-making process while determining the suitability of a species for urban tree planation.

I excluded the economic factor from consideration, because a roadside plantation drive in an urban area shouldn't primarily focus on making a profit for the horticultural department, but rather should focus on improving air quality at the plantation site and downwind. The plantation should also not induce additional healthcare burden on residents due to the plantation of species that emit windblown allergenic pollen.

Ideally, urban plantations should reduce the economic burden of residents by reducing heating and cooling needs. This reduces anthropogenic emissions and, therefore, provides an indirect air quality benefit. Due to this, I suggested that winter deciduous trees should not receive a negative score in the AQII index. They are actually desirable in winter cold climates. The original API considered all deciduous trees as undesirable, because of the inconvenience leaf litter causes to municipal authorities. However, winter deciduous trees allow better sunlight penetration during cold season, than evergreen trees. This reduces heating related emissions and fogginess. At the same time, winter deciduous trees carry leaves that reduce the urban heat island via evapotranspiration and sequester pollutants during the hot and dry season. Hence, they should not be considered as a-priory undesirable in all locations.

I also made some changes in how the suitability of species is assessed based on the tree habit and crown structure. The original API awarded negative marks to short trees and shrubs with small canopies. Recent research has shown, that short vegetation elements such as green walls and hedges between the road and the sidewalk reduce the particulate matter exposure of pedestrians more efficiently than tall alley trees. Alley trees tend to reduce wind speeds and, therefore, the ventilation within the street canyon, which results in hyperlocal pollution accumulation. In my new index, I do not award a negative score for short vegetation and instead evaluate the plant based on its leaf aera index, stomatal conductance and the ability of the leaves to capture particulate matter via the process of dry deposition.

To ensure all aspects that are important for the air quality impact of plantation are considered equally my new AQII ensures all parameters with an impact on the air quality are awarded a maximum of 3 pluses and up to a maximum of 3 minuses and, therefore, carry equal weightage.

After designing the new index, grades were allotted to 149 species for all those properties for which the required input data was previously available or presented for the first time as part of this thesis. For 98 species, AQII was calculated and for 52 species the AQII could be contrasted with their old API score. I recommend species with AQII score ≥ 17 as good choices for urban plantations. Such a high score results from a species having low isoprene and monoterpene emission potential and no allergenic windblown pollen. On the other hand, species with AQII score ≤ 11 are usually not very well suited for urban plantation or at the very least require a careful site-specific impact assessment. Usually, species which such a low score are prolific emitters of isoprene and monoterpenes and have allergenic windblown pollen. Hence their plantation is best avoided in urban areas. A moderate score between 11 and 17 is usually either due to the high ozone or aerosol precursor emission potential or due to allergenic windblown pollen. Occasionally, a moderate or low score is caused by the fact that the APTI and pollution uptake potential of a species have not been quantified or are very low. Hence, species with a moderate score can be considered for urban plantation but with site-specific assessment that evaluates how important the parameter that causes the low score is in a particular plantation context.

Which different modelling approaches exist for estimating the air pollution uptake potential of trees and how does their performance compare in the urban environment?
The leaves of vegetation serve as surface for dry deposition and sequester trace gases including ozone (O_3) and O_3 precursors through stomatal uptake. Flux-based models that model the opening and closing process of stomata have become the state of the art in assessing stomatal uptake of air pollutants by vegetation in recent years. There are two fundamental approaches used in modelling stomatal behavior, namely the more widely used multiplicative approach or Jarvis algorithm (Jarvis et al., 1976), which assumes that stomatal conductance for a species is influenced by temperature, irradiance, vapor pressure deficit (VPD), phenology, and soil moisture (SM). The second approach is called Ball-Berry, and is a photosynthesis-based algorithm (Ball et al., 1987), that postulates dependency of stomatal conductance on CO_2 exchange rate and is linked to the photosynthesis model of Farquhar et al. (1980).
In my thesis I use the well-known DO_3SE (Deposition of Ozone for Stomatal Exchange) model (Emberson et al., 2000). This model is widely used for example under the Convention on Long-Range Transboundary Air Pollution European Monitoring and Evaluation Programme (CLRTAP-EMEP). DO_3SE as a dry deposition model, which allows parameterization of environmental variables, based on Jarvis' multiplicative algorithm or the use of the photosynthetic algorithm, to obtain stomatal response and O_3 flux. I optimize the DO_3SE model for *Mangifera Indica* both in the photosynthetic and multiplicative mode with the help of four years of measured meteorological data, ambient O_3 mixing ratios measuredCO_2 mixing rations as the input file and 7657 stomatal conductance measurements as validation data.

The multiplicative model has been argued to perform better for leaf-level and regional level application in the past. However, my thesis shows with the help of measurements performed on *Mangifera indica* that the photosynthetic model is superior to the multiplicative model even for leaf-level applications. Specifically, I found that the multiplicative model overestimated the daytime stomatal conductance, when compared with measured stomatal conductance of water, and prescribed zero conductance at night. This becomes a problem when stomatal conductance is used to assess the stomatal uptake of pollutants that are primarily emitted at night. The photosynthetic model has the advantage of already being integrated into the carbon and water cycle module in Earth system models. Adopting this model more widely means that the corresponding modules in earth system models can be modified to incorporate photosynthesis-based stomatal uptake flux estimates of other trace gasses.

Do these models contain all the feedback processes which affect plant stomatal aperture or are there missing processes?

Comparison of output data, for four consecutive years (2018 – 2021), with measured stomatal conductance in the field shows a systematic overestimation of stomatal conductance and daytime pollutant uptake of *Mangifera indica* by the multiplicative model. The overestimation was highest on days with high ozone levels. This indicates the presence of a reversible ROS-induced stomatal closure in this species. A tunable function that can model the reversible ROS-induced stomatal closure in addition to the currently available function that models the O_3-induced leaf senescence would improve model measurement agreement. These two functions describe two different biochemical processes.

The photosynthetic model too would benefit from modifications. Several studies have reported a circadian rhythm that regulates stomatal conductance independently of assimilation exists in most trees. This diurnal cycle of opening and closing of stomata persists for several days even if the plant is transferred to an environment with constant light, constant darkness or without CO_2. My data indicates that the inclusion of this circadian rhythm of stomatal conductance into the model would improve the model performance particularly under twilight conditions and on cloudy days.

Which changes in the existing model would improve its performance in reproducing the measured plant stomatal conductance?

The following changes in the model would enable the multiplicative approach to reproduce my measured *Mangifera indica* data better:

1)A return to the original formulation of the DO_3SE model proposed by Emberson et al. (2000) which permits the use of the parameter f_{min} to model nighttime fluxes.

2)To better model performance, I proposed allowing the loading of mearsued soil moisture data. This would make using the model for single-site research simpler. In particular, when moisture influx is caused by irrigation and hasn't been accurately measured or when the soil structure is complex.

3) A tunable function that can model the reversible ROS-induced stomatal closure observed in addition to the currently available function that models the O_3-induced leaf senescence. These two functions describe two different biochemical processes.

The photosynthetic DO_3SE model too, would benefit from further improvements listed below:

1) The photosynthetic model can be improved by incorporating a non-linear approach of finding the relation between assimilation rate and conductance, represented in the model by tuning m.

2) The parameters V_{cmax} and J_{max} in the model control the net photosynthesis rate, which depends on the rate of carboxylation and electron transport. The photosynthetic DO_3SE only permits one set of these parameters to put in while tunning, which remains constant irrespective of the influence of factors like season, light and soil moisture. The model can be embedded with the ability to change V_{cmax} and J_{max} seasonally or, at the very least, have distinct values for the dormancy, reproductive, and vegetative growth stages. This would improve model performance.

3) Inclusion of the circadian rhythm that regulates stomatal conductance independently of assimilation, via a sine curve which tapers off overs several days when the plant is transferred to an environment with constant light, constant darkness or without CO_2.

4) My findings suggest that the photosynthetic model overestimates carbon assimilation during twilight conditions. This is possibly due to the linear relationship between stomatal conductance and assimilation in the current formulation and the optimization of the light

response function to reproduce stomatal conductance on cloudy days. I propose that stomatal conductance on overcast days must be managed using a separate circadian rhythm of stomatal conductance. This should allow to tune the light response function in a manner that lessens the overestimation of stomatal conductance during twilight conditions in the early morning and evening hours.

Are trees helpful in mitigating the exposure to air pollutants and trace gases for which emissions peak in the evening post sunset and or the early morning before sunrise, for example compounds emitted by traffic (NOx and PAHs)?

Many trees do not close their stomata fully at night and *Mangifera indica* is one such tree. While stomatal pollutant uptake is higher for ozone with 2.09 kg per tree and year than for gasses whose concentrations peak in the evening or at night such as NO_2 (0.93 kg per tree and year) and SO_2 (0.22 kg per tree and year) the stomatal uptake of gases that display higher mixing ratios at night is still significant. The nocturnal flux quantified by the photosynthetic model contributes 64%, 39%, 46%, and 88% of the total for NO_2 uptake in winter, summer, monsoon, and post-monsoon, respectively. The nocturnal uptake for SO_2 amounts to 38%, 30%, 31%, and 48% in winter, summer, monsoon, and post-monsoon, respectively.

Which uptake models are best capable of assessing the nighttime stomatal flux?

Assessment of nighttime uptake by trees is vital as stomata are not fully closed in the night hours. In the present formulation, the stomatal conductance of the multiplicative model is zero by definition at night. Even though the minimal value of conductance is set in the model, the multiplicative model writes zero flux values into the output file at night when solar radiation is less than 50 W m^{-2}. As a result, the current version of the multiplicative model is unsuitable for assessing the nighttime stomatal uptake of trace gases. A return to the original formulation of the DO_3SE model proposed by Emberson et al. (2000) which permits the use of the parameter f_{min} to model nighttime fluxes would enable the use of this model for the purpose.

The photosynthetic model has a parameter *gsto0 which can be used to set the stomatal conductance at night to the measured value. Hence the model can be used to assess night time fluxes in its current formulation. The photosynthetic model simulates the nocturnal stomatal conductance more precisely and is thus at present more suited to determine the pollutant uptake for pollutants mainly emitted at night. I also showed that the observed CO_2 flux can be simulated using the photosynthetic model. Thus, by using field measurements taken on

Mangifera indica, I showed that the photosynthetic model is superior to the multiplicative model, even for leaf-level research.

Additional findings beyond the original questions

My thesis shows that while isoprene and monoterpene emission rates under standardized conditions are available for many trees, the environmental response functions and the seasonality of emissions have been discussed to a much lesser degree. Experimental observations of stomatal conductance are still rare. Such data is available only for a very limited set of tropical trees. The environmental response functions of tropical tree species still leave a lot of room for new discoveries. In *Mangifera indica*, I found an exceptional tolerance to hot and dry air. The tree is capable of maintaining maximum stomatal conductance till a VPD_{max} of 8 kPa. This is more than double the highest VPD_{max} observed for any other tropical tree species so far studied and may be a peculiar adaptation of plant species that evolved to flower and fruit during the drought that precedes the onset of the rainy season in tropical winter dry climates. The high cooling potential of mango orchards during the hottest season of the year which is accompanied by high pollution tolerance may indeed by one of the key reasons why urban planners favor such plantations despite the fact that they fuel tropospheric ozone formation.

Future research can usefully extend and improve this work in many ways.

The final AQII can currently only be determined for 18 species. 80 species have a partial score mostly because their APTI and or stomatal conductance has not been studied till date. For 51 species with known isoprene emission potential the score cannot be computed because monoterpene emissions or pollen allergy potential have not been studied till date. Even detailed environmental response functions for most of the 18 tropical tree species for which the maximum stomatal conductance has been reported are not available in the literature till date.

List of Figures

List of Tables

List of Abbreviations

AOT40: Accumulated ozone exposure over a threshold of 40 ppb

API: Anticipated performance index

APTI: Air pollution tolerance index

AQII: Air Quality Impact Index

BDL: Below detection limit

BETHY: Biosphere Energy Transfer Hydrology

BVOCs: Biogenic volatile organic compounds

°C: Degree celsius

cm: centimetre

CO_2: Carbon dioxide

CLTRAP-EMEP: Convention on Long-Range Transboundary Air Pollution European Monitoring and Evaluation Programme

CRDS: Cavity ring-down spectrometer

CTEM: Canadian Terrestrial Ecosystem Model

DO_3SE: Deposition of Ozone for Stomatal Exchange

DDT: Dry deciduous tree

DS: Deciduous shrub

DT: Deciduous tree

EC: Evergreen conifer

ES: Evergreen shrub

ESMs: Earth System Models

ET: Evergreen tree

hPa: hecta pascal

ID: Internal diameter

IEP: Isoprene emission potential

J_{max}: Electron transport rate

JULES: Joint UK Land Environment Simulator

kg: Kilogram

kPa: kilo Pascal

L: Litre

LIA: Leaf area index

m: metre

MEGAN: Model of Emissions of Gases and Aerosols from Nature

MEP: Monoterpene emission potential

MIR: Maximum incremental reactivity coefficient

mL: millilitre

mm: millimetre

MSC: Maximum stomatal conductance

NE: Non-emitter

NO_2: Nitrogen dioxide

NOx: Nitrogen oxides

NW-IGP: Northwest Indo Gangetic Plain

O_3: Ozone

OD: Outer diameter

OFP: Ozone formation potential

OUP: Ozone uptake potential

PAHs: Polycyclic aromatic hydrocarbons

PAR: Photosynthetic active radiation

PI: Pollen impact

PM: Particulate matter

PO3M: Portable ozone monitor

ppb: Parts per billion

PTR-MS: Proton transfer reaction mass spectrometer

RH: Relative humidity

RMA: Reduced major axis

sccm: Standard cubic centimeter per minute

SM: Soil moisture

SO_2: Sulphur dioxide

SOA: Secondary organic aerosol

SOAFP: Secondary organic aerosol formation potential

Tg: Tera gram (= 10^{12} gram)

TO: Tropospheric ozone

UV: Ultraviolet

V_{cmax}: Rate of carboxylation

VOCs: Volatile organic compounds

VPD: Vapor pressure deficit

Bibliography

Abhijith, K.V., Kumar, P., Gallagher, J., McNabola, A., Baldauf, R., Pilla, F., Broderick, B., Di Sabatino, S., Pulvirenti, B., 2017. Air pollution abatement performances of green infrastructure in open road and built-up street canyon environments – A review. Atmospheric Environment 162, 71-86.

Alcock, I., White, M., Cherrie, M., Wheeler, B., Taylor, J., McInnes, R., Otte im Kampe, E., Vardoulakis, S., Sarran, C., Soyiri, I., Fleming, L., 2017. Land cover and air pollution are associated with asthma hospitalisations: A cross-sectional study. Environment international 109, 29-41.

Allan, D.J., Ratner, K., Giller, Y.E., Gussakovsky, E.E., Shahak, Y., Ort, D.A., 2000. An overnight chill induces a delayed inhibition of photosynthesis at midday in mango (Mangifera indica L.). Journal of Experimental Botany 51, 1893-1902.

Alonso, R., Elvira, S., Sanz, M.J., Gerosa, G., Emberson, L.D., Bermejo, V., Gimeno, B.S., 2008. Sensitivity analysis of a parameterization of the stomatal component of the DO3SE model for Quercus ilex to estimate ozone fluxes. Environmental Pollution 155, 473-480.

Anake, W., Bayode, F.O., Omonhinmin, C., Williams, A.B., 2018. Ambient air pollution control using air pollution tolerance index and anticipated performance index of trees. International Journal of Civil Engineering and Technology 9, 417-425.

Anderegg, W.R.L., Berry, J.A., Field, C.B., 2012. Linking definitions, mechanisms, and modeling of drought-induced tree death. Trends in Plant Science 17, 693-700.

Assis, P.I., Alonso, R., Meirelles, S.T., Moraes, R.M., 2015. DO3SE model applicability and O3 flux performance compared to AOT40 for an O3-sensitive tropical tree species (Psidium guajava L. 'Paluma'). Environ Sci Pollut Res Int 22, 10873-10881.

Atkinson, R., Arey, J., 2003. Atmospheric Degradation of Volatile Organic Compounds. Chemical Reviews 103, 4605-4638.

Baille, M., Baille, A., Laury, J.C., 1994. A simplified model for predicting evapotranspiration rate of nine ornamental species vs. climate factors and leaf area. Scientia Horticulturae 59, 217-232.

Bakiyaraj, R., Ayyappan, D., 2014. Air pollution tolerance index of some terrestrial plants around an industrial area International Journal of Modern Research and Reviews 2, 1-7.

Ball, J.T., Woodrow, I.E., Berry, J.A., 1987. A model predicting stomatal conductance and its contribution to the control of photosynthesis under different environmental conditions, Progress in photosynthesis research. Springer, pp. 221-224.

Barwise, Y., Kumar, P.J.N.C., Science, A., 2020. Designing vegetation barriers for urban air pollution abatement: a practical review for appropriate plant species selection. 3, 1-19.

Behbehani, N., Arifhodzic, N., Al-Mousawi, M., Marafie, S., Ashkanani, L., Moussa, M., Al-Duwaisan, A., 2004. The seasonal variation in allergic rhinitis and its correlation with outdoor allergens in Kuwait. Int Arch Allergy Immunol 133, 164-167.

Benjamin, M.T., Winer, A.M., 1998. Estimating the ozone-forming potential of urban trees and shrubs. Atmospheric Environment 32, 53-68.

Bharti, S., Trivedi, A., Kumar, N., 2017. Air pollution tolerance index of plants growing near an industrial site. Urban Climate 24.

Bhattacharya, K., Sircar, G., Dasgupta, A., Gupta Bhattacharya, S., 2018. Spectrum of Allergens and Allergen Biology in India. Int Arch Allergy Immunol 177, 219-237.

Biswas, S., Bala, S., Mazumdar, A., 2014. Diurnal and seasonal carbon sequestration potential of seven broadleaved species in a mixed deciduous forest in India. Atmospheric Environment 89, 827-834.

Bonan, G., Williams, M., Fisher, R., Oleson, K., 2014. Modeling stomatal conductance in the Earth system: Linking leaf water-use efficiency and water transport along the soil-plant-atmosphere continuum. Geoscientific Model Development 7, 2193-2222.

Bonan, G.B., 1995. Land-atmosphere CO2 exchange simulated by a land surface process model coupled to an atmospheric general circulation model. J. Geophys. Res. 100D, 2817-2831.

Bonn, B., von Schneidemesser, E., Butler, T., Churkina, G., Ehlers, C., Grote, R., Klemp, D., Nothard, R., Schäfer, K., von Stülpnagel, A., Kerschbaumer, A., Yousefpour, R., Fountoukis, C., Lawrence, M.G., 2018. Impact of vegetative emissions on urban ozone and biogenic secondary organic aerosol: Box model study for Berlin, Germany. Journal of Cleaner Production 176, 827-841.

Boral, D., Chatterjee, S., Bhattacharya, K., 2004. The occurrence and allergising potential of airborne pollen in West Bengal, India. 11, 45-52.

Buck, A.L., 1981. New equations for computing vapor pressure and enhancement factor. Journal of Applied Meteorology and Climatology 20, 1527-1532.

Büker, P., Emberson, L.D., Ashmore, M.R., Cambridge, H.M., Jacobs, C.M., Massman, W.J., Müller, J., Nikolov, N., Novak, K., Oksanen, E., Schaub, M., de la Torre, D., 2007. Comparison of different stomatal conductance algorithms for ozone flux modelling. Environ Pollut 146, 726-735.

Büker, P., Feng, Z., Uddling, J., Briolat, A., Alonso, R., Braun, S., Elvira, S., Gerosa, G., Karlsson, P.E., Le Thiec, D., Marzuoli, R., Mills, G., Oksanen, E., Wieser, G., Wilkinson, M., Emberson, L.D., 2015. New flux based dose–response relationships for ozone for European forest tree species. Environmental Pollution 206, 163-174.

Cabaraban, M.T.I., Kroll, C.N., Hirabayashi, S., Nowak, D.J., 2013. Modeling of air pollutant removal by dry deposition to urban trees using a WRF/CMAQ/i-Tree Eco coupled system. Environmental Pollution 176, 123-133.

Caird, M.A., Richards, J.H., Donovan, L.A.J.P.p., 2007. Nighttime stomatal conductance and transpiration in C3 and C4 plants. 143, 4-10.

Calfapietra, C., Fares, S., Manes, F., Morani, A., Sgrigna, G., Loreto, F., 2013. Role of Biogenic Volatile Organic Compounds (BVOC) emitted by urban trees on ozone concentration in cities: A review. Environmental Pollution 183, 71-80.

Campbell, G.S., Norman, J.M., 2000. Water Vapor and Other Gases, in: Campbell, G.S., Norman, J.M. (Eds.), An Introduction to Environmental Biophysics (2nd edition). Springer USA, New York, NY, p. 286.

Cariñanos, P., Casares-Porcel, M., 2011. Urban green zones and related pollen allergy: A review. Some guidelines for designing spaces with low allergy impact. Landscape and Urban Planning 101, 205-214.

Cariñanos, P., Grilo, F., Pinho, P., Casares-Porcel, M., Branquinho, C., Acil, N., Andreucci, M.B., Anjos, A., Bianco, P.M., Brini, S., Calaza-Martínez, P., Calvo, E., Carrari, E., Castro, J., Chiesura, A., Correia, O., Gonçalves, A., Gonçalves, P., Mexia, T., Mirabile, M., Paoletti, E., Santos-Reis, M., Semenzato, P., Vilhar, U., 2019. Estimation of the Allergenic Potential of Urban Trees and Urban Parks: Towards the Healthy Design of Urban Green Spaces of the Future. Int J Environ Res Public Health 16.

Carlton, A.G., Wiedinmyer, C., Kroll, J.H., 2009. A review of Secondary Organic Aerosol (SOA) formation from isoprene. Atmos. Chem. Phys. 9, 4987-5005.

Carter, W.P.L., 1994. Development of Ozone Reactivity Scales for Volatile Organic Compounds. Air & Waste 44, 881-899.

Carter, W.P.L., 2010. Development of the SAPRC-07 chemical mechanism. Atmospheric Environment 44, 5324-5335.

Cassimiro, J.C., Moura, B.B., Alonso, R., Meirelles, S.T., Moraes, R.M., 2016. Ozone stomatal flux and O3 concentration-based metrics for Astronium graveolens Jacq., a Brazilian native forest tree species. Environmental Pollution 213, 1007-1015.

Chakraborty, P., Ghosal, K., Sarkar, E., Bhattacharya, S.G., 2016. Atmospheric pollen grains of a suburban area near India-Bangladesh border with reference to their allergenic potential and probable effect on asthma-related hospital admission. Current Science 111, 1486-1491.

Chan, A., Chan, M.N., Surratt, J., Chhabra, P., Loza, C., Crounse, J., Yee, L., Flagan, R., Wennberg, P., Seinfeld, J., 2010. Role of aldehyde chemistry and NOx concentrations in secondary organic aerosol formation. Atmospheric Chemistry and Physics 10, 7169-7188.

Chandrappa, R., Chandra Kulshrestha, U., 2016. Fundamentals of Treatment, and Process Design for Air Pollution Control, in: Chandrappa, R., Chandra Kulshrestha, U. (Eds.), Sustainable Air Pollution Management: Theory and Practice. Springer International Publishing, Cham, pp. 141-206.

Chaparro-Suarez, I., Meixner, F., Kesselmeier, J., 2011. Nitrogen dioxide (NO2) uptake by vegetation controlled by atmospheric concentrations and plant stomatal aperture. Atmospheric Environment 45, 5742-5750.

Chaturvedi, R., Prasad, S., Rana, S., Obaidullah, S., Pandey, V., Singh, H., 2013. Effect of dust load on the leaf attributes of the tree species growing along the roadside. Environmental Monitoring and Assessment 185.

Chaudhary, P., Singh, R., Shabin, M., Sharma, A., Bhatt, S., Sinha, V., Sinha, B., 2022. Replacing the greater evil: Can legalizing decentralized waste burning in improved devices reduce waste burning emissions for improved air quality? Environmental Pollution 311, 119897.

Chauhan, S.V.S., Goyal, R., 2006. Pollen calendar of Agra city with special reference to allergenic significance. Journal of Environmental Biology 27, 275-281.

Chaurasia, S., 2017. Pollen morphotypes of some common tree flora of Allahabad. International Journal of Multidisciplinary Research and Development 4, 151-157.

Chen, D., Wang, Y., Liu, S., Wei, X., Wang, X., 2014. Response of relative sap flow to meteorological factors under different soil moisture conditions in rainfed jujube (Ziziphus jujuba Mill.) plantations in semiarid Northwest China. Agricultural Water Management 136, 23-33.

Chun, B., Guldmann, J.-M., 2018. Impact of greening on the urban heat island: Seasonal variations and mitigation strategies. Computers Environment and Urban Systems 71, 165-176.

Churkina, G., Grote, R., Butler, T.M.a., Lawrence, M., 2015. Natural selection? Picking the right trees for urban greening. Environmental Science & Policy 47, 12-17.

Churkina, G., Kuik, F., Bonn, B., Lauer, A., Grote, R., Tomiak, K., Butler, T.M., 2017. Effect of VOC Emissions from Vegetation on Air Quality in Berlin during a Heatwave. Environ Sci Technol 51, 6120-6130.

Corchnoy, S.B., Arey, J., Atkinson, R., 1992. Hydrocarbon emissions from twelve urban shade trees of the Los Angeles, California, Air Basin. Atmospheric Environment. Part B. Urban Atmosphere 26, 339-348.

Cox, P.M., Huntingford, C., Harding, R.J., 1998. A canopy conductance and photosynthesis model for use in a GCM land surface scheme. Journal of Hydrology 212-213, 79-94.

da Silva, C.M., Corrêa, S.M., Arbilla, G., 2018. Isoprene Emissions and Ozone Formation in Urban Conditions: A Case Study in the City of Rio de Janeiro. Bulletin of Environmental Contamination and Toxicology 100, 184-188.

Dabadge, A., Sreenivas, A., Josey, A., 2018. What has the Pradhan Mantri Ujjwala Yojana achieved so far. Econ Polit Wkly 53, 69-75.

Daley, M.J., Phillips, N.G., 2006. Interspecific variation in nighttime transpiration and stomatal conductance in a mixed New England deciduous forest. Tree physiology 26, 411-419.

Damour, G., Simonneau, T., Cochard, H., Urban, L., 2010. An overview of models of stomatal conductance at the leaf level. Plant Cell Environ 33, 1419-1438.

Danielsson, H., Karlsson, G.P., Karlsson, P.E., Pleijel, H., 2003. Ozone uptake modelling and flux-response relationships—an assessment of ozone-induced yield loss in spring wheat. Atmospheric Environment 37, 475-485.

Darmayanti, A.S., Fiqa, A.P., 2017. The Canopy Structure and Its Impact on Hydrological Performance of Five Local Trees Species Grown in the Purwodadi Botanic Garden. The Journal of Tropical Life Science 7, 40-47.

Das, S., Prasad, P., 2010. Seasonal variation in air pollution tolerance indices and selection of plant species for industrial areas of Rourkela. Indian Journal of Environmental Protection 30, 978-988.

Datta, S., Sharma, A., Parkar, V., Hakkim, H., Kumar, A., Chauhan, A., Tomar, S.S., Sinha, B., 2021. A new index to assess the air quality impact of urban tree plantation. Urban Climate 40, 100995.

Dawson, T.E., Burgess, S.S., Tu, K.P., Oliveira, R.S., Santiago, L.S., Fisher, J.B., Simonin, K.A., Ambrose, A.R., 2007. Nighttime transpiration in woody plants from contrasting ecosystems. Tree physiology 27, 561-575.

De Kauwe, M.G., Kala, J., Lin, Y.S., Pitman, A.J., Medlyn, B.E., Duursma, R.A., Abramowitz, G., Wang, Y.P., Miralles, D.G., 2015. A test of an optimal stomatal conductance scheme within the CABLE land surface model. Geosci. Model Dev. 8, 431-452.

Dios de, V.R., Gessler, l., 2018. Circadian regulation of photosynthesis and transpiration from genes to ecosystems. Environmental and Experimental Botany 152, 37-48.

Dodd, A.N., Kusakina, J., Hall, A., Gould, P.D., Hanaoka, M., 2014. The circadian regulation of photosynthesis. Photosynthesis Research 119, 181-190.

Dusart, N., Vaultier, M.-N., Olry, J.-C., Buré, C., Gérard, J., Jolivet, Y., Le Thiec, D., 2019. Altered stomatal dynamics of two Euramerican poplar genotypes submitted to successive ozone exposure and water deficit. Environmental Pollution 252, 1687-1697.

Eisenman, T., Churkina, G., Jariwala, S., Kumar, P., Lovasi, G., Pataki, D., Weinberger, K., Whitlow, T., 2019. Urban trees, air quality, and asthma: An interdisciplinary review. Landscape and Urban Planning 187, 47-59.

Eisikowitch, D., Ghara, M., 2017. An overview on Ficus pollination. Acta Horticulturae 1173, 143-148.

Elsheery, N.I., Cao, K.-F., 2008. Gas exchange, chlorophyll fluorescence, and osmotic adjustment in two mango cultivars under drought stress. Acta Physiologiae Plantarum 30, 769-777.

Emberson, L.D., Ashmore, M.R., Cambridge, H.M., Simpson, D., Tuovinen, J.P., 2000. Modelling stomatal ozone flux across Europe. Environ Pollut 109, 403-413.

Emberson, L.D., Büker, P., Ashmore, M.R., 2007. Assessing the risk caused by ground level ozone to European forest trees: a case study in pine, beech and oak across different climate regions. Environ Pollut 147, 454-466.

Endres, L., 2007. Daily and seasonal variation of water relationship in sugar apple (Annona squamosa L.) under different irrigation regimes at semi-arid Brazil. Scientia Horticulturae 113, 149-154.

Erskine, P.D., Lamb, D., Borschmann, G., 2005. Growth performance and management of a mixed rainforest tree plantation. New Forests 29, 117-134.

Evans, R.C., Tingey, D.T., Gumpertz, M.L., Burns, W.F., 1982. Estimates of Isoprene and Monoterpene Emission Rates in Plants. Botanical Gazette 143, 304-310.

Fares, S., Gentner, D.R., Park, J.-H., Ormeno, E., Karlik, J., Goldstein, A.H., 2011. Biogenic emissions from Citrus species in California. Atmospheric Environment 45, 4557-4568.

Fares, S., Matteucci, G., Mugnozza, G., Morani, A., Calfapietra, C., Salvatori, E., Fusaro, L., Manes, F., Loreto, F., 2013. Testing of models of stomatal ozone fluxes with field measurements in a mixed Mediterranean forest. Atmospheric Environment 67, 242-251.

Farquhar, G.D., von Caemmerer, S., Berry, J.A., 1980. A biochemical model of photosynthetic CO2 assimilation in leaves of C3 species. Planta 149, 78-90.

Flato, G.M., 2011. Earth system models: an overview. WIREs Clim Change 2, 783-800.

Gargi, Sinha, A.K., 2017. Floral biology and breeding behaviour in Terminalia belerica and Terminalia chebula. Indian Forester 143, 499-504.

Georgi, N.J., Zafiriadis, K., 2006. The impact of park trees on microclimate in urban areas. Urban Ecosystems 9, 195-209.

Geron, C., Harley, P., Guenther, A.J.A.E., 2001. Isoprene emission capacity for US tree species. 35, 3341-3352.

Geron, C., Owen, S., Guenther, A., Greenberg, J., Rasmussen, R., Hui Bai, J., Li, Q.-J., Baker, B., 2006. Volatile organic compounds from vegetation in southern Yunnan Province, China: Emission rates and some potential regional implications. Atmospheric Environment 40, 1759-1773.

Gessler, A., Rienks, M., Rennenberg, H., 2000. NH3 and NO2 fluxes between beech trees and the atmosphere – correlation with climatic and physiological parameters. New Phytologist 147, 539-560.

Giri, S., Shrivastava, D., Deshmukh, K., Dubey, P., 2013. Effect of air pollution on chlorophyll content of leaves. Current Agriculture Research Journal 1, 93-98.

Gómez, M.C., Durana, N., García, J.A., de Blas, M., Sáez de Cámara, E., García-Ruiz, E., Gangoiti, G., Torre-Pascual, E., Iza, J., 2020. Long-term measurement of biogenic volatile organic compounds in a rural background area: Contribution to ozone formation. Atmospheric Environment 224, 117315.

Gonzalez–Fernandez, I., Kaminska, A., Dodmani, M., Goumenaki, E., Quarrie, S., Barnes, J.D., 2010. Establishing ozone flux–response relationships for winter wheat: analysis of uncertainties based on data for UK and polish genotypes. Atmospheric Environment 44, 621-630.

Govindarajulu, D., 2014. Urban green space planning for climate adaptation in Indian cities. Urban Climate 10.

Grantz, D.A., Garner, J.H.B., Johnson, D.W., 2003. Ecological effects of particulate matter. Environment international 29, 213-239.

Grote, R., Samson, R., Alonso, R., Amorim, J., Carinanos, P., Churkina, G., Fares, S., Le Thiec, D., Niinemets, Ü., Mikkelsen, T., Tiwary, A., Calfapietra, C., 2016. Functional traits of urban trees: Air pollution mitigation potential. Frontiers in Ecology and the Environment 14, 543-550.

Guenther, A., Greenberg, J., Harley, P., Helmig, D., Klinger, L., Vierling, L., Zimmerman, P., Geron, C.J.T.P., 1996. Leaf, branch, stand and landscape scale measurements of volatile organic compound fluxes from US woodlands. 16, 17-24.

Guenther, A., Hewitt, C.N., Erickson, D., Fall, R., Geron, C., Graedel, T., Harley, P., Klinger, L., Lerdau, M., Mckay, W.A., Pierce, T., Scholes, B., Steinbrecher, R., Tallamraju, R., Taylor, J., Zimmerman, P., 1995. A global model of natural volatile organic compound emissions. Journal of Geophysical Research 100, 8873-8892.

Guenther, A., Karl, T., Harley, P., Wiedinmyer, C., Palmer, P.I., Geron, C., 2006. Estimates of global terrestrial isoprene emissions using MEGAN (Model of Emissions of Gases and Aerosols from Nature). Atmos. Chem. Phys. 6, 3181-3210.

Guenther, A.B., Jiang, X., Heald, C.L., Sakulyanontvittaya, T., Duhl, T., Emmons, L.K., Wang, X., 2012. The Model of Emissions of Gases and Aerosols from Nature version 2.1 (MEGAN2.1): an extended and updated framework for modeling biogenic emissions. Geoscientific Model Development 5, 1471-1492.

Guidi, L., Panicucci, A., Lorenzini, G., Soldatini, G., 1993. Ozone-induced changes in chlorophyll fluorescence kinetics and CO2 assimilation in Vicia faba. Journal of plant physiology 141, 545-550.

Gulia, S., Shiva Nagendra, S.M., Khare, M., Khanna, I., 2015. Urban air quality management-A review. Atmospheric Pollution Research 6, 286-304.

Gurjar, B.R., Ravindra, K., Nagpure, A.S., 2016. Air pollution trends over Indian megacities and their local-to-global implications. Atmospheric Environment 142, 475-495.

Guttikunda, S.K., Goel, R., Pant, P., 2014. Nature of air pollution, emission sources, and management in the Indian cities. Atmospheric Environment 95, 501-510.

Hakkim, H., Kumar, A., Sinha, B., Sinha, V., 2022. Air pollution scenario analyses of fleet replacement strategies to accomplish reductions in criteria air pollutants and 74 VOCs over India. Atmospheric Environment: X 13, 100150.

Hakkim, H., Sinha, V., Chandra, B.P., Kumar, A., Mishra, A.K., Sinha, B., Sharma, G., Pawar, H., Sohpaul, B., Ghude, S.D., Pithani, P., Kulkarni, R., Jenamani, R.K., Rajeevan, M., 2019. Volatile organic compound measurements point to fog-induced biomass burning feedback to air quality in the megacity of Delhi. Science of The Total Environment 689, 295-304.

Hao, G.-Y., Sack, L., Wang, A.-Y., Cao, K.-F., Goldstein, G., 2010. Differentiation of leaf water flux and drought tolerance traits in hemiepiphytic and non-hemiepiphytic Ficus tree species. Functional Ecology 24, 731-740.

Hatamimanesh, M., Mortazavi, S., Solgi, E., Mohtadi, A.J.J.o.A.i.E.H.R., 2021. Assessment of Tolerance of Some Tree Species to Air Con-tamination Using Air Pollution Tolerance and Anticipated Performance Indices in Isfahan City, Iran. 9, 31-44.

Haverd, V., Smith, B., Nieradzik, L., Briggs, P.R., Woodgate, W., Trudinger, C.M., Canadell, J.G., Cuntz, M., 2018. A new version of the CABLE land surface model (Subversion revision r4601) incorporating land use and land cover change, woody vegetation demography, and a novel optimisation-based approach to plant coordination of photosynthesis. Geosci. Model Dev. 11, 2995-3026.

Helmig, D., Ortega, J., Duhl, T., Tanner, D., Guenther, A., Harley, P., Wiedinmyer, C., Milford, J., Sakulyanontvittaya, T., 2007. Sesquiterpene emissions from pine trees--identifications, emission rates and flux estimates for the contiguous United States. Environ Sci Technol 41, 1545-1553.

Hennessey, T.L., Freeden, A.L., Field, C.B., 1993. Environmental effects on circadian rhythms in photosynthesis and stomatal opening. Planta 189, 369-376.

Hirons, A., Sjöman, H., 2019. Tree species selection for green infrastructure: a guide for specifiers. Trees & Design Action Group.

Hoshika, Y., Fares, S., Savi, F., Gruening, C., Goded, I., De Marco, A., Sicard, P., Paoletti, E., 2017. Stomatal conductance models for ozone risk assessment at canopy level in two Mediterranean evergreen forests. Agricultural Forest Meteorology 234, 212-221.

Hoshika, Y., Osada, Y., de Marco, A., Peñuelas, J., Paoletti, E., 2018. Global diurnal and nocturnal parameters of stomatal conductance in woody plants and major crops. 27, 257-275.

Hu, W., Chen, L., Qiu, X., Lu, H., Wei, J., Bai, Y., He, N., Hu, R., Sun, L., Zhang, H., Shen, G., 2016. Morphological, Physiological and Proteomic Analyses Provide Insights into the Improvement of Castor Bean Productivity of a Dwarf Variety in Comparing with a High-Stalk Variety. Frontiers in plant science 7, 1473-1473.

Huang, Y., Wang, Y.-P., Ziehn, T., 2021. Nonlinear interactions of land carbon cycle feedbacks in Earth System Models. Global change biol. 28, 296-306.

Hussain, M.M., Mandal, J., Bhattacharya, K., 2014. Aerobiological, clinical, and immunobiochemical studies on Alstonia scholaris pollen from eastern India. Environmental Monitoring and Assessment 186, 457-467.

Jaganmohan, M., Vailshery, L., Mundoli, S., Nagendra, H., 2018. Biodiversity in sacred urban spaces of Bengaluru, India. Urban Forestry & Urban Greening 32, 64–70

Jarvis, P.G., Monteith, J.L., Weatherley, P.E., 1976. The interpretation of the variations in leaf water potential and stomatal conductance found in canopies in the field. Phil. Trans. R. Soc. Lond. 273, 593-610.

Jat, H.S., Mann, J.S., Sharma, S.C., Chand, R., 2010. Identification of best performing ardu (Ailanthus excelsa) genotypes in semi-arid ecosystems of Rajasthan. Indian Journal of Agricultural Sciences 80, 227-230.

Jhou, H.C., Wang, Y.N., Wu, C.S., Yu, J.C., Chen, C.I., 2017. Photosynthetic gas exchange responses of Swietenia macrophylla King and Melia azedarach L. plantations under drought conditions. Bot Stud 58, 57.

Jiang, L., O'Neill, B.C., 2017. Global urbanization projections for the Shared Socioeconomic Pathways. Global Environmental Change 42, 193-199.

Jiang, N., Yin, J., Mak, P., Wen, L.J.I.J.o.A., Asthma, Immunology, 2015. Occupational allergy to peach (Prunus persica) tree pollen and potential cross-reactivity between rosaceae family pollens. 14, 483-492.

Jing, X., Lun, X., Fan, C., Ma, W., 2020. Emission patterns of biogenic volatile organic compounds from dominant forest species in Beijing, China. Journal of Environmental Sciences 95, 73-81.

Kalinganire, A., Harwood, C., Slee, M., Simons, A., 2001. Pollination and fruit-set of Grevillea robusta in western Kenya. Austral ecology 26, 637-648.

Kamble, P., Bodhane, P.S., Beig, G., Awale, M., Mukkannawar, U., Mane, A.V., Mujumdar, M., Kuchekar, S.R., Patil, V.N., 2021. Impact of transport sector emissions on biochemical characteristics of plants and mitigation strategy in Pune, India. Environmental Challenges 4, 100081.

Kapoor, C.S., Bamniya, B.R., Kapoor, K., 2013. Efficient control of air pollution through plants, a cost-effective alternative: studies on Dalbergia sissoo Roxb. Environmental Monitoring and Assessment 185, 7565-7580.

Karlik, J.F., Pittenger, D. R., 2012. Urban Trees and Ozone Formation: A Consideration for Large-Scale Plantings.

Karmakar, D., Deb, K., Padhy, P.K., 2021. Ecophysiological responses of tree species due to air pollution for biomonitoring of environmental health in urban area. Urban Climate 35, 100741.

Karmakar, D., Ghosh, T., Padhy, P.K., 2019. Effects of air pollution on carbon sequestration potential in two tropical forests of West Bengal, India. Ecological Indicators 98, 377-388.

Kashyap, R., Sharma, R., Uniyal, S.K., 2018. Bioindicator responses and performance of plant species along a vehicular pollution gradient in western Himalaya. Environmental Monitoring and Assessment 190, 302.

Kaur, M., Nagpal, A.K., 2017. Evaluation of air pollution tolerance index and anticipated performance index of plants and their application in development of green space along the urban areas. Environmental Science and Pollution Research 24, 18881-18895.

Keller, T., 1986. The electrical conductivity of Norway spruce needle diffusate as affected by certain air pollutants. Tree physiology 1, 85-94.

Keller, T., Schwager, H., 1977. Air pollution and ascorbic acid. European Journal of Forest Pathology 7, 338-350.

Khera, N., Mehta, V., Sabata, B.C., 2009. Interrelationship of birds and habitat features in urban greenspaces in Delhi, India. Urban Forestry & Urban Greening 8, 187-196.

Kim, J.I., Kim, G., 2016. Country-level socioeconomic indicators associated with healthy life expectancy: income, urbanization, schooling, and internet users: 2000–2012. Social Indicators Research 129, 391-402.

Klinger, L., Li, Q., Guenther, A., Greenberg, J., Baker, B., Bai, J., 2002. Assessment of volatile organic compound emissions from ecosystems of China. Journal of Geophysical Research 107, 4603-4603.

Koedsin, W., Yasen, K., 2016. Estimating Leaf Area Index of Rubber Tree Plantation Using Worldview-2 Imagery. Journal of Life Sciences and Technologies 4, 1-6.

Koricho, H.H., Seboka, A.D., Song, S., 2020. Ecosytem Services Assessment of Urban Forests of Adama City, Ethiopia. preprint 10.21203/rs.3.rs-24636/v1.

Körner, C., 2003. Carbon limitation in trees. J. Ecol. 91, 4-17.

Körner, C., 2015. Paradigm shift in plant growth control. Current Opinion in Plant Biology 25, 107-114.

Krishen, P., 2006. Trees of Delhi: A field guide. Penguin Books, New Delhi India.

Krishnaveni, M., Kalimuthu, R., Ponraj, K., Lavanya., K., Magesh, P., Jasbin, S.G., 2014. Air Pollution Tolerance Index Assessment of Yercaud Road Side Plants. International Journal of Pharmaceutical Sciences Review and Research 26, 177-181.

Kumar, V., Sarkar, C., Sinha, V., 2016. Influence of post-harvest crop residue fires on surface ozone mixing ratios in the N.W. IGP analyzed using 2 years of continuous in situ trace gas measurements. Journal of Geophysical Research: Atmospheres 121, 3619-3633.

Lamarque, J.F., Bond, T.C., Eyring, V., Granier, C., Heil, A., Klimont, Z., Lee, D., Liousse, C., Mieville, A., Owen, B., Schultz, M.G., Shindell, D., Smith, S.J., Stehfest, E., Van Aardenne, J., Cooper, O.R., Kainuma, M., Mahowald, N., McConnell, J.R., Naik, V., Riahi, K., van Vuuren, D.P., 2010. Historical (1850–2000) gridded anthropogenic and biomass burning emissions of reactive gases and aerosols: methodology and application. Atmos. Chem. Phys. 10, 7017-7039.

Landrigan, P., 2017. Air pollution and health. The Lancet Public Health 2, e4-e5.

Laothawornkitkul, J., Taylor, J.E., Paul, N.D., Hewitt, C.N., 2009. Biogenic volatile organic compounds in the Earth system. New Phytologist 183, 27-51.

Lee, E.H., 1991. Plant resistance mechanisms to air pollutants: rhythms in ascorbic acid production during growth under ozone stress. Chronobiology international 8, 93-102.

Lelieveld, J., Dentener, F.J., Peters, W., Krol, M.C., 2004. On the role of hydroxyl radicals in the self-cleansing capacity of the troposphere. Atmos. Chem. Phys. 4, 2337-2344.

Li, S., Dai, L., Wang, H., Wang, Y., He, Z., Lin, S., 2017. Estimating Leaf Area Density of Individual Trees Using the Point Cloud Segmentation of Terrestrial LiDAR Data and a Voxel-Based Model. Remote Sensing 9.

Liu, H., Cui, W., Zhang, M., 2022. Exploring the causal relationship between urbanization and air pollution: Evidence from China. Sustainable Cities and Society 80, 103783.

Liu, X., Lu, Y., Xie, Y., Xue, Y., 2015. The positive interaction between two nonindigenous species, Casuarina (Casuarina equisetifolia) and Acacia (Acacia mangium), in the tropical coastal zone of south China: stand dynamics and soil nutrients. Tropical Conservation Science 8, 598-609, 512.

Mäenpää, M., Riikonen, J., Kontunen-Soppela, S., Rousi, M., Oksanen, E.J.T.p., 2011. Vertical profiles reveal impact of ozone and temperature on carbon assimilation of Betula pendula and Populus tremula. 31, 808-818.

Mage, D., Ozolins, G., Peterson, P., Webster, A., Orthofer, R., Vandeweerd, V., Gwynne, M., 1996. Urban air pollution in megacities of the world. Atmospheric Environment 30, 681-686.

Malik, T.G., Gajbhiye, T., Pandey, S.K., 2018. Plant specific emission pattern of biogenic volatile organic compounds (BVOCs) from common plant species of Central India. Environ Monit Assess 190, 631.

Mandal, J., Chakraborty, P., Roy, I., Chatterjee, S., Gupta-Bhattacharya, S., 2008. Prevalence of allergenic pollen grains in the aerosol of the city of Calcutta, India: a two year study. Aerobiologia 24, 151-164.

Marselle, M.R., Bowler, D.E., Watzema, J., Eichenberg, D., Kirsten, T., Bonn, A., 2020. Urban street tree biodiversity and antidepressant prescriptions. Scientific reports 10, 1-11.

Massman, W.J., 1998. A review of the molecular diffusivities of H2O, CO2, CH4, CO, O3, SO2, NH3, N2O, NO, and NO2 in air, O2 and N2 near STP. Atmospheric Environment 32, 1111-1127.

Matyssek, R., Wieser, G., Nunn, A., Kozovits, A., Reiter, I., Heerdt, C., Winkler, J., Baumgarten, M., Häberle, K.-H., Grams, T.J.A.E., 2004. Comparison between AOT40 and ozone uptake in forest trees of different species, age and site conditions. 38, 2271-2281.

McAdam, E.L., Brodribb, T.J., McAdam, S.A.J.P., Cell, Environment, 2017. Does ozone increase ABA levels by non-enzymatic synthesis causing stomata to close? 40, 741-747.

Mills, G., Harmens, H., Hayes, F., Pleijel, H., Büker, P., González, I., Alonso, R., Bender, J., Bergmann, E., Bermejo, V., Braun, S., Danielsson, H., Gerosa, G., Grünhage, L., Karlsson, P., Marzuoli, R., Schaub, M., Simpson, D., 2017. MAPPING CRITICAL LEVELS FOR VEGETATION Revised Chapter 3 of the Manual on Methodologies and Criteria for Modelling and Mapping Critical Loads and Levels and Air Pollution Effects, Risks and Trends.

Mishra, R.P., Singh, B., Oommachan, M., 2002. Airborne pollen flora of Jabalur–the central India. Aerobiologia 18, 73-81.

Mo, L., li, W., Ye, Y., Zhou, Y., Liu, S., Su, Z., 2014. Using Hemispherical Photography to Determine Leaf Area Index of Landscape Trees in Urban Green Space of Dongguan, South China. Advanced Materials Research 955-959, 4034-4038.

Mohammed, K., Kumari, R., and, Ramteke, P.W., 2011. Studies on air pollution tolerance of selected plants in Allahabad city, India. E3 Journal of Environmental Research and Management 2, 42-46.

Molnár, V.É., Tőzsér, D., Szabó, S., Tóthmérész, B., Simon, E.J.P., 2020. Use of leaves as bioindicator to assess air pollution based on composite proxy measure (APTI), dust amount and elemental concentration of metals. 9, 1743.

Mondal, A.K., Mondal, S., Mandal, S., 1998. Pollen production in some plant taxa with a supposed role in allergy in Eastern India. Aerobiologia 14, 397.

Morecroft, M.D., Roberts, J.M., 1999. Photosynthesis and stomatal conductance of mature canopy Oak (Quercus robur) and Sycamore (Acer pseudoplatanus) trees throughout the growing season. Functional Ecology 13, 332-342.

Moura, B.B., Brunetti, C., Engela, M.R.G.d.S., Hoshika, Y., Paoletti, E., Ferrini, F., 2021. Experimental assessment of ozone risk on ecotypes of the tropical tree Moringa oleifera. Environmental Research 201, 111475.

Murthy, R., Barron-Gafford, G., Dougherty, P.M., Engel, V.C., Grieve, K., Handley, L., Klimas, C., Potosnak, M.J., Zarnoch, S.J., Zhang, J., 2005. Increased leaf area dominates carbon flux response to elevated CO2 in stands of Populus deltoides (Bartr.). Global Change Biology 11, 716-731.

Mushtaq, Kurubar, A.R., Umesh, M.R., Patil, S., Hugar, A., 2019. Nutrient requirement, canopy development and fruit yield of high density guava (Psidium guajava L.) production in subtropics of Northern Karnataka. Journal of Applied and Natural Science 11, 440-444.

Nadgórska–Socha, A., Kandziora-Ciupa, M., Trzęsicki, M., Barczyk, G.J.C., 2017. Air pollution tolerance index and heavy metal bioaccumulation in selected plant species from urban biotopes. 183, 471-482.

Neinavaz, E., Skidmore, A., Darvishzadeh, R., Groen, T.A., 2016. Leaf area index retrieved from thermal hyperspectral data. International Archives of the Photogrammetry, Remote Sensing and Spatial Information Sciences XLI-B7, 99-105.

Ng, N.L., Chhabra, P.S., Chan, A.W.H., Surratt, J.D., Kroll, J.H., Kwan, A.J., McCabe, D.C., Wennberg, P.O., Sorooshian, A., Murphy, S.M., Dalleska, N.F., Flagan, R.C., Seinfeld, J.H., 2007. Effect of NOx level on secondary organic aerosol (SOA) formation from the photooxidation of terpenes. Atmos. Chem. Phys. 7, 5159-5174.

Nikolov, N.T., Massman, W.J., Schoettle, A.W., 1995. Coupling biochemical and biophysical processes at the leaf level: an equilibrium photosynthesis model for leaves of C3 plants. Ecological Modelling 80, 205-235.

Nirgude, V., Karuna, K., Mankar, A., Kumar, V., Spandana, M., 2016. Response of NPK fertigation on pheno-physiological status of Citrus sinensis Osbeck cv. Mosambi under high density planting. Journal of Applied and Natural Science 8, 1306-1311.

Noe, S.M., Peñuelas, J., Niinemets, U., 2008. Monoterpene emissions from ornamental trees in urban areas: a case study of Barcelona, Spain. Plant Biology 10, 163-169.

Novick, R.R., Dick, C.w., Lemes, M.R., Navarro, C., Caccone, A., Bermingham, E., 2003. Genetic structure of Mesoamerican populations of Big-leaf mahogany (Swietenia macrophylla) inferred from microsatellite analysis. 12, 2885-2893.

Nowak, D.J., Civerolo, K.L., Trivikrama Rao, S., Gopal, S., Luley, C.J., E. Crane, D., 2000. A modeling study of the impact of urban trees on ozone. Atmospheric Environment 34, 1601-1613.

Nowak, D.J., Crane, D.E., Stevens, J.C., 2006. Air pollution removal by urban trees and shrubs in the United States. Urban Forestry & Urban Greening 4, 115-123.

Ortega, J., Helmig, D., 2008. Approaches for quantifying reactive and low-volatility biogenic organic compound emissions by vegetation enclosure techniques - part A. Chemosphere 72, 343-364.

Ortega, J., Helmig, D., Daly, R.W., Tanner, D.M., Guenther, A.B., Herrick, J.D., 2008. Approaches for quantifying reactive and low-volatility biogenic organic compound emissions by vegetation enclosure techniques - part B: applications. Chemosphere 72, 365-380.

Osborne, S., Pandey, D., Mills, G., Hayes, F., Harmens, H., Gillies, D., Büker, P., Emberson, L., 2019. New insights into leaf physiological responses to ozone for use in crop modelling. Plants 8, 84.

Ottelé, M., van Bohemen, H.D., Fraaij, A.L., 2010. Quantifying the deposition of particulate matter on climber vegetation on living walls. Ecological engineering 36, 154-162.

Owen, S.M., Boissard, C., Hagenlocher, B., Hewitt, C.N.J.J.o.G.R.A., 1998. Field studies of isoprene emissions from vegetation in the Northwest Mediterranean region. 103, 25499-25511.

Owen, S.M., MacKenzie, A.R., Stewart, H., Donovan, R., Hewitt, C.N., 2003. Biogenic volatile organic compound (voc) emission estimates from an urban tree canopy. 13, 927-938.

Padhy, P.K., Varshney, C.K., 2005. Emission of volatile organic compounds (VOC) from tropical plant species in India. Chemosphere 59, 1643-1653.

Pandey, A., Brauer, M., Cropper, M.L., Balakrishnan, K., Mathur, P., Dey, S., Turkgulu, B., Kumar, G.A., Khare, M., Beig, G., 2021. Health and economic impact of air pollution in the states of India: the Global Burden of Disease Study 2019. The Lancet Planetary Health 5, e25-e38.

Pandey, A.K., Pandey, M., Mishra, A., Tiwary, S.M., Tripathi, B.D., 2015. Air pollution tolerance index and anticipated performance index of some plant species for development of urban forest. Urban Forestry & Urban Greening 14, 866-871.

Pathak, V., Tripathi, B.D., Mishra, V.K., 2011. Evaluation of Anticipated Performance Index of some tree species for green belt development to mitigate traffic generated noise. Urban Forestry & Urban Greening 10, 61-66.

Pawar, H., Garg, S., Kumar, V., Sachan, H., Arya, R., Sarkar, C., Chandra, B., Sinha, B., 2015. Quantifying the contribution of long-range transport to particulate matter (PM) mass loadings at a suburban site in the north-western Indo-Gangetic Plain (NW-IGP). Atmospheric Chemistry and Physics 15, 9501-9520.

Pazouki, N., Sankian, M., Nejadsattari, T., Khavari-Nejad, R.A., Varasteh, A.R., 2008. Oriental plane pollen allergy: identification of allergens and cross-reactivity between relevant species. Allergy Asthma Proc 29, 622-628.

Peng, C., Ma, Z., Lei, X., Zhu, Q., Chen, H., Wang, W., Liu, S., Li, W., Fang, X., Zhou, X.J.N.c.c., 2011. A drought-induced pervasive increase in tree mortality across Canada's boreal forests. 1, 467-471.

Peñuelas, J., Staudt, M., 2010. BVOCs and global change. Trends in Plant Science 15, 133-144.

Pfanz, H., Martinoia, E., Lange, O.-L., Heber, U., 1987. Mesophyll resistances to SO2 fluxes into leaves. Plant Physiology 85, 922-927.

Pichersky, E., Gershenzon, J., 2002. The formation and function of plant volatiles: perfumes for pollinator attraction and defense. Current Opinion in Plant Biology 5, 237-243.

Pleijel, H., Danielsson, H., Emberson, L., Ashmore, M., Mills, G., 2007. Ozone risk assessment for agricultural crops in Europe: further development of stomatal flux and flux–response relationships for European wheat and potato. Atmospheric Environment 41, 3022-3040.

Pleijel, H., Danielsson, H., Vandermeiren, K., Blum, C., Colls, J., Ojanperä, K., 2002. Stomatal conductance and ozone exposure in relation to potato tuber yield—results from the European CHIP programme. European Journal of Agronomy 17, 303-317.

Pohekar, H.R., Kalkar, S.A., 2016. Pollen Survey of Mahatma Jyotiba Phule Campus RTMNU Nagpur. Bulletin of Environment, Pharmacology and Life Sciences 5, 71-77.

Pokorska, O., Dewulf, J., Amelynck, C., Schoon, N., Šimpraga, M., Steppe, K., Van Langenhove, H.J.A.e., 2012. Isoprene and terpenoid emissions from Abies alba: identification and emission rates under ambient conditions. 59, 501-508.

Prajapati, S.K., Tripathi, B.D., 2008. Anticipated Performance Index of some tree species considered for green belt development in and around an urban area: a case study of Varanasi city, India. J Environ Manage 88, 1343-1349.

Rai, A., Mandal, R., 2020. Performance of Cinnamomum camphora, Ficus benjamina, Ficus elastica, Prunus cerasoides and Syzygium cumini against Air Pollution in Kathmandu Valley Nepal. Journal of applied biomaterials & biomechanics (JABB) 25, 1-8.

Rajan, S., Kumar, R., Negi, S., 2001. Variation in canopy characteristics of mango (Mangifera indica L.) cultivars from diverse eco-geographical regions. Journal of Applied Horticulture 3, 95-97.

Raju, A.J.S., Rao, S.P., 2006. Explosive pollen release and pollination as a function of nectar-feeding activity of certain bees in the biodiesel plant, Pongamia pinnata (L.) Pierre (Fabaceae). Current Science 90, 960-967.

Ramírez, F., Davenport, T.L., 2010. Mango (Mangifera indica L.) flowering physiology. Scientia Horticulturae 126, 65-72.

Rane, A., D., Narkhede, S., S., Bhave, S., G., Burondkar, M., M., 2017. Quantification of CO2 Atrsorption Rates of Few Tropical Trees of Konkan Region of Maharashtra. Advanced Agricultural Research and technology Journal 1, 19.

Reich, P.B., 1995. Phenology of tropical forests: patterns, causes, and consequences. Canadian Journal of Botany 73, 164-174.

Riley, W.J., Zhu, Q., Tang, J.Y., 2018. Weaker land–climate feedbacks from nutrient uptake during photosynthesis-inactive periods. Nature Climate Change 8, 1002-1006.

Rogers, A., 2014. The use and misuse of Vc,max in Earth System Models. Photosynthesis Research 119, 15-29.

Sahney, M., Chaurasia, S., 2008. Seasonal variations of airborne pollen in Allahabad, India. Ann Agric Environ Med 15, 287-293.

Sahu, C., Basti, S., Sahu, S.K., 2020. Air pollution tolerance index (APTI) and expected performance index (EPI) of trees in sambalpur town of India. SN Applied Sciences 2, 1327.

Sakai, S., Harrison, R.D., Momose, K., Kuraji, K., Nagamasu, H., Yasunari, T., Chong, L., Nakashizuka, T., 2006. Irregular droughts trigger mass flowering in aseasonal tropical forests in Asia. American Journal of Botany 93, 1134-1139.

Sarkar, R., 2019. Urbanization in India before and after the economic reforms: what does the census data reveal? Journal of Asian and African Studies 54, 1213-1226.

Satheeshkumar, S., Vittal, B.P.R., 1998. A preliminary survey of airborne pollen in Madras City. Aerobiologia 14, 69-73.

Schiestl, F.P., Johnson, S.D., 2013. Pollinator-mediated evolution of floral signals. Trends Ecol Evol 28, 307-315.

Schneider, C.A., Rasband, W.S., Eliceiri, K.W., 2012. NIH Image to ImageJ: 25 years of image analysis. Nature Methods 9, 671-675.

Seinfeld, J.H., 1989. Urban air pollution: state of the science. Science 243, 745-752.

Sellers, P.J., Randall, D.A., Collatz, G.J., Berry, J.A., Field, C.B., Dazlich, D.A., Zhang, C.,, Collelo, G.D., Bounoua, L., 1996. A revised land surface parameterization (SiB2) foratmospheric GCMs, Part I: model formulation. J. Clim. 9, 676-705.

Selmi, W., Weber, C., Rivière, E., Blond, N., Mehdi, L., Nowak, D.J.U.f., greening, u., 2016. Air pollution removal by trees in public green spaces in Strasbourg city, France. 17, 192-201.

Sermin, S., Koley, D., Ganguly, A., Ghosh, N., Talukdar, P., 2019. A study on respiratory allergy problems among local people of Serampore sub-division of West Bengal, India during spring season. World News of Natural Sciences 26.

Shannigrahi, A.S., Fukushima, T., Sharma, R.J.I.J.o.E.S., 2004. Anticipated air pollution tolerance of some plant species considered for green belt development in and around an industrial/urban area in India: an overview. International Journal of Environmental Studies 61, 125 - 137.

Shannigrahi, A.S., Sharma, R., Fukushima, T., 2003. Air pollution control by optimal green belt development around the Victoria Memorial monument, Kolkata (India). International Journal of Environmental Studies 60, 241-249.

Sharkey, T.D., Wiberley, A.E., Donohue, A.R., 2007. Isoprene Emission from Plants: Why and How. Annals of Botany 101, 5-18.

Sharma, G., Annadate, S., Sinha, B., 2022. Will open waste burning become India's largest air pollution source? Environmental Pollution 292, 118310.

Sharma, G., Sinha, B., 2023. Future emissions of greenhouse gases, particulate matter and volatile organic compounds from municipal solid waste burning in India. Science of The Total Environment 858, 2, 159708.

Shukla, R.P., Ramakrishnan, P.S., 1984. Biomass allocation strategies and productivity of tropical trees related to successional status. Forest Ecology and Management 9, 315-324.

Sicard, P., Agathokleous, E., Araminiene, V., Carrari, E., Hoshika, Y., De Marco, A., Paoletti, E., 2018. Should we see urban trees as effective solutions to reduce increasing ozone levels in cities? Environmental Pollution 243, 163-176.

Simon, H., Fallmann, J., Kropp, T., Tost, H., Bruse, M., 2019. Urban Trees and Their Impact on Local Ozone Concentration—A Microclimate Modeling Study, Atmosphere.

Singh, A.A., Eram, R., Agrawal, M., Agrawal, S.B., 2022. Air Pollution: Sources and its Effects on Humans and Plants. INTERNATIONAL JOURNAL OF PLANT AND ENVIRONMENT 8, 10-24.

Singh, A.B., Shahi, S., 2008. Aeroallergens in clinical practice of allergy in India- ARIA Asia Pacific Workshop report. Asian Pac J Allergy Immunol 26, 245-256.

Singh, A.P., Singh, R., Mina, U., Singh, M.P., Varshney, C.K., 2011. Emissions of monoterpene from tropical Indian plant species and assessment of VOC emission from the forest of Haryana state. Atmospheric Pollution Research 2, 72-79.

Singh, R., Singh, A.P., Singh, M.P., Kumar, A., Varshney, C.K., 2008. Emission of isoprene from common Indian plant species and its implications for regional air quality. Environ Monit Assess 144, 43-51.

Singh, R., Singh, M.P., Singh, A.P., 2014. Ozone forming potential of tropical plant species of the Vidarbha region of Maharashtra state of India. Urban Forestry & Urban Greening 13, 814-820.

Singh, S.K., Rao, D.N., Agrawal, M., Pandey, J., Naryan, D., 1991. Air pollution tolerance index of plants. Journal of Environmental Management 32, 45-55.

Sinha, V., Kumar, V., Sarkar, C., 2014. Chemical composition of pre-monsoon air in the Indo-Gangetic Plain measured using a new air quality facility and PTR-MS: high surface ozone and strong influence of biomass burning. Atmos. Chem. Phys. 14, 5921-5941.

Sinha, V., Williams, J., Meyerhöfer, M., Riebesell, U., Paulino, A.I., Larsen, A., 2007. Air-sea fluxes of methanol, acetone, acetaldehyde, isoprene and DMS from a Norwegian fjord following a phytoplankton bloom in a mesocosm experiment. Atmos. Chem. Phys. 7, 739-755.

Snyder, K.A., James, J.J., Richards, J.H., Donovan, L.A., 2008. Does hydraulic lift or nighttime transpiration facilitate nitrogen acquisition? Plant Soil 306, 159-166.

Song, Q., Sun, C., Deng, Y., Bai, H., Zhang, Y., Yu, H., Zhang, J., Sha, L., Liu, Y., 2020. Tree Surface Temperature in a Primary Tropical Rain Forest. Atmosphere 11, 798.

Spreer, W., Ongprasert, S., Hegele, M., Wünsche, J.N., Müller, J., 2009. Yield and fruit development in mango (Mangifera indica L. cv. Chok Anan) under different irrigation regimes. Agricultural Water Management 96, 574-584.

Stasik, O., Jones, H.G., 2007. Response of photosynthetic apparatus to moderate high temperature in contrasting wheat cultivars at different oxygen concentrations. Journal of Experimental Botany 58, 2133-2143.

Sulistijorini, Mas'Ud, Z.A., Nasrullah, N., Bey, A., Tjitrosemito, S., 2008. Tolerance Levels of Roadside Trees to Air Pollutants Based on Relative Growth Rate and Air Pollution Tolerance Index. HAYATI Journal of Biosciences 15, 123-129.

Swain, S.S., Mishra, P., 2020. Determinants of adoption of cleaner cooking energy: Experience of the Pradhan Mantri Ujjwala Yojana in rural Odisha, India. Journal of Cleaner Production 248, 119223.

Szczepanek, K., Myszkowska, D., Worobiec, E., Piotrowicz, K., Ziemianin, M., Bielec-Bąkowska, Z., 2017. The long-range transport of Pinaceae pollen: an example in Kraków (southern Poland). Aerobiologia 33, 109-125.

Taha, H., 1996. Modeling impacts of increased urban vegetation on ozone air quality in the South Coast Air Basin. Atmospheric Environment 30, 3423-3430.

Tahir, F., Ibrahim, M., Hamid, K., 2003. Effect of drought stress on vegetative and reproductive growth behaviour of mango (Mangifera indica L.). Asian Journal of Plant Sciences.

Thakur, P.S., Kaur, H., 2001. Variation in photosynthesis, transpiration, water use efficiency, light transmission and leaf area index in multipurpose agroforestry tree species. Indian Journal of Plant Physiology 6, 249-253.

Thien, L.B., 1974. Floral biology of Magnolia. American Journal of Botany 61, 1037-1045.

Toh, J., Jariwala, S., Rosenstreich, D., Zou, K., 2012. Association Between Asthma-related Emergency Department Visits, And Tree Pollen Concentrations In The Bronx, 2001 - 2008. Journal of Allergy and Clinical Immunology 129, AB167.

Tor-ngern, P., Leksungnoen, N., 2020. Investigating carbon dioxide absorption by urban trees in a new park of Bangkok, Thailand. BMC Ecology 20.

Tubby, K.V., Webber, J.F., 2010. Pests and diseases threatening urban trees under a changing climate. Forestry: An International Journal of Forest Research 83, 451-459.

Urban, L., Le Roux, X., Sinoquet, H., Jaffuel, S., Jannoyer, M.J.T.P., 2003. A biochemical model of photosynthesis for mango leaves: evidence for the effect of fruit on photosynthetic capacity of nearby leaves. 23, 289-300.

Urban, L., Mathieu, L., Lu, P., 2004. Effect of fruit load and girdling on leaf photosynthesis in Mangifera indica L. Journal of Experimental Botany 55, 2075-2085.

Vahisalu, T., Puzõrjova, I., Brosché, M., Valk, E., Lepiku, M., Moldau, H., Pechter, P., Wang, Y.S., Lindgren, O., Salojärvi, J., 2010. Ozone-triggered rapid stomatal response involves the production of reactive oxygen species, and is controlled by SLAC1 and OST1. The Plant Journal 62, 442-453.

Vainonen, J.P., Kangasjärvi, J., 2015. Plant signalling in acute ozone exposure. Plant, cell environment 38, 240-252.

Varshney, C.K., Singh, A.P., 2003. Isoprene emission from Indian trees. Journal of Geophysical Research: Atmospheres 108, n/a-n/a.

Vettikkat, L., Sinha, V., Datta, S., Kumar, A., Hakkim, H., Yadav, P., Sinha, B., 2020. Significant emissions of dimethyl sulfide and monoterpenes by big-leaf mahogany trees: discovery of a missing dimethyl sulfide source to the atmospheric environment. Atmospheric Chemistry and Physics 20, 375-389.

Viippola, V., Whitlow, T.H., Zhao, W., Yli-Pelkonen, V., Mikola, J., Pouyat, R., Setälä, H., 2018. The effects of trees on air pollutant levels in peri-urban near-road environments. Urban Forestry & Urban Greening 30, 62-71.

Vos, P.E.J., Maiheu, B., Vankerkom, J., Janssen, S., 2013. Improving local air quality in cities: To tree or not to tree? Environmental Pollution 183, 113-122.

Vrinceanu, D., Berghi, O.N., Cergan, R., Dumitru, M., Ciuluvica, R.C., Giurcaneanu, C., Neagos, A., 2021. Urban allergy review: Allergic rhinitis and asthma with plane tree sensitization (Review). Exp Ther Med 21, 275.

Wahala, S., De Costa, J., Ranasinqhe, D., 2013. An assessment of vegetation and canopy structure of moderately exploited natural forest area in Yagirala forest reserve. Proceedings of International Forestry and Environment Symposium.

Wang, Q., Wang, X., Li, R., Society, 2022. Does urbanization redefine the environmental Kuznets curve? An empirical analysis of 134 Countries. Sustainable Cities and Society 76, 103382.

Wang, Y., Anderegg, W.R., Venturas, M.D., Trugman, A.T., Yu, K., Frankenberg, C., 2021. Optimization theory explains nighttime stomatal responses. New Phytologist 230, 1550-1561.

Wang, Z.H., Bai, Y.H., Liu, Z.R., Wang, X.S., Li, Q.J., Klinger, L.F., 2005. Investigation of natural VOC emitted from tropical vegetations in China. J Environ Sci (China) 17, 8-13.

Wei, N., Xia, J., Wang, Y.-P., Zhang, X., Zhou, J., Bian, C., Luo, Y., 2022. Nutrient Limitations Lead to a Reduced Magnitude of Disequilibrium in the Global Terrestrial Carbon Cycle. Journal of geophysical research: biogeosciences 127, e2021JG006764.

Wesely, M.L., 1989. Parameterization of surface resistances to gaseous dry deposition in regional-scale numerical models. Atmospheric Environment (1967) 23, 1293-1304.

Wieser, G., Emberson, L., 2004. Evaluation of the stomatal conductance formulation in the EMEP ozone deposition model for Picea abies. Atmospheric Environment 38, 2339-2348.

Wittig, V.E., Ainsworth, E.A., Long, S.P., 2007. To what extent do current and projected increases in surface ozone affect photosynthesis and stomatal conductance of trees? A meta-analytic review of the last 3 decades of experiments. Plant Cell Environ 30, 1150-1162.

Wolf, A., Akshalov, K., Saliendra, N., Johnson, D.A., Laca, E.A., 2006. Inverse estimation of Vcmax, leaf area index, and the Ball-Berry parameter from carbon and energy fluxes. Journal of Geophysical Research: Atmospheres 111.

Wolfe, B.T., Van Bloem, S.J., 2012. Subtropical dry forest regeneration in grass-invaded areas of Puerto Rico: Understanding why Leucaena leucocephala dominates and native species fail. Forest Ecology and Management 267, 253-261.

Wu, C., Yang, C., Huang, T., Chen, S., 2006. Forensic pollen evidence from clothes by the tape adhesive method. Taiwania 51, 123.

Yang, J., Chang, Y., Yan, P., 2015. Ranking the suitability of common urban tree species for controlling PM2.5 pollution. Atmospheric Pollution Research 6, 267-277.

Yu, K., Goldsmith, G.R., Wang, Y., Anderegg, W.R., 2019. Phylogenetic and biogeographic controls of plant nighttime stomatal conductance. New Phytologist 222, 1778-1788.

Zaharah, S.S., Razi, I.M., 2009. Growth, stomata aperture, biochemical changes and branch anatomy in mango (Mangifera indica) cv. Chokanan in response to root restriction and water stress. Scientia Horticulturae 123, 58-67.

Zhang, L., He, Z., 2014. Technical Note: An empirical algorithm estimating dry deposition velocity of fine, coarse and giant particles. Atmos. Chem. Phys. 14, 3729-3737.

Zhang, W., Zhang, Z., Meng, H., Zhang, T.J.F., 2018. How does leaf surface micromorphology of different trees impact their ability to capture particulate matter? Forests 9, 681.

Ziemianin, M., Waga, J., Czarnobilska, E., Myszkowska, D., 2021. Changes in qualitative and quantitative traits of birch (Betula pendula) pollen allergenic proteins in relation to the pollution contamination. Environmental Science and Pollution Research 28, 39952-39965.

Zimmerman, P.R., Chatfield, R.B., Fishman, J., Crutzen, P.J., Hanst, P.L., 1978. Estimates on the production of CO and H2 from the oxidation of hydrocarbon emissions from vegetation. 5, 679-682.